Environment Canada Environnement Canada

National Hydrology Research Institute

NHRI PAPER NO. 31
IWD SCIENTIFIC SERIES NO. 160

Hydrogeological Characterization of the East Bull Lake Research Area

K.G. Raven,* D.J. Bottomley, R.A. Sweezey, J.A. Smedley and T.J. Ruttan

*Now with:
INTERA Technologies Ltd.
1525 Carling Avenue, Suite 600
Ottawa, Ontario, Canada
K1Z 8R9

This is the final report on hydrogeological studies conducted by the Contaminant Hydrogeology Section, National Hydrology Research Institute, Inland Waters/Lands Directorate, Environment Canada for the Applied Geoscience Branch, Atomic Energy of Canada Ltd., Pinawa, Manitoba, Canada R0E 1L0.

NHRI

INLAND WATERS / LANDS DIRECTORATE
NATIONAL HYDROLOGY RESEARCH INSTITUTE
NATIONAL HYDROLOGY RESEARCH CENTRE
SASKATOON, SASKATCHEWAN, 1987
(Disponible en français sur demande)

Published by authority of
the Minister of the Environment

© Minister of Supply and Services Canada 1987

Cat. No. En 36-502/160E

ISBN 0-662-15782-6

Contents

	Page
ABSTRACT	vii
RÉSUMÉ	viii
ACKNOWLEDGMENTS	ix
1. INTRODUCTION	1
2. SITE DESCRIPTION	2
Site location	2
Surface drainage pattern	2
Geology	2
3. DRILLING PROGRAM	9
4. HYDRAULIC CONDUCTIVITY TESTING	15
P-Series boreholes	15
Methodology	15
Open-borehole pump tests	15
Packer tests	15
Results and interpretation	16
EBL-Series boreholes	18
Methodology	18
1983 Tests	18
1984 Tests	21
1985 Tests	22
Results and interpretation	22
Borehole EBL-1	22
Borehole EBL-2	25
Borehole EBL-3	26
Borehole EBL-4	26
5. INSTALLATION OF MULTIPLE-PACKER CASINGS	30
6. HYDRAULIC HEAD MONITORING	35
Methodology	35
Results and interpretation	35
P-Series boreholes	35
EBL-Series boreholes	36
7. HYDROGEOCHEMICAL INVESTIGATIONS	40
Methodology	40
Results	41
Sample representativeness	41
1984 Sampling	45
Major and minor elements and trace metals	45
Dissolved gases	47
Environmental isotopes	48
1985 Sampling	49
Discussion	50

Contents (Cont.)

Page

8. SYNTHESIS AND SUMMARY 52

REFERENCES 54

APPENDIX A. Summary of straddle-packer test results, boreholes P-1 to P-14 57

APPENDIX B. Summary of hydraulic head measurements, boreholes EBL-1, 2, 3 and 4, October 1984 to October 1985 65

APPENDIX C. Analytical methods for major and minor elements and trace metals 73

Tables

1. Borehole lengths and orientations 9
2. Relative borehole locations and elevations of surface casings 9
3. Open-borehole hydraulic properties of the P-series Boreholes 16
4. Summary of 1983 packer test results for borehole EBL-1 23
5. Summary of 1983 packer test results for borehole EBL-2 23
6. Summary of 1984 PIP test results for EBL-series boreholes 23
7. Summary of 1985 hydraulic tests completed in EBL-series boreholes 24
8. Summary of multiple-packer casing installations in the EBL-series boreholes 30
9. Elevations of test intervals in EBL-series boreholes 30
10. Hydraulic heads of the 050 and 130 lineament structures in the base of the troctolite horizon 36
11. Hydraulic heads measured during 1984 PIP testing 36
12. Results of integrity check on multiple-packer casings in boreholes EBL-1 and EBL-2 37
13. Summary of most representative analyses for 1984 of ground-water chemistry (major and minor elements) for P-series and EBL-series boreholes 42
14. Summary of 1984 trace metal concentrations in ground waters from the P-series and EBL-series boreholes 43
15. The most representative chemical analyses (major and minor elements) of ground-water samples collected from selected intervals in the EBL-series boreholes, 1985 43
16. Representative trace metal concentrations in ground waters from selected intervals in the EBL-series boreholes, 1985 44
17. Dissolved gas composition of East Bull Lake ground waters 44
18. Helium and neon concentrations and $^{3}He/^{4}He$ ratios in 1984 EBL ground waters . . . 44
19. Isotopic composition of 1984 East Bull Lake ground waters 45

Illustrations

Page

Figure 1. Location map of the East Bull Lake research area 3
Figure 2. Regional topography and surface drainage patterns of the East Bull Lake research area 4
Figure 3. Topography and borehole locations in the detailed study area – East Bull Lake research area 5
Figure 4. Geology of the central plateau of the East Bull Lake pluton 6
Figure 5. Borehole locations and air photo-identified lineaments in the detailed study area – East Bull Lake research area 7
Figure 6. Summary lithologic and structural log of borehole EBL-1 10
Figure 7. Summary lithologic and structural log of borehole EBL-2 11
Figure 8. Summary lithologic and structural log of borehole EBL-3 12
Figure 9. Summary lithologic and structural log of borehole EBL-4 13
Figure 10. Schematic of straddle-packer probe used to complete bail-recovery tests in the P-series boreholes 15
Figure 11. Histogram of the distribution of the common logarithm of equivalent rock mass hydraulic conductivity, K_{erm}, determined from packer tests completed from 0 to 75-m depth at the East Bull Lake and Chalk River research areas 17
Figure 12. Cumulative probability plot of the common logarithm of equivalent rock mass hydraulic conductivity, K_{erm}, determined from packer tests completed from 0 to 75-m depth at the East Bull Lake and Chalk River research areas 17
Figure 13. Umbilical cable and electrically driven cable reel used during packer testing of borehole EBL-1 in 1983 19
Figure 14. Schematic of straddle-packer probe and umbilical cable used during packer testing of borehole EBL-1 in 1983 19
Figure 15. Details of the downhole piston and downhole valve incorporated in the straddle-packer probe used to hydraulically test borehole EBL-1 in 1983 19
Figure 16. Schematic of flow measurement and pressure application equipment used during packer testing of borehole EBL-1 in 1983 20
Figure 17. Schematic of data acquisition system used during packer testing of borehole EBL-1 in 1983 20
Figure 18. Schematic of equipment used for hydraulic testing with a work-over rig showing details of swabber and production-injection packer (PIP) 21
Figure 19. Flow rate per unit head ($Q/\Delta H$) profiles for boreholes EBL-1 and EBL-2 determined from 1983 packer tests and 1984 PIP tests 24
Figure 20. Change in hydraulic head in EBL observation intervals and change in barometric pressure versus log-time during EBL-1 pump test of troctolite fracture zone at 210-m depth 25
Figure 21. Log-drawdown versus log-time response of open-borehole pump test in EBL-1 26
Figure 22. Results of borehole EBL-4 flow meter survey completed by United States Geological Survey in 1984 27
Figure 23. Plot of specific conductance of withdrawn fluid versus cumulative produced fluid volume for four periods of pumping from 454-m depth fracture zone in borehole EBL-4 28
Figure 24. Log-drawdown versus log-time response of open-borehole pump test in EBL-4 28

Illustrations (Cont.)

		Page
Figure 25.	Results of step-drawdown pump test of borehole EBL-4	29
Figure 26.	Composite lithological and hydrogeological log for borehole EBL-1	31
Figure 27.	Composite lithological and hydrogeological log for borehole EBL-2	32
Figure 28.	Composite lithological and hydrogeological log for borehole EBL-3	33
Figure 29.	Composite lithological and hydrogeological log for borehole EBL-4	34
Figure 30.	Plot of electrical conductivity vs. volume of water withdrawn from EBL-4 (429-456 m) in 1985	43
Figure 31.	Water table map for EBL based on water level measurements in all boreholes on May 2, 1984, and the topography of the area	46
Figure 32.	Concentrations of N_2 and Ar in the EBL-series and P-series ground waters	47
Figure 33.	Plot of the stable isotope (^{18}O-^{2}H) compositions of EBL ground waters based upon the most representative sample collected from each test interval	48
Figure 34.	Trilinear plot of the major ion composition of EBL ground waters	50

Abstract

In the period 1983-1985, the National Hydrology Research Institute in co-operation with Atomic Energy of Canada Limited undertook hydrogeological research studies at the East Bull Lake research area, a gabbro-anorthosite pluton located near Massey, Ontario. This report describes the methodology, results and interpretation of the borehole investigations completed at East Bull Lake to measure the fundamental hydrogeological parameters of hydraulic conductivity, hydraulic head and ground-water chemistry. These parameters were measured in four deep boreholes (440-850 m in depth) and 14 shallow boreholes (40-100 m in depth) using a variety of testing, monitoring and sampling methods developed for use in open boreholes and in boreholes equipped with packer assemblies and multiple-packer casings. The results of the borehole investigations are interpreted in the context of a regional ground-water flow system for the East Bull Lake area.

The borehole investigations reliably demonstrate that the hydraulic conductivity of the gabbro-anorthosite decreases with depth from an average near-surface value of 10^{-8} $m \cdot s^{-1}$ to less than 10^{-12} $m \cdot s^{-1}$ below 400-500 m. Superimposed on this general hydraulic conductivity-depth trend are several permeable fracture zones which are shown to be important to the development of both local and deeper regional flow systems. Of particular hydrogeological significance are the 050 and 130 structural discontinuities, fracturing associated with the base of the troctolite unit and with a porphyritic dyke near the basal contact of the pluton and the regional-scale Folson Lake Fault.

The ground-water chemistry in the upper 300 m of the pluton is the Ca/HCO_3 type at shallow depths near ground-water recharge areas which evolves to high pH, Na/HCO_3 water along the direction of flow. The chemical evolution is the result of ion exchange reactions on fracture infilling minerals and is not controlled by the bulk rock composition. Saline, Na/Cl waters are present below about 400 m in the deep, regional flow system. The Br/Cl ratio of the saline water suggests that it is derived from an ancient infiltration of sea water, formation water or from lateral flow from adjacent Precambrian metasedimentary formations.

The East Bull Lake ground waters exhibit a remarkable range in $\delta^{18}O$ of 7.6 ‰. The isotopically lightest ground waters are Na/HCO_3 waters found in the troctolite in the northeastern region of the pluton. A glacial meltwater component appears to be present in these waters. The saline Na/Cl waters have an isotopic composition similar to that of the modern, shallow ground water in the pluton, indicating they have a different origin and are part of a different flow system than the isotopically light Na/HCO_3 waters.

Résumé

De 1983 à 1985, l'Institut national de recherche en hydrologie en coopération avec Énergie atomique du Canada Ltée, a entrepris des recherches hydrogéologiques dans la zone de recherches du lac East Bull, un pluton de gabbro-anorthosite située près de Massey en Ontario. Le présent rapport porte sur la méthodologie, les résultats et l'interprétation des recherches par sondage accomplies au lac East Bull pour mesurer les paramètres hydrogéologiques fondamentaux, à savoir la conductivité hydraulique, la hauteur piézométrique et la chimie de l'eau souterraine. Ces paramètres ont été mesurés dans quatre forages profonds (440 à 850 m de profondeur) et 14 forages peu profonds (40 à 100 m de profondeur) par diverses méthodes d'essai, de contrôle et d'échantillonnage mises au point pour servir dans des sondages ouverts et des sondages équipés de packers et de tubages pour packers multiples. Les résultats des recherches par les sondages sont interprétés dans le contexte d'un système régional d'écoulement d'eau souterraine pour la région du lac East Bull.

Les sondages ont démontré clairement que la conductivité hydraulique du gabbro-anorthosite diminue avec la profondeur d'une valeur moyenne près de la surface de 10^{-8} $m \cdot s^{-1}$ à moins de 10^{-12} $m \cdot s^{-1}$ sous 400-500 m. En plus de cette tendance générale de la conductivité hydraulique en fonction de la profondeur, il y a plusieurs zones de fractures perméables qui ont joué un rôle important dans l'évolution des systèmes d'écoulement locaux et régionaux plus profonds. Les discontinuités structurales 050 et 130 sont particulièrement importantes sur le plan hydrogéologique; il s'agit de fractures associés à la base du troctolite et à un dyke porphyritique près du contact avec la base du pluton et de la faille régionale du lac Folson.

La chimie de l'eau souterraine dans les 300 m supérieurs du pluton est de type Ca/HCO_3 aux faibles profondeurs près des zones de recharge des eaux souterraines et passe à des pH élevés, avec de l'eau de type Na/HCO_3 le long de la direction de l'écoulement. L'évolution chimique est le résultat de réactions d'échange d'ions sur les minéraux de remplissage des fractures et n'est pas contrôlée par la composition de la masse rocheuse. Des eaux salines (Na/Cl) se trouvent sous 400 m dans le réseau d'écoulement régional profond. Le rapport Br/Cl de l'eau saline indique qu'elle provient d'une infiltration ancienne d'eau de mer ou d'eau de formation, ou d'un écoulement latéral venu de formations métasédimentaires précambriennes adjacentes.

La teneur en $\delta^{18}O$ des eaux souterraines du lac East Bull varie de façon remarquable de 7.6 ‰. Les eaux souterraines isotopiquement les moins denses sont celles qui contiennent du Na/HCO_3 et qui se trouvent dans le troctolite de la partie nord-est du pluton. Elles semblent contenir de l'eau de fonte glaciaire. Les eaux salines, contenant du Na/Cl, ont une composition isotopique semblable à celles de l'eau souterraine contemporaine et peu profonde dans le pluton, ce qui indique qu'elles ont une origine différente et font partie d'un système d'écoulement différent que ceux des eaux isotopiquement moins denses contenant du Na/HCO_3.

Acknowledgments

The authors gratefully acknowledge the following individuals for their contributions to the East Bull Lake project: J. Gorrie, Atomic Energy of Canada Ltd. (AECL), for borehole testing and sampling; J. Ross, AECL, for ground-water sampling; K. Inch, National Hydrology Research Institute (NHRI), for laboratory chemical analyses of ground waters; E. Kozak, AECL, and K.S. Novakowski, NHRI, for installation of multiple-packer casings in boreholes; R. Dickin, Gartner Lee and Associates, for installation of production-injection packers; and S. Denhoed, D. Hutchinson, M. Jensen, B. Kueper, P. Kornelsen, P. Lapcevic, I. MacDonald, C. Van der Grient and A. Vorauer, all of AECL, for their capable field assistance in all aspects of the hydrogeological investigations undertaken at East Bull Lake.

We also wish to extend special thanks to R. Pearson and M. Gascoyne, AECL, for help in co-ordinating the East Bull Lake study.

Introduction

Atomic Energy of Canada Ltd. (AECL) is currently evaluating the concept of deep disposal of nuclear fuel cycle wastes in geologically stable rock formations. As part of this ten-year (1981-1990) concept assessment phase, AECL is expected to provide geological and hydrogeological data characteristic of plutonic rocks within the Canadian Shield. Since 1977, the National Hydrology Research Institute (NHRI) of Environment Canada, in conjunction with AECL, has carried out a research program to examine and develop methods of characterizing the hydrogeology of fractured plutonic rocks at several study sites or research areas within the Canadian Shield. The focus of this research program has been the reliable measurement of the ground-water flow, chemistry, and solute transport properties of fractured plutonic rocks to depths of 1000 m.

In 1983, NHRI began hydrogeological studies at AECL's East Bull Lake (EBL) research area (RA-7) located near Massey, Ontario. During 1983, reconnaissance-level hydrogeological investigations were completed in four, deep, diamond-cored boreholes (EBL-series) and 14 shallow, air-percussion drilled boreholes (P-series). The results of these studies, which included drill water tagging, packer testing, pump testing, production-injection packer installation and ground-water sampling, are summarized by Raven *et al.* (1984).

Hydrogeological testing and monitoring continued at the East Bull Lake research area in 1984 and 1985. Detailed measurements of hydraulic conductivity, hydraulic head and ground-water chemistry were obtained from both the EBL-series and the P-series boreholes during this period.

Hydrogeological testing in the P-series boreholes in 1984 and 1985 focussed on systematic single-packer and straddle-packer testing to determine the distribution of hydraulic conductivity and hydraulic head. Ground-water sampling was also completed from selected packer-isolated intervals in each P-series borehole to characterize the chemical and isotopic composition of EBL ground waters in the near surface (0 to 100-m depth).

During 1984, hydrogeological testing was performed in the deep boreholes EBL-1, 2 and 4 using production-injection packers (PIPs) that were installed in the boreholes during October and November 1983. The PIPs created a network of 14 test intervals in the three boreholes and reduced mixing of ground waters from different hydraulic head regimes along each borehole. Hydraulic conductivity and hydraulic head were measured in each PIP-isolated test interval. Ground-water samples were obtained from each of the test intervals to characterize the chemical and isotopic composition of EBL ground waters to depths of 600-800 m.

During October and November 1984, multiple-packer casings were permanently installed in boreholes EBL-1, 2, 3 and 4. Hydraulic conductivity tests, detailed hydraulic head monitoring, and ground-water sampling were completed in 1985 using these multiple-packer casings.

This report summarizes the results of the hydrogeological testing, monitoring and sampling completed in boreholes at the East Bull Lake research area during 1983, 1984 and part of 1985. Some isotopic results and hydraulic head data obtained after October 1985 were not available for inclusion in this report. The available hydrogeological data from 1983, 1984 and 1985 studies have been interpreted in the context of a regional ground-water flow system for the East Bull Lake area.

Site Description

SITE LOCATION

The East Bull Lake research area is located in the Algoma Regional District, 35 km east of Elliot Lake, and north of Ontario Highway 17 between Sault Ste. Marie and Sudbury (Fig. 1). Access to the site is provided by gravel highway (Ontario Highway 553), which extends northward approximately 35 km from Massey. Local and regional terrain characteristics are described by Leech and Cooper (1982). Regional topography and the distribution of surface waters are shown in Figure 2.

All boreholes were drilled in a 3 to 4 km^2 area selected for detailed geological and hydrogeological study (Ermanovics *et al.*, 1982). This detailed study area is located immediately northwest of Moon Lake between East Bull and Folson lakes (Fig. 1). The study area is further situated on the plateau area (elevation in excess of 380 m a.s.l.) in the central part of the East Bull Lake pluton. The topography of the study area and the locations of the boreholes are shown in Figure 3.

SURFACE DRAINAGE PATTERN

There are two major drainage routes (Fig. 2) from the plateau area of the study site to River aux Sables which drains south to Lake Huron. Surface drainage from the northern half of the plateau area is collected through two intersecting streams that follow two major structural lineaments. These streams empty into Little Bull Lake through a connecting stream from Moon Lake. Drainage from Moon Lake is westward to Burnett Lake, and then northward and eastward to River aux Sables. Surface drainage from the southern half of the plateau area is to the south and southeast to Moon Lake and the topographic low created by the regional Folson Lake Fault (see below). Drainage is channelled along the Folson Lake Fault to the southeast through Parisien Lake and to River aux Sables.

GEOLOGY

Most of the geological and geophysical activities completed to date at the East Bull Lake research area have been confined to the central plateau portion of the East Bull Lake gabbro-anorthosite body (Ermanovics *et al.*, 1983). The surface geology of this central area is described in detail by Kamineni *et al.* (1984) (Fig. 4), McCrank *et al.* (1983), and James and Born (1985). Previous mapping in the area includes that of Moore and Armstrong (1943), Born (1978), Born and James (1978), and Brown and Kamineni (1981). Subsurface geology of the central area based on EBL-series borehole core logging is described by McCrank *et al.* (1984) and Ejeckam *et al.* (1984). Reconnaissance airborne and ground geophysical surveys including gravity (Watson, 1982; Redford, 1983a), aeromagnetics and airborne EM VLF surveys (Redford, 1983b) were used to define the general geology and location of major structural discontinuities.

The results of the surveys and mapping indicate that the plateau area is the central portion of a layered gabbro-anorthosite intrusion, which is elliptical and measures 13 km by 4 km. The pluton, which is likely of Proterozoic age, is a shallow (700 to 800 m deep), layered basin-like intrusion with anorthositic rocks at the base and gabbroic rocks near the top. In the map area (Fig. 4), the pluton is underlain by gneissic rocks, granodiorites and metavolcanics of Archean age.

The gabbro-anorthosite pluton has been subdivided into eight textural and compositional units that reflect percentages of pyroxene, amphibolite and plagioclase, and compositional layering. Detailed descriptions of these units are given by McCrank *et al.* (1983) and Kamineni *et al.* (1984). Rocks in the study area were also intruded by abundant Proterozoic dykes and sheets of amphibolite and diabase. These dyke swarms generally trend northwesterly through the plateau area and are shown in Figure 4.

The detailed study area was also mapped for major structural discontinuities or lineaments using local-scale and regional-scale aerial photographs. Identification of major fracture zones and faults is important in groundwater flow system investigations, as these discontinuities are likely to form short-circulating pathways of high permeability and no-flow barriers of low permeability in otherwise uniformly fractured and permeable rock. The resultant map of lineaments identified on air photos is shown in Figure 5. Both major and minor lineaments were identified, with major lineaments generally being in excess of 1 km in length and transecting the upper plateau area.

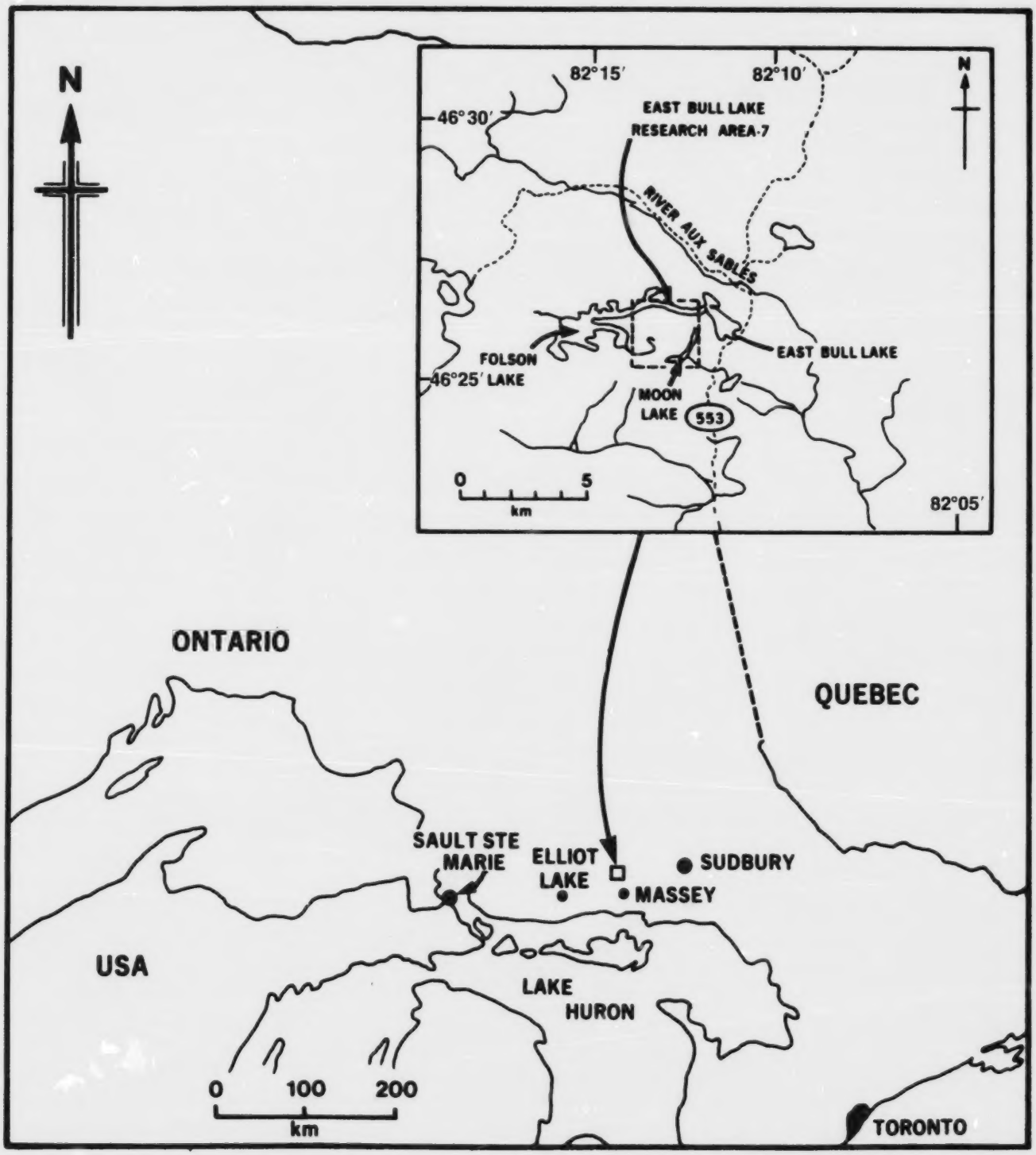

Figure 1. Location map of the East Bull Lake research area.

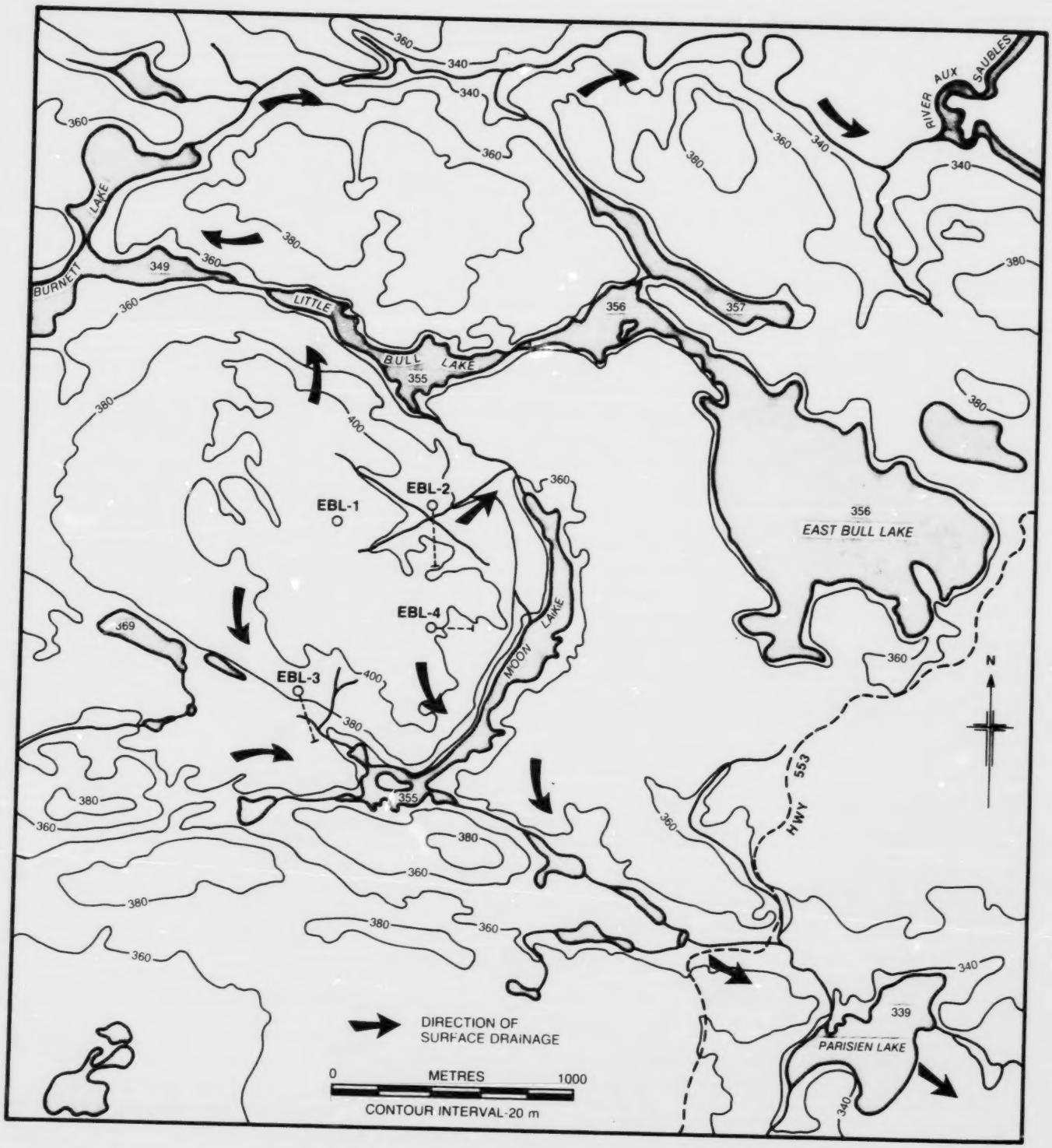

Figure 2. Regional topography and surface drainage patterns of the East Bull Lake research area.

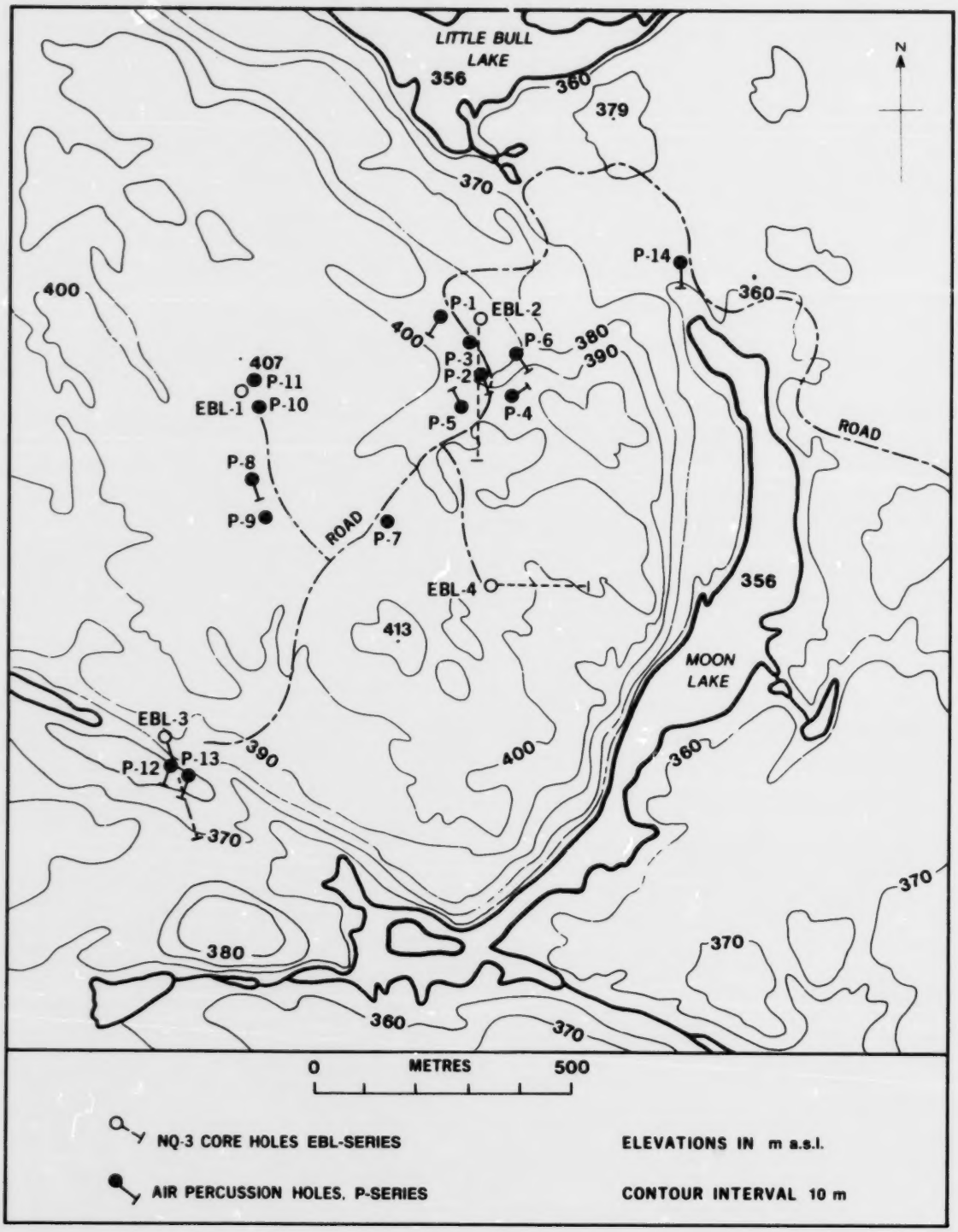

Figure 3. Topography and borehole locations in the detailed study area – East Bull Lake research area.

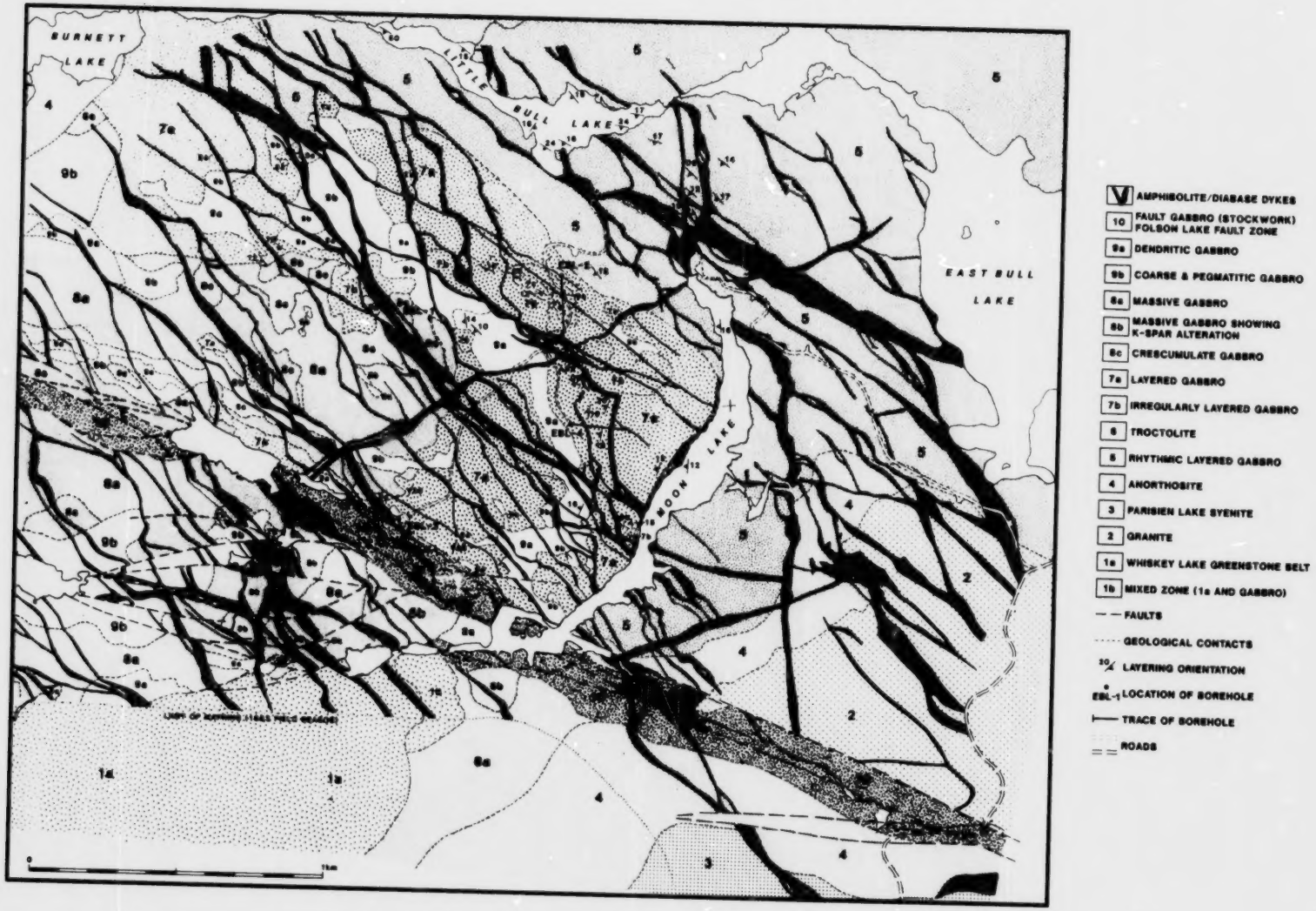

Figure 4. Geology of the central plateau of the East Bull Lake pluton (after Kamineni *et al.*, 1984).

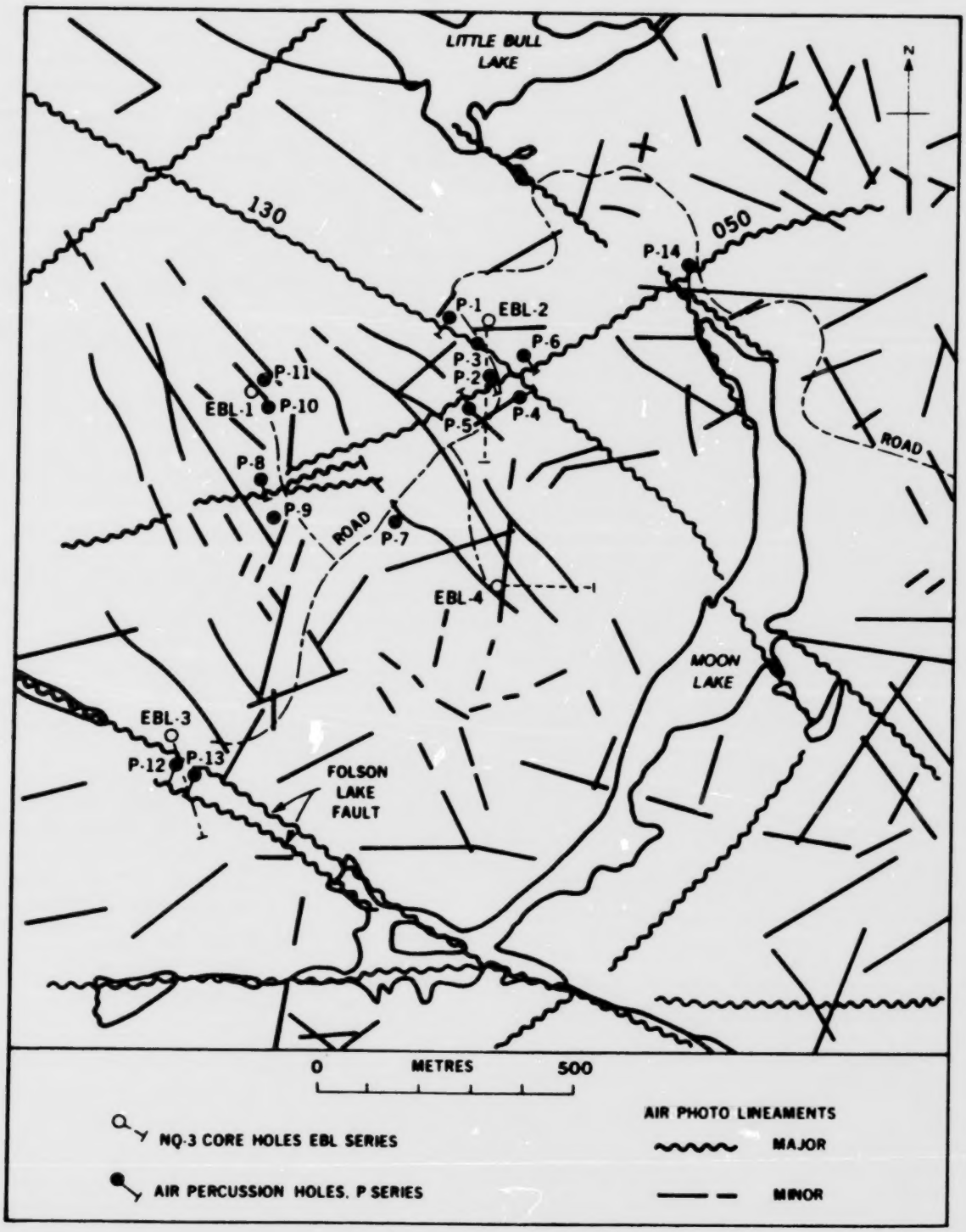

Figure 5. Borehole locations and air photo-identified lineaments in the detailed study area – East Bull Lake research area.

Three of the structural lineaments identified in Figure 5 are particularly noteworthy; the 050, the 130, and the Folson Lake Fault. The 050 and 130 lineaments criss-cross the northern portion of the plateau area and were also identified as water-bearing in the near surface from aerial thermography surveys completed in spring 1983 (D. Lee, AECL, pers. comm.). These lineaments channel surface drainage and likely ground-water discharge from the northern half of the plateau area northward to Little Bull Lake.

Comparison of the lineament and geological maps suggests that the 130 lineament is associated with a steeply north dipping, northwest striking mafic dyke. The 050 lineament may not be related to mafic dykes and is therefore likely associated with a large fracture zone or fault. As evident in Figure 5, the lineaments were intersected by both deep diamond drilling and shallow air-percussion drilling to create a borehole array for hydrogeological testing. The results of the drilling program (Raven *et al.*, 1984) suggest both lineaments are steeply north dipping.

The Folson Lake Fault lineament or series of lineaments are part of a large regional-scale fault trending northwesterly through the study area. Splays of this fault structure are intersected by boreholes EBL-3 and P-12 and P-13.

Drilling Program

The drilling program completed at East Bull Lake during 1983 included deep diamond-core drilling and shallow air-percussion drilling. Four diamond-cored boreholes and 14 air-percussion boreholes were completed for total lengths of 2617 m and 740 m, respectively. Diamond-core drilling was supervised by the Geological Survey of Canada; air-percussion drilling was supervised by NHRI. Statistics of the drilling program are summarized in Table 1. Table 2 lists the relative borehole locations and elevations of the surface casings as determined from surveying. Locations of the boreholes are shown in Figures 3 and 5.

The results of the diamond drilling program are presented and discussed in detail by Ejeckam *et al.* (1984) and Raven *et al.* (1984). The results of the air-percussion drilling program are summarized by Raven *et al.* (1984).

Table 1. Borehole Lengths and Orientations

Borehole	Length (m)	Orientation
EBL-Series		
NQ – diamond cored		
EBL-1	850.7	Vertical
EBL-2	835.6	177°/75-71°*
EBL-3	441.6	161-159°/60-57°
EBL-4	488.7	91-95°/69-65°
P-Series		
0.16-m diameter air-percussion		
P-1	53.3	210°/68°
P-2	38.1	148°/75°
P-3	38.1	Vertical
P-4	55.0	0°/65°
P-5	97.6	320°/70°
P-6	68.0	140°/80°
P-7	39.6	Vertical
P-8	45.2	160°/68°
P-9	43.2	Vertical
P-10	98.7	Vertical
P-11	49.2	Vertical
P-12	48.6	210°/75°
P-13	48.7	194°/65°
P-14	43.3	184°/70°

*Range of orientations from top to bottom of borehole as determined from gyroscopic directional surveys completed by Sperry Sun of Canada.

Table 2. Relative Borehole Locations and Elevations of Surface Casings

Borehole	Location		Casing elevation* (m a.s.l.)
	Northing (m)	Easting (m)	
EBL-1	42 523.17	6421.72	405.85
EBL-2	42 661.89	6877.85	397.76
EBL-3	41 859.42	6314.96	386.71
EBL-4	42 713.84	6878.68	404.54
P-1	42 676.04	6807.86	395.08
P-2	42 568.38	6884.36	391.29
P-3	42 621.11	6852.81	390.78
P-4	42 537.99	6925.11	393.13
P-5	42 489.20	6824.64	396.40
P-6	42 613.70	6941.14	399.67
P-7	42 349.19	6721.04	403.18
P-8	42 365.71	6449.80	401.02
P-9	42 306.28	6474.94	401.51
P-10	42 496.84	6443.14	405.42
P-11	42 536.04	6429.95	405.56
P-12	41 810.55	6330.29	378.36
P-13	41 807.89	6334.48	378.47
P-14	42 806.18	7285.23	362.92

*Reference elevation is lowest point on top of borehole casing m a.s.l. = Metres above sea level.

Detailed structural and lithologic logs completed by Ejeckam *et al.* (1984) for boreholes EBL-1, 2, 3 and 4 are shown in Figures 6 to 9.

In addition to structural and lithologic logs, borehole acoustic televiewer logs and selected geophysical logs were completed in the EBL-series boreholes by the Geological Survey of Canada and the United States Geological Survey. Borehole acoustic televiewer surveys were also completed in selected P-series boreholes by the Geological Survey of Canada.

Brief summaries of the important geological features intersected by each EBL-series borehole are provided below from Raven *et al.* (1984) based on work by Ejeckam *et al.* (1984) and the Geological Survey of Canada. These summaries supplement hydrogeological data presented in Chapters 4, 6 and 7. In this report, depth refers to length along the borehole from the top of the surface casing.

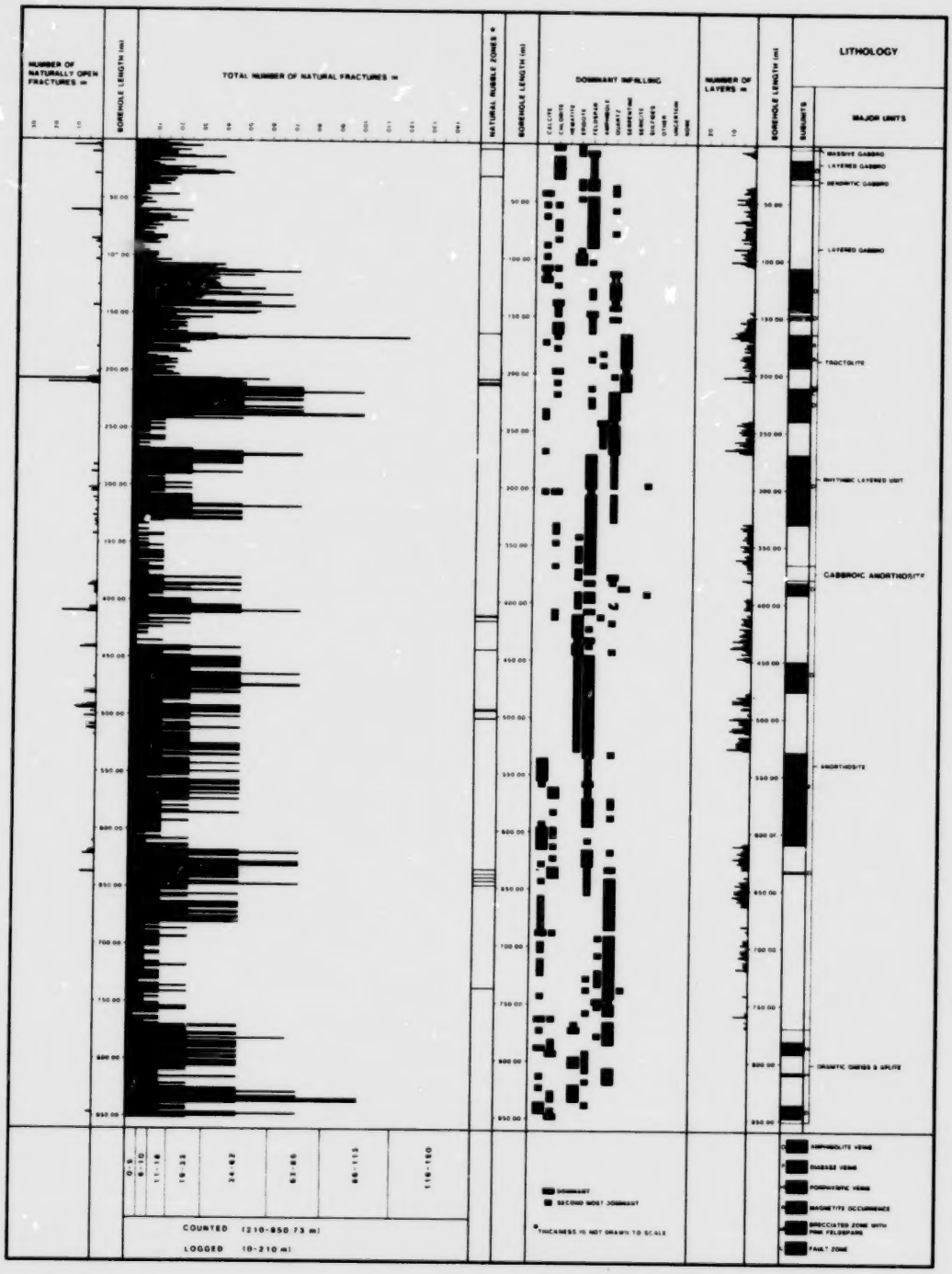

Figure 6. Summary lithologic and structural log of borehole EBL-1 (after Ejeckam *et al.*, 1984).

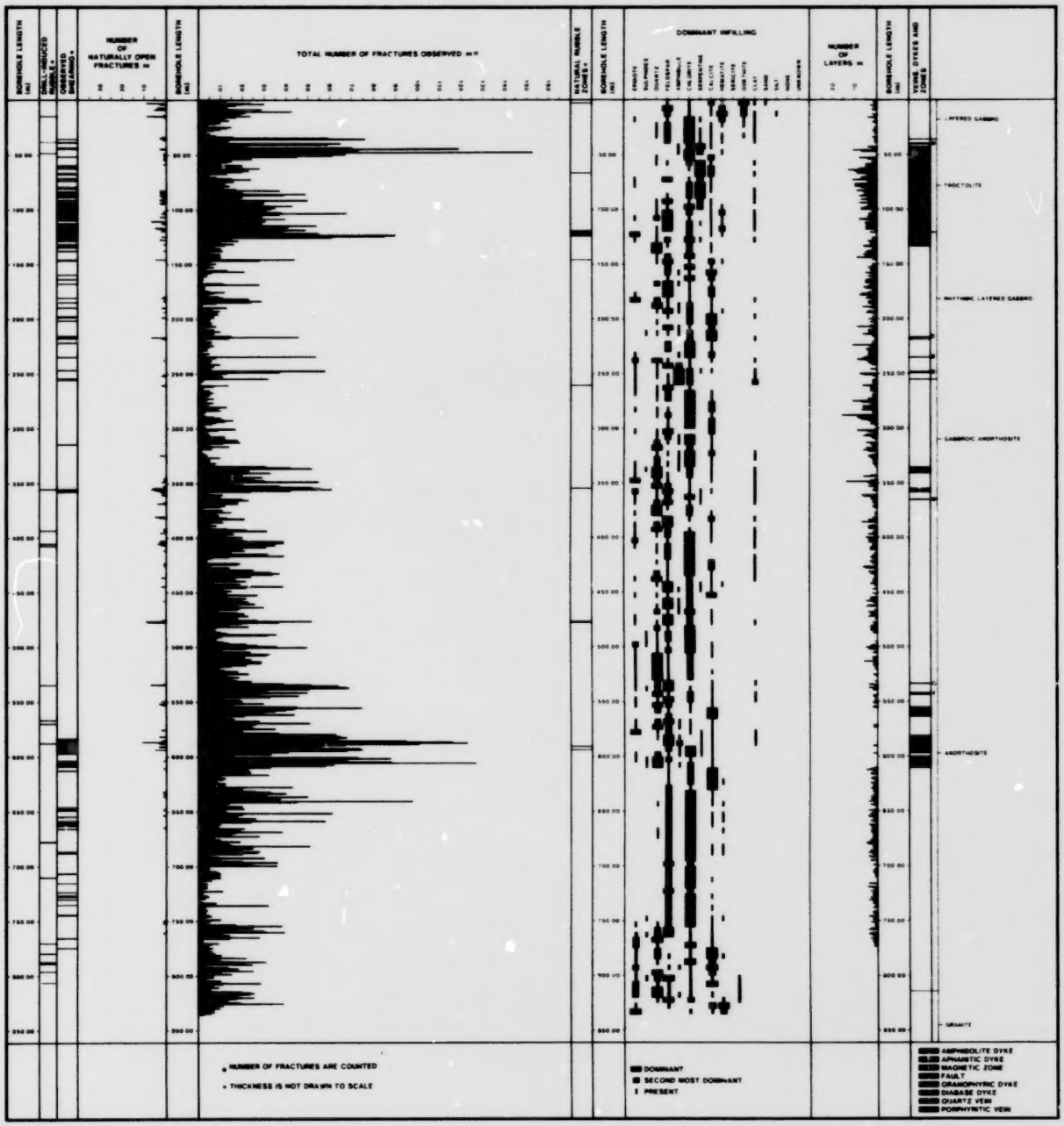

Figure 7. Summary lithologic and structural log of borehole EBL-2 (after Ejeckam *et al.*, 1984).

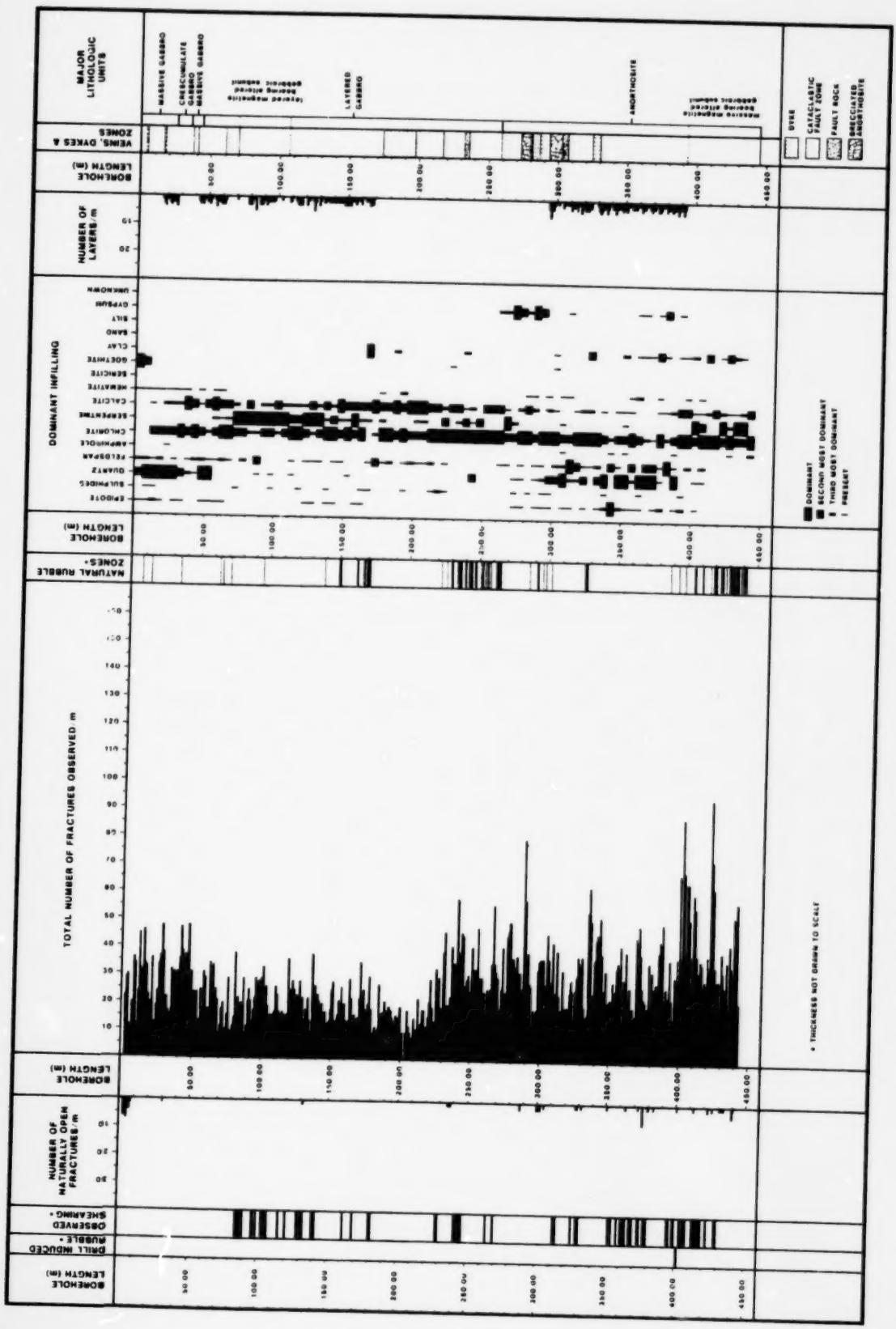

Figure 8. Summary lithologic and structural log of borehole EBL-3 (after Ejeckam *et al.*, 1984).

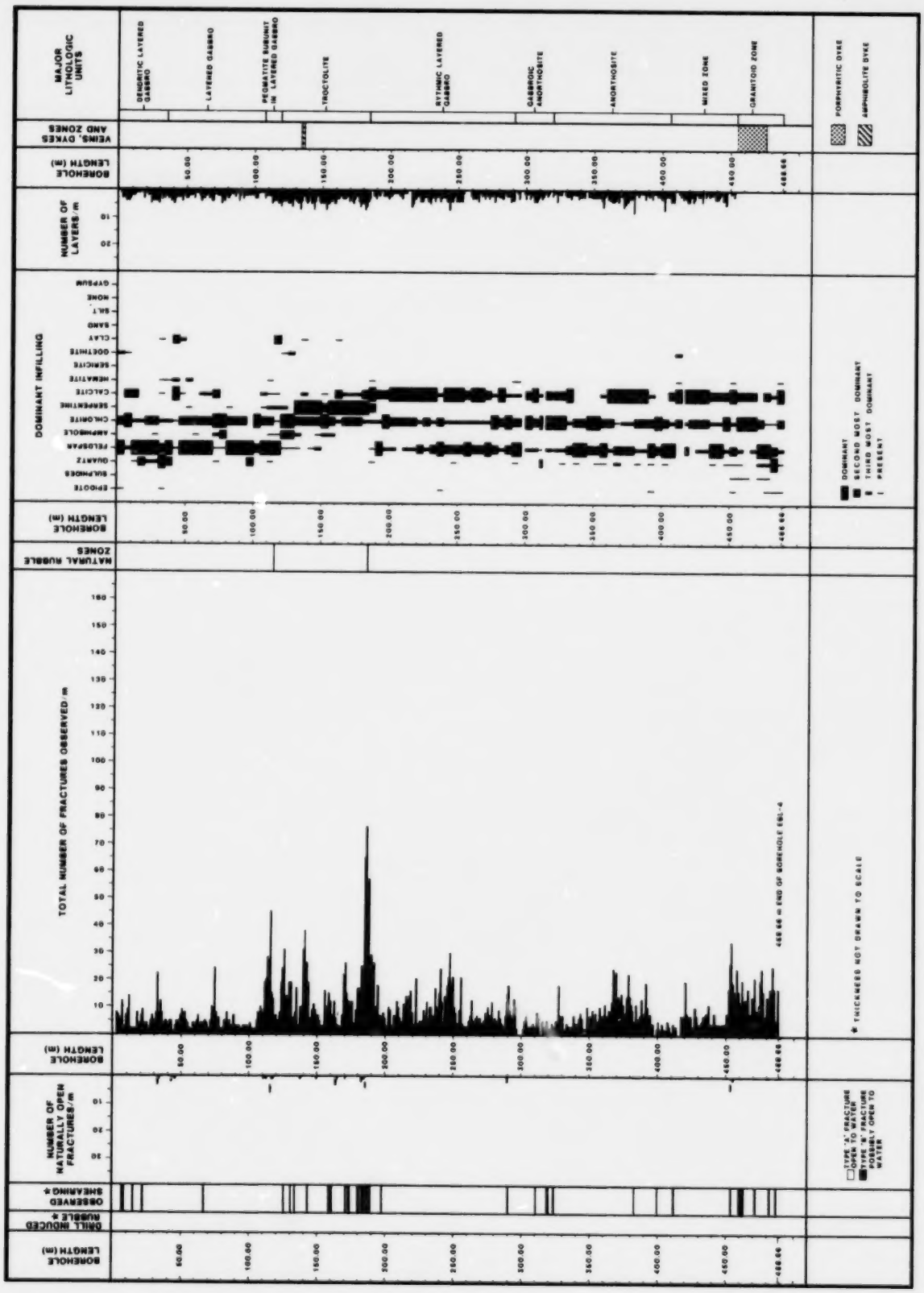

Figure 9. Summary lithologic and structural log of borehole EBL-4 (after Ejeckam *et al.*, 1984).

Borehole EBL-1 was drilled in an area without surface expression of major faults and fracture zones. The borehole was located to confirm interpretation of gravity data that suggested the area under borehole EBL-1 was the thickest part of the pluton. Based on core logs and acoustic televiewer surveys, borehole EBL-1 encountered several open fracture zones at depths of about 65, 87, 210, 410, 440, 475, 490, 510, 620 and 640 m. Basement granitic rock was encountered at 770-m depth. The most significant hydrogeological feature intersected by borehole EBL-1 is fracturing associated with the base of a magnetite-rich and spotty nonmagnetic layer of serpentinized troctolite at 210-m depth. Long sections of borehole EBL-1 also intersect amphibolite and diabase dykes and sills.

Boreholes EBL-2 and EBL-3 were drilled to investigate the geology and hydrogeology of major air-photo lineaments and faults. Borehole EBL-2 intersected both the 130 and 050 lineaments at possible depths of 110-126 m and 355 m and basement granitic rocks at approximately 814-m depth. Based on core logging and acoustic televiewer surveys of borehole EBL-2, fracture zones were intersected at depths of 35, 60, 123, 216, 250, 355, 405 and 580 m. The troctolite horizon was intersected at depths from 51 to 122 m.

Borehole EBL-3 was drilled to intersect highly fractured and extremely altered rock associated with the Folson Lake Fault. The major zone of faulting was intersected at depths of 197 to 220 m, with minor related shearing and fractures intersected throughout the borehole length. Acoustic televiewer surveys and core logs show open fractures at depths of 10, 237, 300, 374 and 400 m. Poor rock quality encountered by borehole EBL-3 resulted in termination of drilling at 442 m.

Borehole EBL-4 was drilled to investigate the geology and hydrogeology of a relatively unfractured area identified by air-photo lineament analysis. The borehole was oriented approximately normal to the strike of layering in the gabbro-anorthosite. The troctolite marker horizon was intersected from depths of 119 to 184 m. Extensive fracturing was evident at the base of the troctolite horizon similar to conditions observed in borehole EBL-1. In addition to this zone, open fractures were observed at depths of 50, 60, 115 and 454 m. A basal granitic contact may have been intersected at approximately 476-m depth.

Hydraulic Conductivity Testing

Hydraulic conductivity was measured in both P-series and EBL-series boreholes under open-borehole conditions and with single-packers and straddle-packer assemblies. This section summarizes the methods, results and interpretation of all borehole tests performed at East Bull Lake to measure the hydraulic conductivity of the gabbro-anorthosite pluton. The methodology, results and interpretation of the hydraulic tests are reported separately for the P-series and EBL-series boreholes.

P-SERIES BOREHOLES

During 1983, open-borehole pump tests were performed in all P-series boreholes. The results of these tests, expressed as transmissivity and storativity, are summarized by Raven *et al.* (1984). In 1984, a program of single-packer and straddle-packer testing was performed to determine the distribution of transmissivity and hydraulic conductivity within the P-series boreholes. This program also identified high-permeability fracture zones for subsequent ground-water sampling (see Chapter 7).

Methodology

Open-Borehole Pump Tests

The methodology used in pump testing the open P-series boreholes is described by Raven *et al.* (1984).

Packer Tests

Detailed borehole testing was performed in the P-series boreholes during 1984 using single-packers and straddle-packer assemblies. The borehole tests were configured as bail-recovery tests (Hvorslev, 1951). During a bail-recovery test, the transient recovery or response of a test interval to an instantaneous withdrawal or bail of water is monitored to determine medium transmissivity and storativity.

Bail-recovery tests using straddle-packers were systematically performed over 4.0-m length intervals in each P-series borehole from the water table to the bottom of the borehole. Similar tests using single-packers were performed only when significant fluid leakage occurred around the straddle packers as a result of highly fractured rock or an irregular borehole wall. In the P-series boreholes 128 bail-recovery tests were successfully completed.

During each straddle-packer test, the borehole probe (Fig. 10) was lowered to the interval of interest using a hand-powered wire-line winch and a tripod. The straddle-packer probe consisted of two steel-reinforced rubber packers, 1.0 m long, and a perforated separation pipe of variable length. The straddle-packer probe was coupled to a plastic standpipe that accessed the test interval through the central mandrel-pipe of the upper packer. The standpipe consisted of 3.05-m lengths of flushed-threaded and O-ring sealed PVC pipe. The pipe measured 52.5 mm inside diameter and 60.3 mm outside diameter.

Packers were inflated with compressed nitrogen to approximately 1000 kPa above ambient fluid pressures. Packer pressures were monitored with a Bourdon gauge.

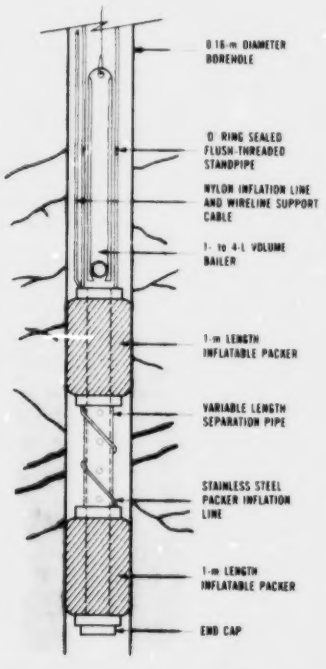
0.16-m DIAMETER BOREHOLE
O RING SEALED FLUSH-THREADED STANDPIPE
NYLON INFLATION LINE AND WIRELINE SUPPORT CABLE
1- to 4-L VOLUME BAILER
1-m LENGTH INFLATABLE PACKER
VARIABLE LENGTH SEPARATION PIPE
STAINLESS STEEL PACKER INFLATION LINE
1-m LENGTH INFLATABLE PACKER
END CAP

Figure 10. Schematic of straddle-packer probe used to complete bail-recovery tests in the P-series boreholes.

Fluid levels were monitored after packer inflation and before removal of a known volume of water to determine an equilibrium fluid level for the test interval. Equilibrium or static fluid levels were usually measured within periods of several hours to tens of hours for test intervals with hydraulic conductivity greater than about 10^{-8} $m \cdot s^{-1}$. Longer periods of time, in the range of several days to weeks, would be required to obtain equilibrium fluid level measurements in test intervals with hydraulic conductivity less than 10^{-8} to 10^{-9} $m \cdot s^{-1}$. For practical testing purposes, the equilibrium fluid levels in these test intervals are assumed to equal the fluid level in the open borehole. This assumption is not overly restrictive, as the average duration of the tests (i.e. several hours) is small compared with the average duration of open borehole conditions prior to testing (i.e. several months).

During each bail-recovery test 3 to 4 L of water was removed from the standpipe and recovery of the fluid level was monitored within the standpipe. The removal of 3 to 4 L of water created an instantaneous drawdown of about 1.5 m. Repeated bailing was often performed in low-permeability test intervals to create larger drawdowns and improve the lower testing limit of the bail-recovery test. With fixed (1) fluid level sensitivity (determined from water-level measurement equipment) and (2) flow rate measurement limits (determined from the diameter of the standpipe and the test duration), the lower testing limit of the bail-recovery test could only be improved by increasing the amount of drawdown in the test interval. Fluid levels were monitored within and outside of the standpipe using an electric-contact water level tape accurate to ±5 mm. Fluid levels were monitored outside the standpipe to detect fluid leakage around the upper packer seal. Several tests showed leakage and these tests were noted (Appendix A) and not analyzed. Prior to testing in each borehole, the straddle-packer probe was pressure-tested for leaks at surface in an artificial borehole made from plastic pipe.

Each successful straddle-packer test was analyzed using the type curve method of Cooper *et al.* (1967) to determine a transmissivity (T) from:

$$T = \frac{\tau r_s^2}{t} \qquad (1)$$

where τ and t are measured match points and r_s is the radius of the standpipe in which the fluid levels are measured. The calculated transmissivity is related to an equivalent rock mass hydraulic conductivity (K_{erm}) by the test interval length (L):

$$K_{erm} = T/L \qquad (2)$$

Tests on low-hydraulic conductivity intervals (<10^{-9} $m \cdot s^{-1}$) often showed negligible fluid level recovery over observation periods of tens of hours. For these test intervals flow rate per unit withdrawal head values ($Q/\Delta H$) were approximated from flow rates determined from two successive fluid level measurements or the fluid level sensitivity limit (10 mm) observed over a specified time and from hydraulic withdrawal heads based on the difference between the average observed fluid level during the test and open borehole fluid levels. The approximated $Q/\Delta H$ values were expressed as transmissivity using a steady-state formula (Hvorslev, 1951)

$$T = \frac{Q}{\Delta H\, 2\pi} \ell n\ (r_b/r_w) \qquad (3)$$

where r_b is the radius of a circular constant-pressure boundary (assumed equal to 10 m) and r_w is the radius of the borehole.

The straddle-packer tests completed in the P-series boreholes were capable of measuring transmissivity in the range of 5×10^{-10} to 5×10^{-5} $m^2 \cdot s^{-1}$. For the 4.0-m length test intervals used at East Bull Lake, this is equivalent to rock mass hydraulic conductivity range of about 1×10^{-10} to 1×10^{-5} $m \cdot s^{-1}$.

Results and Interpretation

The results of open-borehole pump tests completed in the P-series boreholes are given by Raven *et al.* (1984) and are reproduced here as Table 3. It lists the open-borehole measures of transmissivity and storativity.

Table 3. Open-Borehole Hydraulic Properties of the P-Series Boreholes

Borehole	Transmissivity ($m^2 \cdot s^{-1}$)	Storativity
P-1	2×10^{-6}	10^{-7}
P-2	8×10^{-7}	10^{-7}
P-3	2×10^{-6}	10^{-7}
P-4	6×10^{-7}	10^{-6}
P-5	4×10^{-6}	10^{-6}
P-6	1×10^{-7}	10^{-7}
P-7	4×10^{-9}	10^{-6}
P-8	2×10^{-6}	10^{-6}
P-9	2×10^{-6}	10^{-7}
P-10	5×10^{-6}	10^{-7}
P-11	2×10^{-7}	10^{-7}
P-12	2×10^{-7}	10^{-7}
P-13	6×10^{-8}	10^{-7}
P-14	7×10^{-8}	10^{-3}

The results of the 128 successful packer tests are tabulated in Appendix A. Appendix A lists the depth, equilibrium hydraulic head, transmissivity and equivalent rock mass hydraulic conductivity of each test.

Permeable fracture zones in each borehole can be identified from comparison of the results of the 1983 pump tests, the 1984 packer tests, and borehole acoustic televiewer logs. These permeable fracture zones can also be related to major lineaments and geological structures using simple subsurface to surface projections.

Using such projections, the hydraulic tests and televiewer logs indicate that the 130 lineament has transmissivity of 6×10^{-7} $m^2 \cdot s^{-1}$ (P-1, 35.3- to 42.0-m depth), 1×10^{-6} $m^2 \cdot s^{-1}$ (P-3, 17.0- to 31.8-m depth) and 3×10^{-7} $m^2 \cdot s^{-1}$ (P-4, 42.0- to 54.0-m depth). The 050 lineament has transmissivity of 8×10^{-7} $m^2 \cdot s^{-1}$ (P-2, 25.0- to 34.6-m depth), 2×10^{-7} $m^2 \cdot s^{-1}$ (P-5, 88.5- to 97.6-m depth), 2×10^{-7} $m^2 \cdot s^{-1}$ (P-6, 41.0- to 49.5-m depth), 1×10^{-6} $m^2 \cdot s^{-1}$ (P-8, 34.4- to 38.5-m depth), and 9×10^{-8} $m^2 \cdot s^{-1}$ (P-14, 23.9- to 28.8-m depth).

In addition to these high-permeability zones, most P-series boreholes showed high transmissivity in the near surface (0 to 16-m depth). Other significant high-transmissivity zones below 16-m depth are intersected by borehole P-4 at depths of 26.8-33.3 m and 37.0-40.0 m; borehole P-5 at depths of 45.0-61.0 m; borehole P-6 at depths of 21.0-25.0 m and 57.0-61.0 m; borehole P-8 at depths of 18.2-18.8 m; borehole P-9 at depths of 33.0-37.0 m, and borehole P-10 at depths of 35.6-35.7 m, 65.0-69.0 m and 89.0-97.0 m. Boreholes P-12 and P-13 intersect splays of the Folson Lake Fault and show variable transmissivities in the range 10^{-8} to 10^{-6} $m^2 \cdot s^{-1}$.

The average transmissivities of the 130 and 050 lineaments are equivalent to average rock mass hydraulic conductivities (K_{erm}) of 6×10^{-8} $m \cdot s^{-1}$ and 1×10^{-7} $m \cdot s^{-1}$, respectively. These hydraulic conductivities are approximately one to one and one-half order of magnitude larger than the average hydraulic conductivity of the East Bull Lake rock mass measured by all straddle-packer bail-recovery tests. The 050 and 130 lineaments therefore represent high-permeability pathways for ground-water flow in the upper 100 m of the East Bull Lake study area.

The distribution of equivalent rock mass hydraulic conductivity measured during testing of the P-series boreholes is shown as a histogram in Figure 11 and as a cumulative probability plot in Figure 12. In both figures the hydraulic conductivity data are plotted as the common logarithm of K_{erm} measured in metres per second. The geometric mean of the distribution is 1×10^{-8} $m \cdot s^{-1}$. The common logarithm of the standard deviation ($\log \sigma$) of the distribution is 0.97. The approximate linear relationship shown on the cumulative probability plot indicates that the hydraulic conductivity data approximate a two-parameter lognormal distribution (Aitchison and Brown, 1957).

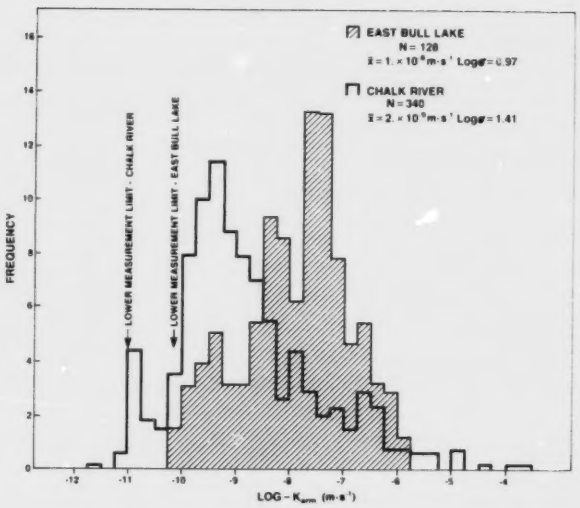

Figure 11. Histogram of the distribution of the common logarithm of equivalent rock mass hydraulic conductivity, K_{erm}, determined from packer tests completed from 0 to 75-m depth at the East Bull Lake and Chalk River research areas.

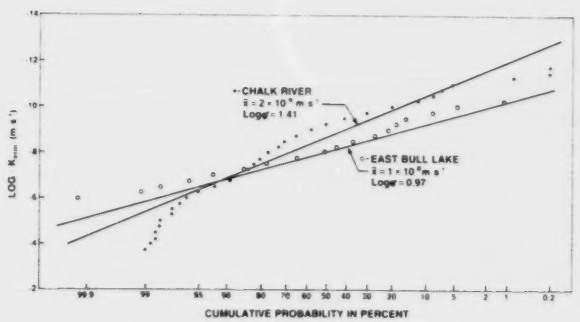

Figure 12. Cumulative probability plot of the common logarithm of equivalent rock mass hydraulic conductivity, K_{erm}, determined from packer tests completed from 0 to 75-m depth at the East Bull Lake and Chalk River research areas.

Figures 11 and 12 also show the distribution of equivalent rock mass hydraulic conductivity measured at the Chalk River Nuclear Laboratories in the FS-series boreholes (Raven, 1986). The Chalk River data shown in Figures 11 and 12 were determined from 340 straddle-packer injection tests (2-m length test interval) completed in the upper 75 m of quartz monzonitic gneiss. Comparison of the two distributions is informative because both data sets are derived from straddle-packer tests completed over a similar depth range (0-75 m) in primarily air-percussion drilled boreholes. Injection tests performed at Chalk River have a measurement range that is one order of magnitude

smaller (i.e. 10^{-11} $m \cdot s^{-1}$) and larger (i.e. 10^{-4} $m \cdot s^{-1}$) than that for the hydraulic tests completed at East Bull Lake. These measurement limits truncate the hydraulic conductivity distribution for East Bull Lake at a lower value of 10^{-10} $m \cdot s^{-1}$; the upper limit on the distribution was not truncated, as no tests were observed with hydraulic conductivity greater than 10^{-6} $m \cdot s^{-1}$.

The two distributions are different, with larger geometric mean and modal value for the East Bull Lake data than for the Chalk River data. The East Bull Lake data also show a smaller standard deviation and better fit to a two-parameter log-normal distribution. The Chalk River data are skewed to larger hydraulic conductivities; these larger hydraulic conductivities are absent from the East Bull Lake distribution.

The larger geometric mean and modal value for the East Bull Lake data reflects the large number of structural lineaments intersected by the P-series boreholes. The Chalk River FS-series boreholes were drilled in an area without major structural lineaments and, consequently, have lower geometric mean and modal hydraulic conductivity than the East Bull Lake data. Hydraulic conductivity data from P-series boreholes that do not intersect major structural lineaments (i.e. P-7, 9, 10, 11 and 14) show lower geometric mean (i.e. 2×10^{-9} $m \cdot s^{-1}$) and modal value than the complete P-series data set and are more consistent with the Chalk River data set.

The absence of hydraulic conductivity larger than 10^{-6} $m \cdot s^{-1}$ from the East Bull Lake tests is significant, as these intervals at Chalk River were important high-permeability fracture zones that controlled the development of ground-water flow systems in the upper 50 m of bedrock (Raven, 1986). The absence of very high-permeability test intervals at East Bull Lake likely reflects a number of important geological differences between the East Bull Lake and Chalk River sites. These differences include lithology, tectonic history, fracture characteristics, state of stress, and fracture infilling mineralogy.

EBL-SERIES BOREHOLES

During 1983, single-packer and straddle-packer tests and open-borehole pump tests were performed in boreholes EBL-1 and EBL-2. The methodology and results of these tests are briefly presented by Raven *et al.* (1984).

In 1984, a follow-up program of hydraulic head monitoring, hydraulic conductivity testing, and ground-water sampling was completed in boreholes EBL-1, 2 and 4. These investigations were performed utilizing a series of semi-permanent packers (Lynes production-injection packers [PIPs]) that were installed during October and November 1983. Single-packer and straddle-packer tests and open-borehole pump tests were also performed in 1984 in boreholes EBL-1, 2 and 4 following removal of the PIPs.

Hydrogeological characterization continued in 1985, using multiple-packer casings that were permanently installed (see Chapter 5) in boreholes EBL-1, 2, 3 and 4 during October and November 1984. Hydraulic property testing was carried out in selected casing intervals in boreholes EBL-1, 2, 3 and 4 in conjunction with hydraulic head monitoring and ground-water sampling that were completed as part of the 1985 characterization program.

The following section summarizes the methodology, results and interpretation of the 1983, 1984 and 1985 hydraulic test programs completed in the EBL-series boreholes.

Methodology

1983 Tests

During 1983, hydraulic conductivity was determined from the results of single-packer tests, straddle-packer tests and open-borehole pump tests. Single-packer and straddle-packer injection and pressure-pulse tests were performed in borehole EBL-1. Single-packer bail-recovery tests were performed in borehole EBL-2. Open-borehole pump tests were performed in boreholes EBL-1 and EBL-2.

EBL-1 Packer Tests

Injection tests and pressure-pulse tests were completed in borehole EBL-1, using a packer probe that was raised and lowered in the borehole using an umbilical cable and an electrically driven cable reel mounted on a large flat-bed trailer (Fig. 13). Details of the umbilical cable and the packer probe configured as a set of straddle packers are shown in Figure 14.

The umbilical cable consisted of two seven-conductor, double armoured, electrical and strain cables; three 9.5-mm nylon tubes; three 9.5-mm nylon filler tubes; and a single 15.9-mm nylon tube. All tubes were low-pressure rated with a burst pressure of about 7.0 MPa. A polyurethane jacket, 1.6 mm thick, was extruded over the cables and tubes to form a 40-mm diameter composite umbilical cable. The cable reel holds 800 m of this composite cable.

The packer probe incorporated a 4- to 20-mA pressure transmitter and hydraulically activated valve and piston.

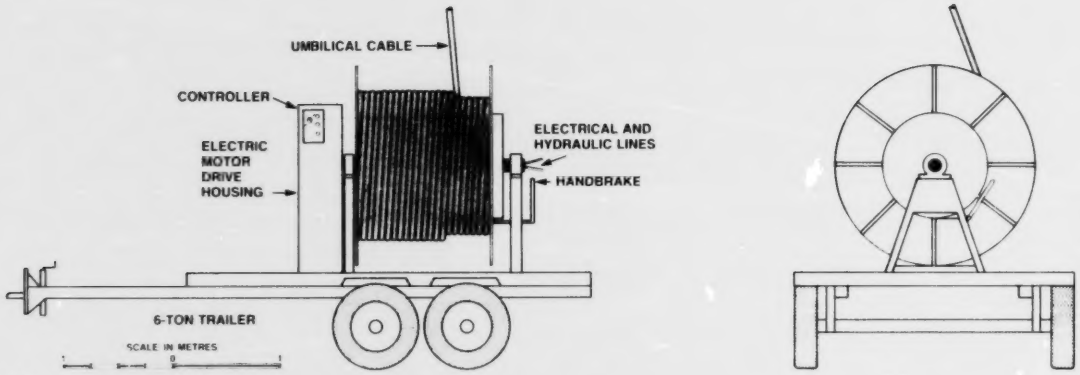

Figure 13. Umbilical cable and electrically driven cable reel used during packer testing of borehole EBL-1 in 1983.

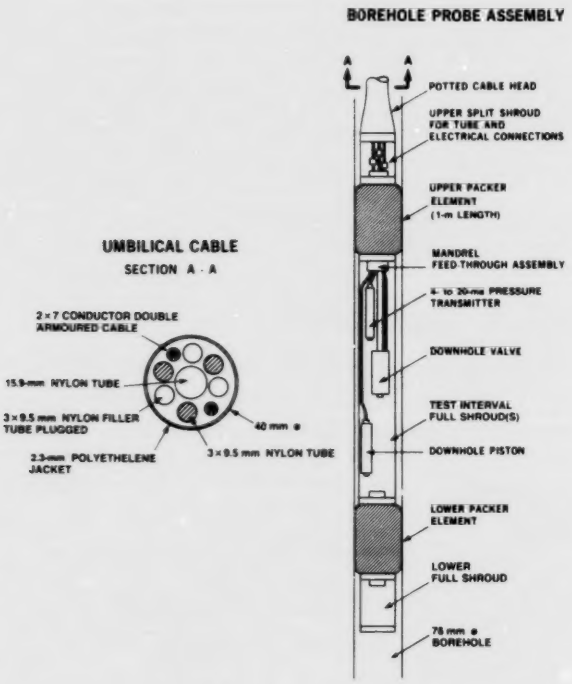
BOREHOLE PROBE ASSEMBLY
POTTED CABLE HEAD
UPPER SPLIT SHROUD FOR TUBE AND ELECTRICAL CONNECTIONS
UPPER PACKER ELEMENT (1-m LENGTH)
MANDREL FEED-THROUGH ASSEMBLY
4- to 20-mA PRESSURE TRANSMITTER
DOWNHOLE VALVE
TEST INTERVAL FULL SHROUD(S)
DOWNHOLE PISTON
LOWER PACKER ELEMENT
LOWER FULL SHROUD
76 mm ø BOREHOLE
UMBILICAL CABLE
SECTION A - A
2 × 7 CONDUCTOR DOUBLE ARMOURED CABLE
15.9-mm NYLON TUBE
3 × 9.5 mm NYLON FILLER TUBE PLUGGED
2.3-mm POLYETHELENE JACKET
40 mm ø
3 × 9.5 mm NYLON TUBE

Figure 14. Schematic of straddle-packer probe and umbilical cable used during packer testing of borehole EBL-1 in 1983.

The current-loop pressure transmitter was preferred over more conventional DC-DC pressure transducers because of reduced line losses associated with signal transmission along the 800-m length electrical cable and therefore greater signal reliability.

The downhole valve was used to isolate the test interval hydraulically from the 800 m of fluid-filled tubing in the borehole and at surface on the cable reel. Isolation of the test interval increased the reliability of the shut in or equilibrium hydraulic head measurement by removing the thermally induced flow and pressure transients frequently observed within the umbilical cable on surface. Isolation of the umbilical tubing from the test interval also allowed for the performance of pressure-pulse tests in test intervals of low permeability. Details of the downhole valve are illustrated in Figure 15. An adjustable spring-assisted reset is incorporated into the valve to permit the valve to open against higher hydraulic head within the umbilical cable above the test interval. These higher hydraulic heads frequently result from decreasing hydraulic head of the test intervals with depth and the additional head imposed by slinging the umbilical cable over a sheave and tripod assembly at surface. The water-filled activation line and spring-assisted reset were used because of the low pressure rating of the tubing.

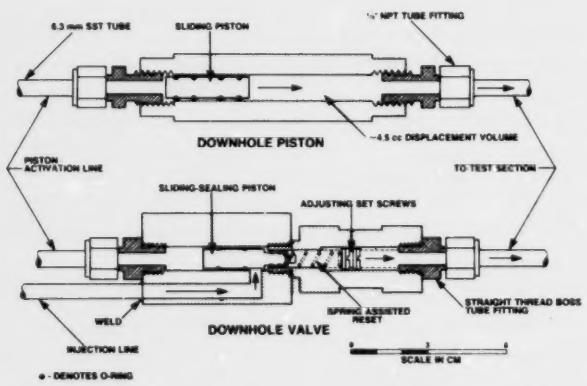

Figure 15. Details of the downhole piston and downhole valve incorporated in the straddle-packer probe used to hydraulically test borehole EBL-1 in 1983.

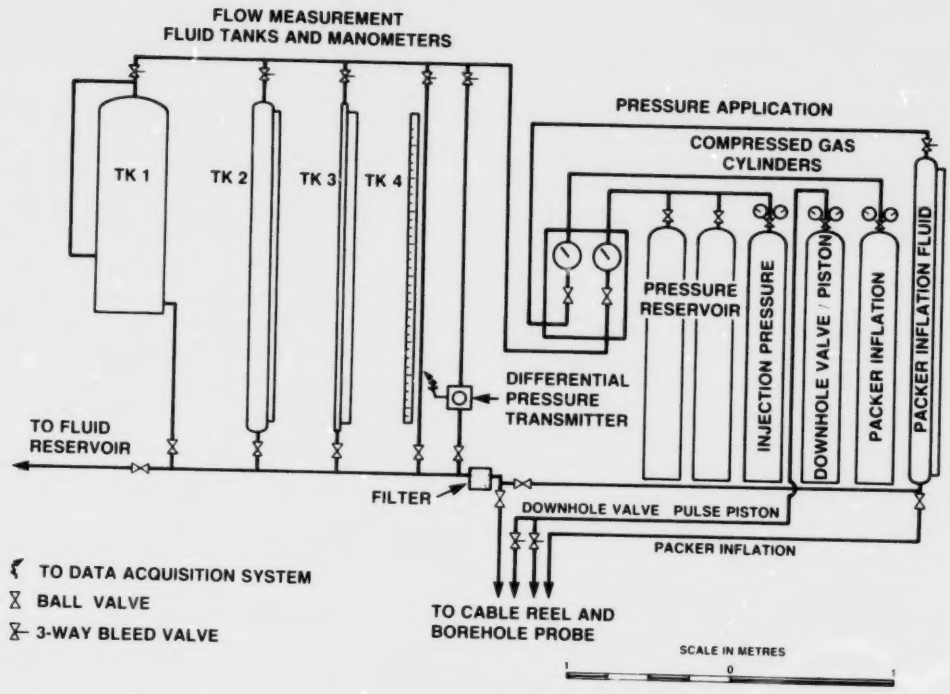

Figure 16. Schematic of flow measurement and pressure application equipment used during packer testing of borehole EBL-1 in 1983.

The downhole piston was used to perform pressure-pulse tests to measure the hydraulic conductivity of the test intervals. Isolation of the test interval from the uncertain and variable compressibility of the tubing and fluid in the umbilical cable significantly reduced the volume-compressibility product of the test interval and increased resolution of the test data and reliability of the test results. The known displacement volume of the piston (≈4.5 mL) together with the observed pressure pulse, provided a calibration value of the volume-compressibility product of the test interval required for analysis of the test data (Raven *et al.*, 1984). The downhole piston was pneumatically or hydraulically activated from the surface; it is illustrated in Figure 15.

During steady-state injection tests, flow rates were measured at surface using a series of constant-head flow tanks of variable diameter and a differential pressure transmitter to indicate fluid level within the tanks. Pressure application for fluid injection, packer inflation and activation of the downhole piston and valve was achieved with compressed nitrogen or air. The flow measurement and pressure application equipment are schematically illustrated in Figure 16. Packers were inflated with water.

Data acquisition, reduction and analysis of hydraulic tests completed in borehole EBL-1 were carried out using an Apple IIE microcomputer with hard copy printer and floppy diskette storage. Strip charts and other analog

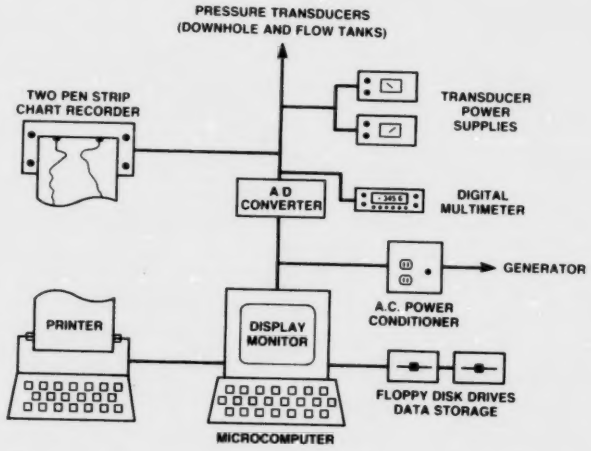

Figure 17. Schematic of data acquisition system used during packer testing of borehole EBL-1 in 1983.

sensing devices were also incorporated into the data acquisition system. The data acquisition system is shown in Figure 17.

Steady-state flow rates (Q) and injection heads (ΔH) were recorded during each injection test. A series of single-packer injection tests were incrementally performed every 50 m from surface to 650-m depth in borehole EBL-1. Straddle-packer tests were performed in the upper 150 m of borehole EBL-1. The flow rate per unit injection head data ($Q/\Delta H$) are related to equivalent rock-mass hydraulic conductivity (K_{erm}) using Equations 2 and 3:

$$K_{erm} = \frac{Q}{\Delta H 2\pi L} \ln (r_b/r_w) \qquad (4)$$

where r_b, r_w and L are as defined previously for Equations 2 and 3.

EBL-2 Packer Tests

Packer testing of borehole EBL-2 was carried out using a work-over rig, AQ standpipe rods and a single-packer assembly. An approximate schematic of this test equipment is shown in Figure 18. Figure 18 shows a PIP, or production-injection packer, attached to the bottom of the AQ rods. During 1983 tests, this PIP was replaced with a single-packer that was hydraulically inflated from surface using a hydraulic hose taped to the outside of the AQ rods. Only limited testing was conducted in borehole EBL-2. Bail-recovery tests were successively completed approximately every 50 m from surface to 250-m depth and at 440-m depth. Drawdowns were created using a swabbing tool attached to a wire-line hoist. The test data were analyzed to determine transmissivity (T) using the method of Cooper *et al.* (1967) and then to determine $Q/\Delta H$ using Equation 3.

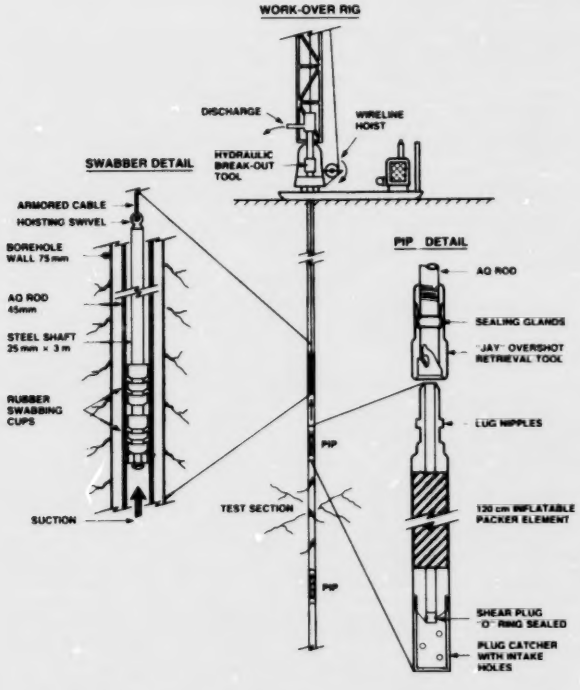

Figure 18. Schematic of equipment used for hydraulic testing with a work-over rig showing details of swabber and production-injection packer (PIP).

Open-Borehole Pump Tests

Open-borehole pump tests were carried out in boreholes EBL-1 and EBL-2. Both boreholes were pumped using a submersible electric pump at approximately 10 $L \cdot min^{-1}$ for 500 min. Drawdown was measured with an electric-contact, water-level tape. The drawdown versus time data were plotted on diagnostic log-log plots.

1984 Tests

Hydraulic conductivity tests were performed in 1984 using PIPs, single-packers, straddle-packer assemblies and open boreholes.

PIP Tests

Production-injection packers were installed in boreholes EBL-1, 2 and 4 during October and November 1983. These packers were installed at depths of 147, 298, 512 and 650 m in borehole EBL-1; 75, 250, 460 and 616 m in borehole EBL-2; and 120, 198 and 396 m in borehole EBL-4. Test intervals created by these PIPs were subject to extensive testing, pumping and monitoring during 1984 in an effort to obtain representative hydraulic data and ground-water samples. Fluid was removed from each PIP-isolated test interval using a combination of air-lift pumping, swabbing and "squeeze" pumping. A schematic of the equipment used during the PIP testing showing details of the PIPs, and the wire-line swabber is given in Figure 18.

The flow rate per unit injection head ($Q/\Delta H$) properties of each PIP-isolated test interval were determined from a variety of tests including slug-recovery tests, bail-recovery tests, pseudo steady-state swabbing and air-lift pumping tests and injection tests. Slug-recovery tests were routinely performed as soon as the shear plug (Fig. 18) was blown from the PIP defining the upper limit of the test interval. Recovery of the fluid level from the top of the AQ rods to an equilibrium value was monitored and analyzed using the methods described previously for bail-recovery tests. Bail-recovery tests were performed in response to

wire-line swabbing. Pseudo steady-state swabbing and air-lift pumping tests were performed in high-permeability test intervals (i.e. EBL 1-4, 4-1, 4-2 and 4-3) where short recovery times prohibited slug or bail-recovery testing. For these test intervals an average flow rate and withdrawal head were estimated from swabbing volume and drawdown measurements recorded over periods of several days. Injection tests were used to measure the $Q/\Delta H$ properties of low-permeability test intervals (i.e. EBL 2-1) by pressurizing the AQ standpipe rods and monitoring changes in fluid level within the rods.

A long-term pump test was performed on May 2-14, 1984, to assess the hydraulic properties and interconnection of the fracture zone at the base of the troctolite horizon. The base of the troctolite horizon intersects boreholes EBL-1, 2 and 4 at depths of 210, 122 and 185 m, respectively. PIP-isolated interval EBL 1-4 (147-298 m) was pumped for 13 days at an average withdrawal rate of 10 $L \cdot min^{-1}$. Intervals EBL 2-4 (75-250 m), 2-5 (0.75 m), 4-3 (120-128 m) and 4-4 (0-120 m) were monitored throughout the pumping period, and until May 15, 1984.

Packer Tests

Several single-packer and straddle-packer tests were conducted in the EBL-series boreholes following the removal of PIPs. Single-packer bail-recovery tests were completed in conjunction with swabbing for geochemical sampling in borehole EBL-4 from depths of 450 to 489 m. A straddle-packer bail-recovery test was also performed to evaluate the hydraulic conductivity of the fracture zone at 405-m depth in borehole EBL-1.

The troctolite horizon at 210 m in borehole EBL-1 was also intermittently pump-tested on July 4-11, 1984, using a single-packer and a submersible electric pump located at 100-m depth. The single-packer isolated the permeable upper 100 m of borehole EBL-1 from the pumping performed over the interval 100-650 m. Because injection tests showed that the base of the troctolite was the most permeable horizon in the pumped interval, we can assume that the observed response reflects the hydraulic properties of the base of the troctolite unit. The single-packer pump test was also performed to substantiate the results of swabbing completed on the PIP-isolated interval EBL 1-4.

Open-Borehole Pump Tests

Three open-borehole pump tests were performed in 1984. Borehole EBL-1 was pumped using a submersible electric pump at an average withdrawal rate of 16 $L \cdot min^{-1}$ from June 24 to July 3, 1984. Drawdown in the pumping well was monitored with a submersible pressure transmitter and the data acquisition system described in the Section on EBL-1 Packer Tests. The drawdown-time data were plotted on diagnostic log-log plots.

Borehole EBL-3 was pumped with a similar pump at 10 $L \cdot min^{-1}$ for 60 min. The observed drawdown-time data indicated persistence of wellbore storage throughout the pumping period. Therefore these data could not be analyzed to determine hydraulic properties of the rock mass. However, because the period of pumping was relatively short compared with the recovery period, the recovery data were analyzed using the method of Cooper *et al.* (1967) to determine borehole transmissivity.

A step-drawdown test of 500-min duration was performed in borehole EBL-4. Pumping rates of 10, 15 and 17.5 $L \cdot min^{-1}$ were used. Drawdowns were measured with an electric-contact, water-level tape. The drawdown response for the 10 $L \cdot min^{-1}$ pumping rate was plotted on a log-log plot. Pseudo steady-state flow rate per unit drawdown data ($Q/\Delta H$) were tabulated for each pumping rate to determine nonlinearity of the pressure-flow rate relation.

1985 Tests

Only limited hydraulic conductivity testing was performed in the EBL-series boreholes in 1985. Most of this testing was performed in conjunction with air-lift pumping from the inside of the multiple-packer casings for groundwater sampling. Intervals tested in 1985 were defined by the location of casing-packers (see Chapter 5). Six intervals in borehole EBL-1, three intervals in borehole EBL-2, and two intervals in borehole EBL-4 were hydraulically tested. Flow rate per unit head data for these intervals were determined from bail-recovery tests performed within the plastic casings and from pseudo steady-state, air-lift pumping.

Results and Interpretation

The results of single-packer and straddle-packer testing completed in boreholes EBL-1 and EBL-2 during 1983 are listed in Tables 4 and 5, respectively, and are plotted in Figure 19. The results of 1984 PIP testing in boreholes EBL-1, 2 and 4 are listed in Table 6 and are also plotted in Figure 19. The results of 1985 hydraulic tests completed within the multiple-packer casings are listed in Table 7. These test results and the results of open-borehole pump tests are discussed and interpreted separately for each borehole.

Borehole EBL-1

We can compare the results of 1983 packer tests and 1984 PIP tests completed over different test interval lengths

by looking at the fundamental flow rate and head data. The flow rate per unit head data (Q/ΔH) for borehole EBL-1 are plotted as the negative common logarithm (p) of Q/ΔH,

Table 4. Summary of 1983 Packer Test Results for Borehole EBL-1

Depth (m)	Q/ΔH ($m^2 \cdot s^{-1}$)	K_{erm} ($m \cdot s^{-1}$)
8.00-13.06	3×10^{-6}	5×10^{-7}
10.00-15.06	2×10^{-6}	3×10^{-7}
15.00-20.06	4×10^{-7}	5×10^{-8}
19.40-24.46	4×10^{-8}	5×10^{-9}
25.40-30.46	7×10^{-8}	1×10^{-8}
30.00-35.06	8×10^{-8}	1×10^{-8}
35.00-40.06	4×10^{-8}	5×10^{-9}
40.00-45.06	3×10^{-7}	5×10^{-8}
45.00-50.06	5×10^{-9}	7×10^{-10}
49.55-54.61	2×10^{-9}	3×10^{-10}
55.60-60.66	4×10^{-10}	5×10^{-11}
60.00-65.06	8×10^{-10}	1×10^{-10}
65.00-70.06	4×10^{-9}	7×10^{-10}
70.00-75.06	3×10^{-9}	5×10^{-9}
75.00-80.06	6×10^{-8}	9×10^{-9}
84.90-89.06	8×10^{-7}	1×10^{-7}
89.34-94.40	–	–
92.50-97.56	6×10^{-10}	1×10^{-10}
95.20-100.26	1×10^{-9}	1×10^{-10}
100.00-105.26	1×10^{-8}	2×10^{-9}
180.00-185.06	2×10^{-10}	4×10^{-11}
150.70-250.00	8×10^{-5}	7×10^{-7}
250.00-300.00	1×10^{-8}	2×10^{-10}
300.00-350.00	2×10^{-8}	3×10^{-10}
350.00-400.00	3×10^{-9}	5×10^{-11}
400.00-448.00	2×10^{-7}	4×10^{-9}
448.00-500.00	3×10^{-7}	3×10^{-9}
500.00-549.00	5×10^{-8}	7×10^{-10}
549.00-600.00	8×10^{-11}	1×10^{-12}
599.00-652.00	9×10^{-11}	1×10^{-12}
652.00-850.70	5×10^{-10}	2×10^{-12}

where Q/ΔH is in square metres per second. The results of both testing programs are similar except for testing of the troctolite horizon in the PIP-isolated interval between 147- and 298-m depth. The 1983 packer testing indicated a Q/ΔH of 8×10^{-5} $m^2 \cdot s^{-1}$ (interval 150- to 250-m depth), whereas the PIP testing yielded a Q/ΔH value of 1×10^{-6} $m^2 \cdot s^{-1}$ (interval 147- to 298-m depth). The different Q/ΔH values likely reflect the different testing techniques and duration of testing. The 1983 results were determined from short duration (i.e. 30-60 min) injection tests and therefore measure the near-borehole hydraulic properties. The PIP-test results were determined from much longer term (i.e. several weeks) swab and pump testing and likely measure the far-field hydraulic properties of the fractures.

Single-packer pump tests completed in 1984 on the interval 100- to 650-m depth and casing-interval withdrawal tests performed in 1985 at 204- to 213-m depth also provide additional reliable measures of the hydraulic conductivity of the base of the troctolite horizon. Both of these tests show a Q/ΔH value of 3×10^{-7} $m^2 \cdot s^{-1}$. For the 9-m test interval of 204- to 213-m depth, this indicates an

Table 5. Summary of 1983 Packer Test Results for Borehole EBL-2

Depth (m)	Q/ΔH ($m^2 \cdot s^{-1}$)	K_{erm} ($m \cdot s^{-1}$)
0.00-50.00	1×10^{-6}	2×10^{-8}
50.00-75.00	8×10^{-7}	2×10^{-8}
75.00-100.00	3×10^{-7}	9×10^{-9}
100.00-150.00	5×10^{-7}	8×10^{-9}
150.00-200.00	2×10^{-8}	3×10^{-10}
200.00-250.00	7×10^{-8}	1×10^{-9}
250.00-440.00	4×10^{-7}	2×10^{-9}
440.00-835.60	2×10^{-8}	5×10^{-11}

Table 6. Summary of 1984 PIP Test Results for EBL-Series Boreholes

Interval	Depth (m)	Static water level* (m)	Q/ΔH ($m^2 \cdot s^{-1}$)	K_{erm} ($m \cdot s^{-1}$)
EBL 1-5	0-147	3.9	2×10^{-6}	1×10^{-8}
EBL 1-4	147-298	6.0	1×10^{-6}	7×10^{-9}
EBL 1-3	298-512	11.0	2×10^{-7}	9×10^{-10}
EBL 1-2	512-650	17.0	5×10^{-8}	3×10^{-10}
EBL 1-1	650-851	---------- Not accessed ----------		
EBL 2-5	0-75	3.5	2×10^{-6}	2×10^{-8}
EBL 2-4	75-250	21.0	6×10^{-7}	3×10^{-9}
EBL 2-3	250-460	30.0	2×10^{-9}	8×10^{-12}
EBL 2-2	460-616	30.0?	1×10^{-9}	6×10^{-12}
EBL 2-1	616-836	30.0?	4×10^{-10}	2×10^{-12}
EBL 3	0-442	9.0	5×10^{-7}	1×10^{-9}
EBL 4-4	0-120	2.9	6×10^{-7}	4×10^{-9}
EBL 4-3	120-198	5.1	2×10^{-7}	2×10^{-9}
EBL 4-2	198-396	20.7	3×10^{-8}	1×10^{-10}
EBL 4-1	396-489	40.0	2×10^{-7}	2×10^{-9}

*Depth in metres below top of borehole casing.

Table 7. Summary of 1985 Hydraulic Tests Completed in EBL-Series Boreholes

Borehole	Casing interval*	Depth (m)	$Q/\Delta H$ ($m^2 \cdot s^{-1}$)	K_{erm} ($m \cdot s^{-1}$)
EBL-1	1	626-650	3×10^{-8}	1×10^{-9}
EBL-1	1-6	504-650	4×10^{-7}	2×10^{-9}
EBL-1	17	204-213	3×10^{-7}	3×10^{-8}
EBL-2	21	156-174	2×10^{-9}	9×10^{-11}
EBL-2	23	111-126	1×10^{-6}	7×10^{-8}
EBL-4	2,3	429-456	3×10^{-7}	1×10^{-8}
EBL-4	22	105-117	4×10^{-7}	3×10^{-8}

*See Table 9 in Chapter 5.

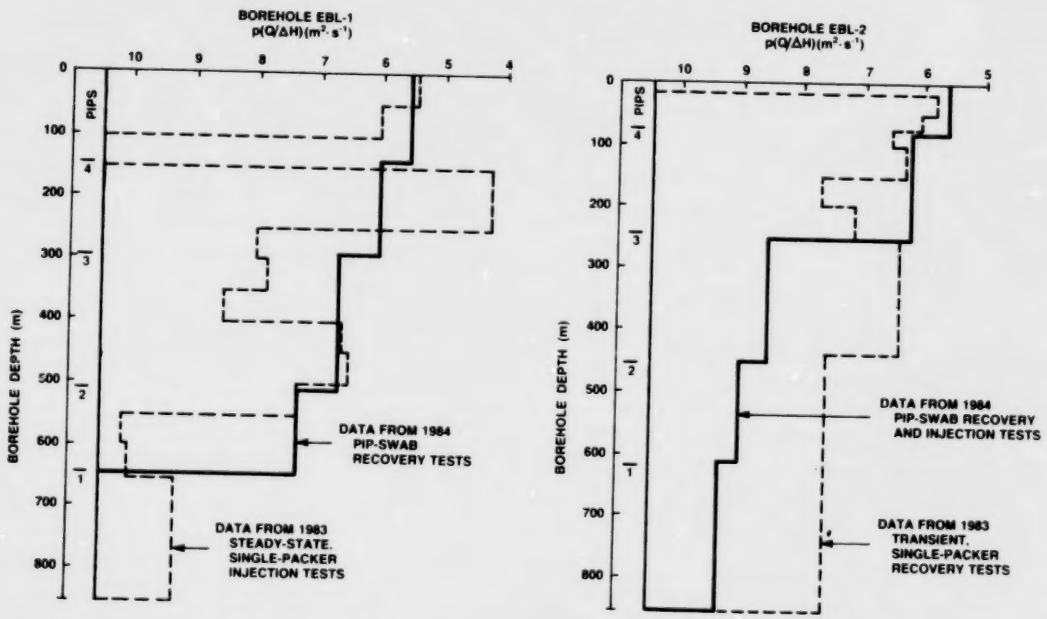

Figure 19. Flow rate per unit head ($Q/\Delta H$) profiles for boreholes EBL-1 and EBL-2 determined from 1983 packer tests and 1984 PIP tests. The test data are plotted as the negative common logarithm (p) of $Q/\Delta H$ expressed in square metres per second.

equivalent rock mass hydraulic conductivity of about 3×10^{-8} $m \cdot s^{-1}$. These hydraulic properties are thought to be the most representative of the troctolite rubble and fracture zone at 210-m depth in the vicinity of borehole EBL-1.

The interference test completed May 2-14, 1984, from the PIP test interval that isolated the troctolite horizon in borehole EBL-1 provides information on the interborehole hydraulic properties of the fractured base of the unit. The drawdown versus log-time data for PIP-isolated test intervals EBL 2-4 and 4-3 that intersect the base of the troctolite unit are shown in Figure 20. The observation intervals show a 0.20- to 0.30-m coincident lowering of fluid levels near the end of the pump test on May 14-16, 1984. Because the amount of observed drawdown was small, possibly reflecting barometric pressure changes, the change in local barometric pressure reported by Environment Canada is also plotted in Figure 20. The barometric pressure record shows that the observed drawdowns are an artifact of an increase in barometric pressure near the end of the pump test.

Because no drawdown was observed in the observation intervals, a maximum hydraulic diffusivity (κ) may be estimated from the observation period (t_o) and the interborehole distance (R) using:

$$\kappa = \frac{CR^2}{t_o} \qquad (5)$$

where C is a constant dependent on the approximations to

the line-source solution of the radial ground-water flow equation. The constant C has been estimated by Cooper and Jacob (1946) as 0.45 and by Johnson *et al.* (1966) as 0.25. Using C of 0.45, maximum hydraulic diffusivities of 7×10^{-2} and 1×10^{-1} $m^2 \cdot s^{-1}$ are calculated between borehole EBL-1 and boreholes EBL-2 and EBL-4, respectively. With a reasonable estimate of storativity of 1×10^{-6}, the maximum diffusivities are equivalent to maximum transmissivities of 7×10^{-8} and 1×10^{-7} $m^2 \cdot s^{-1}$, similar to the $Q/\Delta H$ value of 3×10^{-7} $m^2 \cdot s^{-1}$ determined from several single-borehole tests in borehole EBL-1.

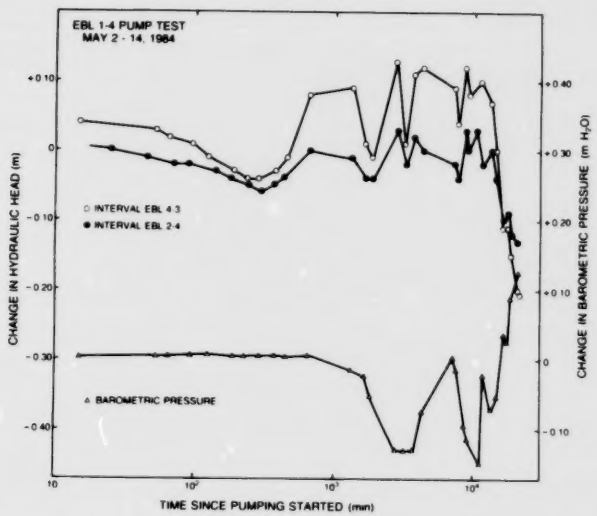
EBL 1-4 PUMP TEST
MAY 2 - 14, 1984
CHANGE IN HYDRAULIC HEAD (m)
CHANGE IN BAROMETRIC PRESSURE (m H2O)
INTERVAL EBL 4-3
INTERVAL EBL 2-4
BAROMETRIC PRESSURE
TIME SINCE PUMPING STARTED (min)

Figure 20. Change in hydraulic head in EBL observation intervals and change in barometric pressure versus log-time during EBL-1 pump test of troctolite fracture zone at 210-m depth.

In addition to the base of the troctolite horizon, hydraulic testing in conjunction with fracture logging identified high-permeability fracture zones at depths of 45, 87, 440, 475, 490 and 510 m. The fractures at depths of 405-410 m identified by fracture logging and thought to be open were hydraulically tested with straddle packers and shown to be tight with $Q/\Delta H$ of 5×10^{-11} $m^2 \cdot s^{-1}$ and K_{erm} of 7×10^{-12} $m \cdot s^{-1}$. Fractures at 510-m depth show $Q/\Delta H$ values in the range 5×10^{-8} $m^2 \cdot s^{-1}$ (1984 PIP tests) to 4×10^{-7} $m^2 \cdot s^{-1}$ (1985 casing tests). Because the casing tests are of relatively short duration compared with the PIP tests, the $Q/\Delta H$ value of 5×10^{-8} $m^2 \cdot s^{-1}$ is likely most representative of the far-field hydraulic properties of the fractures. Fractures at 45- and 87-m depth showed $Q/\Delta H$ values of 3×10^{-7} and 8×10^{-7} $m^2 \cdot s^{-1}$, respectively. Fractures at 440-m depth have a $Q/\Delta H$ value of 2×10^{-7} $m^2 \cdot s^{-1}$ based on 1983 packer tests. Fractures at 475- and 490-m depth are thought to be permeable with a combined $Q/\Delta H$ of 3×10^{-7} $m^2 \cdot s^{-1}$ based on 1983 packer tests and 1984 PIP tests. Resolution of the hydraulic properties of each fracture zone will require more detailed hydraulic testing.

The results of 1983, 1984 and 1985 hydraulic tests performed in borehole EBL-1 and expressed as equivalent rock mass hydraulic conductivity (K_{erm}) show a logarithmic decrease in depth. With 50- to 100-m test interval lengths, K_{erm} values decrease from 1×10^{-8} to 1×10^{-12} $m \cdot s^{-1}$ from surface to depth. Below 510-m depth the rock mass shows low hydraulic conductivity, generally less than 2×10^{-12} $m \cdot s^{-1}$.

The results of an open-borehole pump test of EBL-1 completed in the period June 24-July 3, 1984, are shown in Figure 21. The drawdown versus time data were analyzed using the single, horizontal, uniform flux fracture model of Gringarten and Ramey (1974). This model was used because the log-drawdown, log-time data show a one-half slope characteristic of linear flow and because the results of recent packer and PIP tests indicate that most (60%-70%) of the pumping flow rate is produced from a sub-horizontal fracture zone at approximately 87-m depth. The visually best-fit type curve to the drawdown-time data is also shown in Figure 21. With estimates of thickness (h) of the rock mass tested and rock mass storativity (S), the type curve matching yields measures of fracture radius (r_f) and the anisotropic rock mass hydraulic conductivities (K_z, K_r). Fracture radius of 45 m, vertical hydraulic conductivity of 7×10^{-8} $m \cdot s^{-1}$, and radial hydraulic conductivity of 1×10^{-8} $m \cdot s^{-1}$ were determined from the Gringarten model based on h of 50 m and S of 10^{-5}. The calculated radial hydraulic conductivities are the same as those measured during PIP testing in the interval 0 to 147-m depth. The slightly higher vertical hydraulic conductivities determined from the model may reflect high-conductivity vertical fractures in the near surface.

Borehole EBL-2

The results of 1983 packer tests and 1984 PIP tests are compared as $Q/\Delta H$ data in Figure 19. The $Q/\Delta H$ data are plotted as the negative common logarithm (p) of $Q/\Delta H$ measured in square metres per second. The results of the 1983 and 1984 tests are similar for the upper two PIP intervals from 0 to 250-m depth. Below 250-m depth the 1983 tests significantly overestimated the $Q/\Delta H$ properties of the rock mass. Because of uncertainty in estimation of static water levels during the 1983 tests and the short duration of the 1983 tests, the results of the 1984 PIP tests are thought to be more reliable than the 1983 test results.

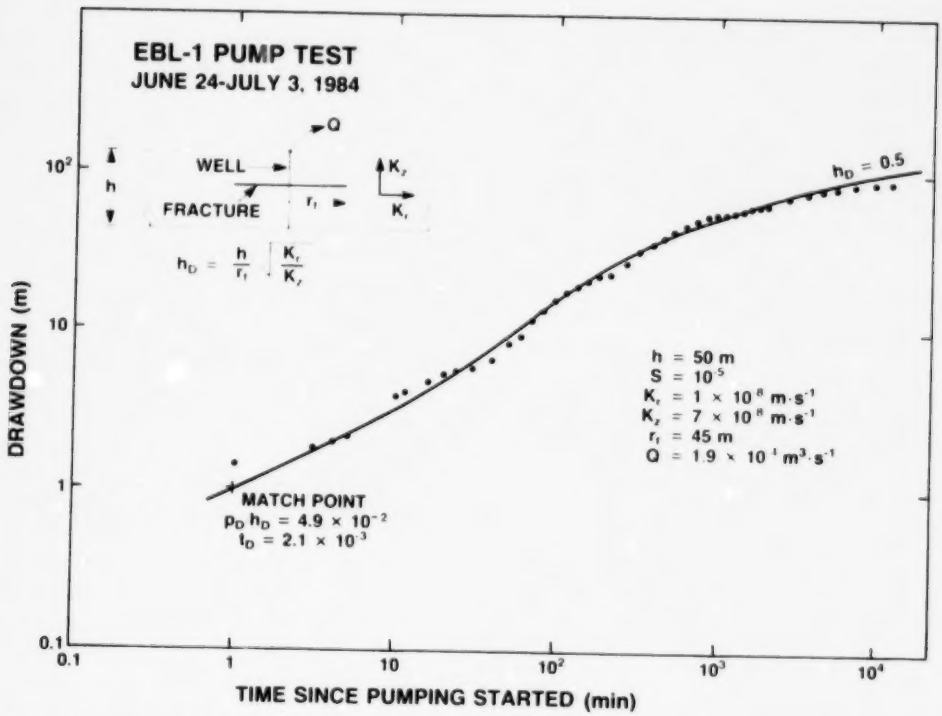

Figure 21. Log-drawdown versus log-time response of open-borehole pump test in EBL-1. Type-curve analysis of the data to determine fracture radius (r_f) and anisotropic hydraulic conductivities (K_r and K_z) of the rock mass are based on the single, horizontal, uniform-flux fracture model of Gringarten and Ramey (1974).

The results of the 1984 PIP tests show relatively high $Q/\Delta H$ in the upper 250 m of rock, with values of 2 × 10^{-6} $m^2 \cdot s^{-1}$ (0-75 m) and 6 × 10^{-7} $m^2 \cdot s^{-1}$ (75-250 m) and very low $Q/\Delta H$ (4 × 10^{-10} to 2 × 10^{-9} $m^2 \cdot s^{-1}$) below 250-m depth. Considering the interval lengths of 75-220 m, the $Q/\Delta H$ data expressed as equivalent rock mass hydraulic conductivity (K_{erm}) show a logarithmic decrease with depth from 2 × 10^{-8} $m \cdot s^{-1}$ to 2 × 10^{-12} $m \cdot s^{-1}$.

Borehole EBL-2 intersected several fracture zones, which on the basis of core logging and acoustic televiewer logging appeared to be open. The results of hydraulic testing, however, indicate that high-conductivity fractures intersect the borehole only in the upper 75 m and at 123- and 216-m depth. Below 250-m depth all fractures have low hydraulic conductivity.

Borehole EBL-2 intersects the 130 and 050 structural lineaments and the base of the troctolite horizon. The base of the troctolite horizon is intersected at 122-m depth. Hydrogeological interpretation of available data suggests that the 130 and 050 lineaments are likely intersected at about 123- and 355-m depth, respectively. The 130 lineament and the base of the troctolite unit have combined $Q/\Delta H$ of between 6 × 10^{-7} $m^2 \cdot s^{-1}$ (1984 PIP tests) and 1 × 10^{-6} $m^2 \cdot s^{-1}$ (1985 casing tests). The close spacing of these two structures prohibits resolution of their individual hydraulic properties. The 050 lineament shows low hydraulic conductivity.

The open-borehole pump test completed in 1983 showed the persistence of wellbore storage throughout the pumping period. As no recovery measurements were recorded, it was not possible to analyze the pump test to determine hydraulic properties.

Borehole EBL-3

Only one hydraulic test was performed in borehole EBL-3. The recovery response to open-borehole pumping was analyzed to determine a composite borehole $Q/\Delta H$ of 5 × 10^{-7} $m^2 \cdot s^{-1}$. Using a borehole length of 442 m, this is equivalent to a K_{erm} of 1 × 10^{-9} $m \cdot s^{-1}$.

Borehole EBL-4

The results of 1984 PIP tests (Table 6) indicate that borehole EBL-4 intersects several high-hydraulic conduc-

tivity fractures in the upper 200 m and one open fracture zone at 454-m depth.

Open fractures occur between surface and 50-m depth, at 105- to 117-m depth, and at the base of the troctolite unit at 184-m depth. The results of 1985 casing tests indicate that most of the fluid produced in the upper 120 m comes from open fractures at 105- to 117-m depth. These fractures show $Q/\Delta H$ of 4×10^{-7} $m^2 \cdot s^{-1}$. Extensive fracturing at the base of the troctolite horizon likely accounts for the most of the $Q/\Delta H$ (2×10^{-7} $m^2 \cdot s^{-1}$) measured in the 120- to 198-m PIP-isolated interval. If this assumption is correct, then the $Q/\Delta H$ value for the base of the troctolite unit in borehole EBL-4 is similar to values measured in borehole EBL-1 (3×10^{-7} $m^2 \cdot s^{-1}$) and likely in borehole EBL-2 (6×10^{-7} $m^2 \cdot s^{-1}$). The interval between 200- and 450-m depth has mostly low to intermediate hydraulic conductivity fractures. Rock mass hydraulic conductivity of about 10^{-10} $m \cdot s^{-1}$ is representative of this section of borehole.

The most significant hydrogeological structure in borehole EBL-4 is a high-hydraulic conductivity, low-hydraulic head (see Chapter 6) fracture zone at 454-m depth. PIP testing and single-packer testing in 1984 and casing testing in 1985 showed that this fracture zone has reproducible $Q/\Delta H$ in the range $2\text{-}3 \times 10^{-7}$ $m^2 \cdot s^{-1}$.

Because of this high permeability and low hydraulic head in conjunction with high permeability and high hydraulic head in the near surface, it was recognized that significant quantities of fluid flow down the borehole and that collection of uncontaminated ground-water samples at depth in borehole EBL-4 would be difficult. From the

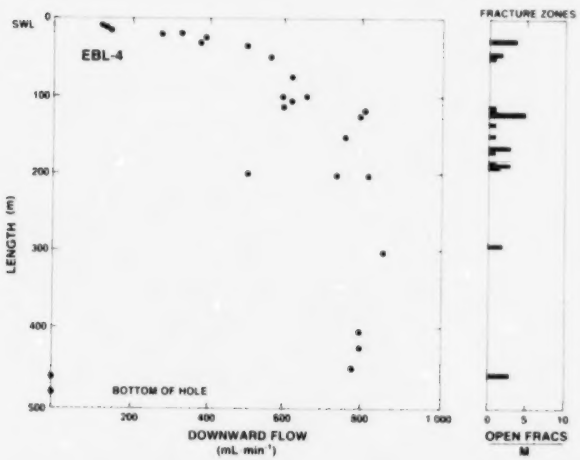

Figure 22. Results of borehole EBL-4 flow meter survey completed by United States Geological Survey in 1984 (after Paillet and Hess, 1986).

results of PIP tests (Table 6) and an estimate of equilibrium open-borehole fluid levels (≈8 m depth), we can estimate the rate of fluid flow down the borehole under equilibrium conditions to be about 500-600 $mL \cdot min^{-1}$. Borehole flow meter measurements performed by the United States Geological Survey (USGS) (Paillet and Hess, 1986) in 1984 provide independent corroboration of this flow rate calculation and therefore the hydraulic properties determined from PIP testing. The results of the borehole flow meter survey are shown in Figure 22. The survey shows that about 800 $mL \cdot min^{-1}$ enters borehole EBL-4 in the upper 150 m, flows down the borehole, and exits the borehole into the fracture zone at 454 m depth. The similarity between the calculated and measured flow rates indicates that the PIP test results for the 454-m depth fracture zone are reliable.

Additional corroboration of the flow rate down borehole EBL-4 is obtained from analysis of the specific conductance of withdrawn fluid versus cumulative produced fluid volume plots (Fig. 23) made from repeated pumping of the 454-m depth fracture zone for geochemical sampling. Because the *in situ* ground waters at 454-m depth are characterized by high salinity and ground waters in the near surface by low salinity, the measurements of specific conductance of the withdrawn fluid from 454-m depth reflect the degree of contamination of the deep *in situ* ground waters with fluids produced from the upper 150 m. As evident in Figure 23, rising fluid conductivity was observed with cumulative produced fluid volume during four periods of pumping. The rate of increase of specific conductance of the withdrawn fluid is variable but in general is directly proportional to the period of time that the borehole was open or without packers prior to pumping. For example, borehole EBL-4 was left open for periods of 15, 60, 3 and 2 days prior to PIP swabbing, first and second single-packer swabbings and casing air-lift pumping, respectively. The downhole flow rate in effect during these periods of open borehole conditions can be calculated, assuming plug flow, from (1) either a measured or extrapolated estimate of the volume of produced fluid necessary during one of the pumping periods to attain the peak specific conductance measured during the previous pumping period and (2) the duration of open-borehole conditions between pumping periods. Using the data shown in Figure 23, we can estimate volumes of 50 000, 3500 and 2600 L required to reach previous peak specific conductances during the first and second single-packer swabbings and the casing air-lift pumping, respectively. The volume and time data indicate downhole flow rates of 580, 800 and 900 $mL \cdot min^{-1}$ between the last three pumping periods very similar to the USGS measured value of 800 $mL \cdot min^{-1}$. The similarity of the borehole flow rates is even more remarkable when one considers that the borehole flow rate

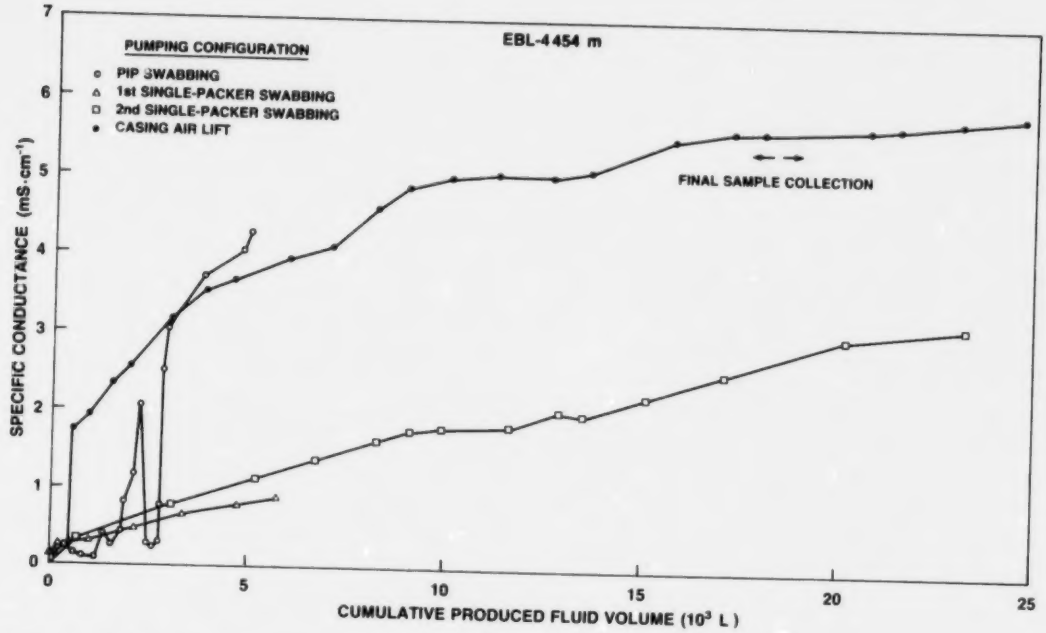

Figure 23. Plot of specific conductance of withdrawn fluid versus cumulative produced fluid volume for four periods of pumping from 454-m depth fracture zone in borehole EBL-4.

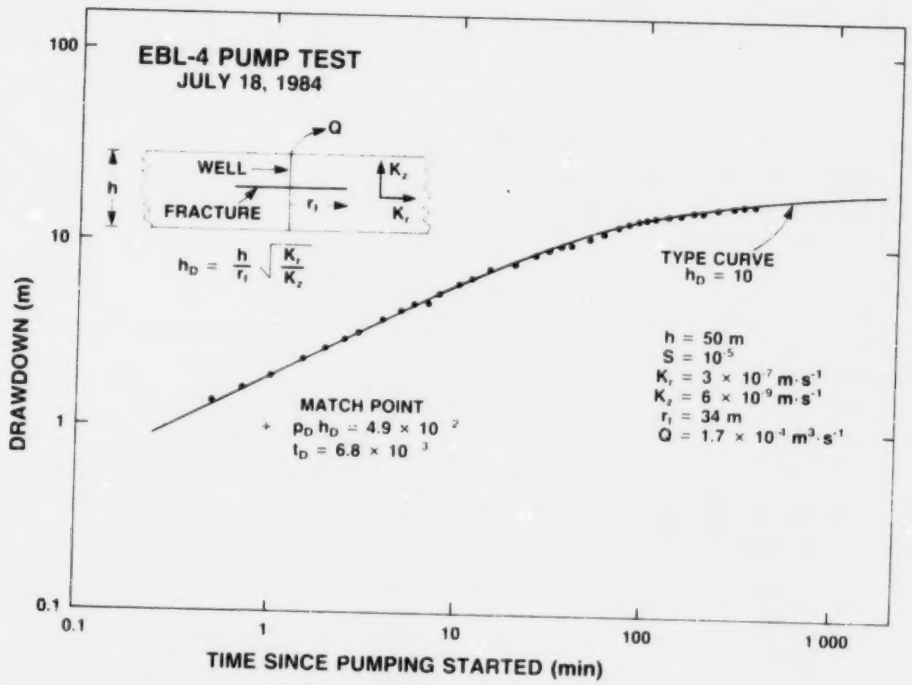

Figure 24. Log-drawdown versus log-time response of open-borehole pump test in EBL-4. Type curve analysis of the data to determine fracture radius (r_f) and anisotropic hydraulic conductivities (K_r and K_z) of the rock mass is based on the single, horizontal, uniform-flux, fracture model of Gringarten and Ramey (1974).

measured by the USGS was obtained during the three-day period between the first and second single-packer swabbings. Our estimate of borehole flow rate between these pumping periods is identical at 800 $mL \cdot min^{-1}$.

The USGS borehole flow rate data also show the location of significant fluid producing fractures at 0 to 50-m depth and at about 115-m depth.

A step-drawdown pumping test was performed in borehole EBL-4 in 1984. The drawdown versus time data for the first pumping step are shown on a log-log plot in Figure 24. Because the drawdown-time data of Figure 24 show a half slope characteristic of linear flow to a high hydraulic conductivity fracture, the pump test was analyzed using the model of Gringarten and Ramey (1974) for flow to a horizontal fracture imbedded on an anisotropic continuum of infinite radial extent and finite thickness. With thickness (h) of 50 m, continuum storativity (S) of 10^{-5} and pumping rate of 10 $L \cdot min^{-1}$, a fracture radius of 34 m and anisotropic hydraulic conductivities of $K_r = 3 \times 10^{-7}$ $m \cdot s^{-1}$ and $K_z = 6 \times 10^{-9}$ $m \cdot s^{-1}$ were determined from type-curve matching the model to the field data. Because most of the fluid pumped from borehole EBL-4 is produced by the fractures in the upper 120 m (likely between 0 to 50-m depth) the model-derived parameters reflect the properties of the near-surface. Enhanced radial permeability is expected at these shallow depths as a result of the occurrence of open horizontal fractures.

Pseudo steady-state flow rate and drawdown conditions were observed during the step-drawdown test. The flow rate versus drawdown data are plotted in Figure 25 in a format proposed by Louis and Maini (1970) to identify turbulence and fracture deformation effects

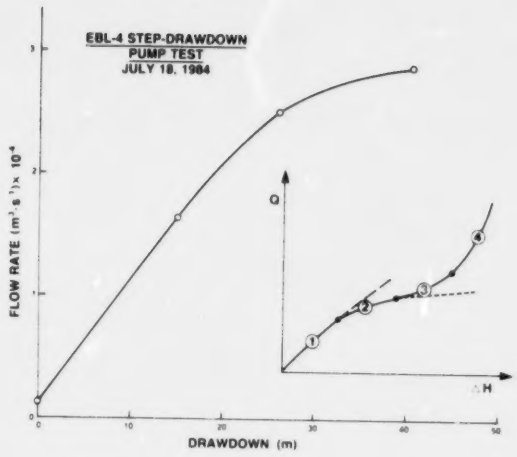

Figure 25. Results of step-drawdown pump test of borehole EBL-4. The inset figure (after Louis and Maini, 1970) shows typical results of fluid injection tests: (1) laminar flow, (2) turbulence effect, (3) turbulence offset by fissure expansion, (4) predominance of fissure expansion effects.

during hydraulic testing of fractured rocks. The inset figure is reproduced from Louis and Maini (1970) and shows potential flow rate-head relations during a step injection test. Because our step test was performed using fluid withdrawal, flow regimes No. 3 and No. 4 resulting from fissure expansion are unlikely. The data from our test suggest the existence of turbulence and possibly fracture closure effects with drawdowns greater than about 20 m. The flow rate at zero drawdown plotted in Figure 25 is the downhole flow rate measured with the USGS borehole flow meter.

Installation of Multiple-Packer Casings

Because of the significant downhole flow rates observed in borehole EBL-4 and suspected in boreholes EBL-1, 2 and 3, it was recognized that reliable measurements of hydraulic head and, to a lesser extent, hydraulic conductivity and the collection of representative groundwater samples could only be obtained with long-term isolation of test intervals. In October and November 1984, multiple-packer casings incorporating water-inflated packers, pressure ports for hydraulic head measurement and pumping ports for hydraulic testing and ground-water sampling were installed in boreholes EBL-1, 2, 3 and 4. The installation and operation of these casings and initial hydraulic head profiles obtained from them are summarized in a report by Novakowski and Flavelle (1985).

Table 8. Summary of the Multiple-Packer Casing Installations in the EBL-Series Boreholes

	EBL-1	EBL-2	EBL-3	EBL-4
Depth (m)	642.0	761.0	256.5	480.0
Packers	31	34	14	30
Pressure ports	33	34	13	28
Pumping ports	29	35	13	25
Test intervals	31	30	13	27

Table 9. Elevations of Test Intervals in EBL-Series Boreholes in Metres above Sea Level

Interval	EBL-1	EBL-2	EBL-3	EBL-4
1	-218.2 to -444.9	-322.3 to -400.1	172.9 to 9.3	-21.0 to -45.1
2	-201.7 to -216.7	-268.3 to -313.8	204.8 to 178.1	8.9 to -15.5
3	-182.2 to -200.2	-238.4 to -266.9	217.9 to 207.2	8.9 to -15.5
4	-132.7 to -180.7	-205.7 to -237.0	237.2 to 219.3	15.7 to -10.2
5	-132.7 to -180.7	-172.8 to -204.3	259.2 to 238.6	33.3 to -17.0
6	-98.2 to -131.2	-154.3 to -171.4	276.0 to 260.6	56.5 to -34.7
7	-63.7 to -96.7	-132.9 to -152.9	292.9 to 277.4	85.2 to -57.9
8	-26.2 to -62.2	-117.1 to -131.5	314.9 to 294.3	103.0 to -86.6
9	-6.7 to -24.7	-87.1 to -115.7	329.3 to 316.3	126.4 to -104.4
10	12.9 to -5.2	-57.1 to -85.6	341.0 to 330.7	144.3 to -127.7
11	41.4 to 14.4	-27.0 to -55.7	358.0 to 342.4	162.2 to -145.7
12	72.9 to 42.9	-1.2 to -25.6	368.4 to 359.4	187.9 to -163.6
13	110.4 to 74.4	40.4 to 0.2	377.6 to 369.9	203.7 to -184.3
14	138.9 to 111.9	64.8 to 41.8		219.0 to -205.1
15	170.4 to 140.4	83.5 to 66.2		225.9 to -220.3
16	186.9 to 171.9	113.7 to 84.9		241.2 to -230.1
17	201.9 to 192.9	143.9 to 115.1		241.2 to -230.1
18	201.9 to 192.9	174.1 to 145.3		256.5 to -245.4
19	206.4 to 203.4	198.6 to 175.7		269.0 to -257.9
20	223.4 to 207.9	228.9 to 200.0		281.6 to -270.4
21	245.4 to 224.4	247.6 to 230.3		294.1 to -282.9
22	266.4 to 246.9	272.2 to 249.0		306.6 to -295.5
23	282.9 to 267.9	290.9 to 276.5		322.0 to -308.0
24	302.4 to 284.4	290.9 to 276.5		334.6 to -323.4
25	311.4 to 303.9	301.0 to 292.3		352.7 to -336.0
26	323.4 to 312.9	314.4 to 302.4		368.1 to -354.1
27	342.9 to 324.9	329.9 to 315.4		380.7 to -369.5
28	353.4 to 344.4	347.2 to 331.3		390.5 to -382.1
29	369.9 to 354.9	347.2 to 331.3		397.5 to -391.9
30	378.9 to 371.4	357.3 to 348.6		
31	386.4 to 380.4	367.4 to 358.7		
32	393.9 to 387.9	374.7 to 368.8		
33	405.8 to 395.4	381.9 to 376.1		
34		387.7 to 383.3		

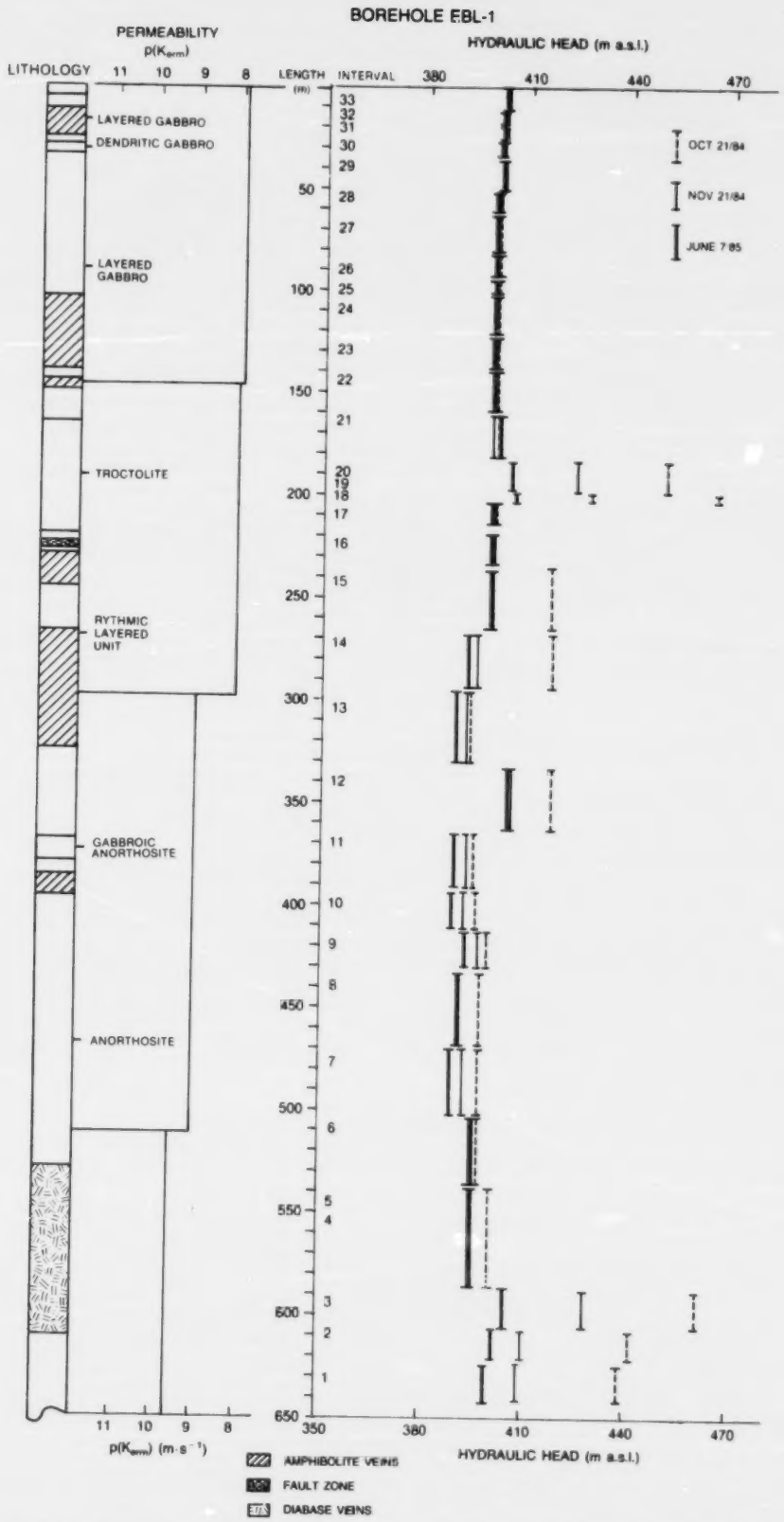

Figure 26. Composite lithological and hydrogeological log for borehole EBL-1; lithological data from core logging, permeability data from PIP testing, and hydraulic head data from pressure profiling in multiple-packer casings.

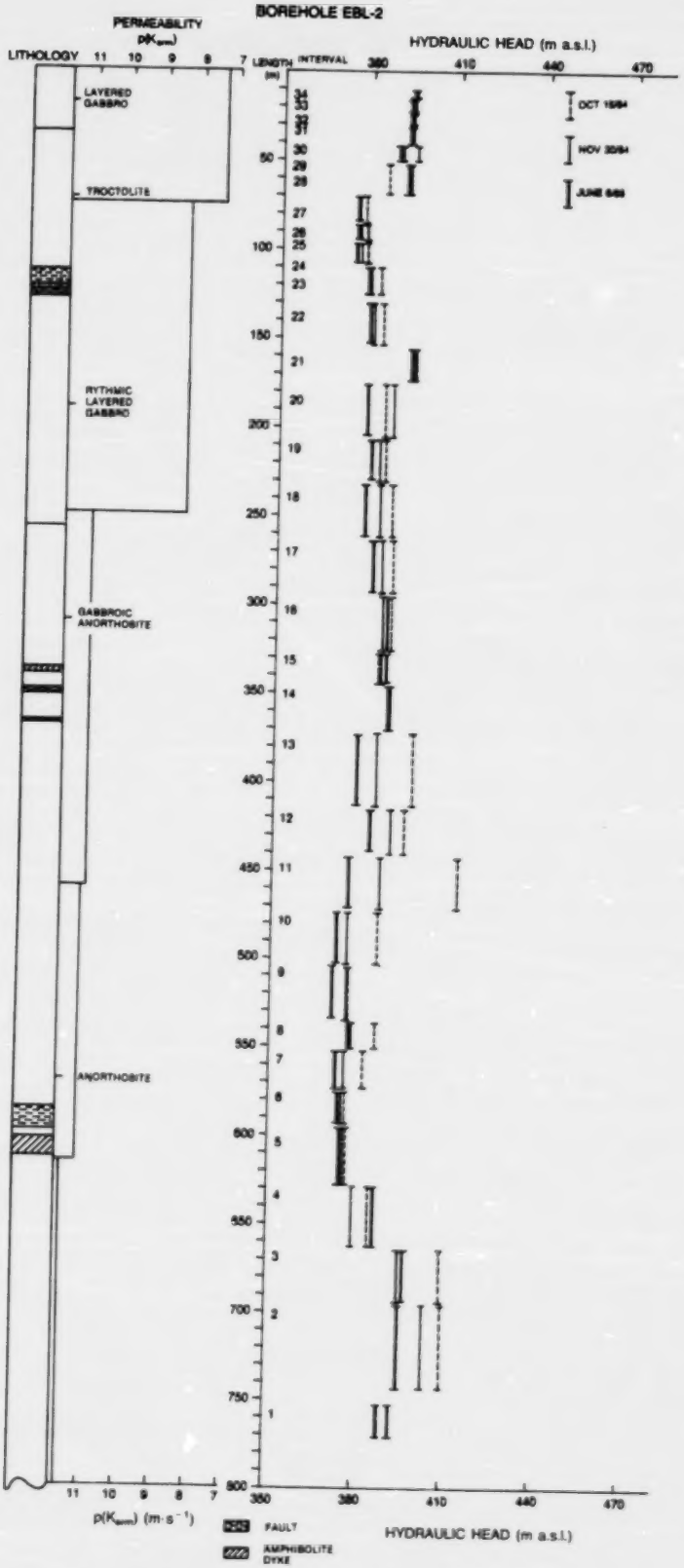

Figure 27. Composite lithological and hydrogeological log for borehole EBL-2; lithological data from core logging, permeability data from PIP testing, and hydraulic head data from pressure profiling in multiple-packer casings.

The depth of installation and number of packers, pressure ports, pumping ports and test intervals for each borehole are listed in Table 8. The elevations of test intervals in each borehole are summarized in Table 9. The elevations of each test interval were determined from the elevation of the top of the surface casing of each borehole and from the results of borehole gyroscopic directional surveys completed by Sperry Sun of Canada Ltd. The distribution of test intervals in each borehole is illustrated in Figures 26 to 29 and described in detail by Novakowski and Flavelle (1985).

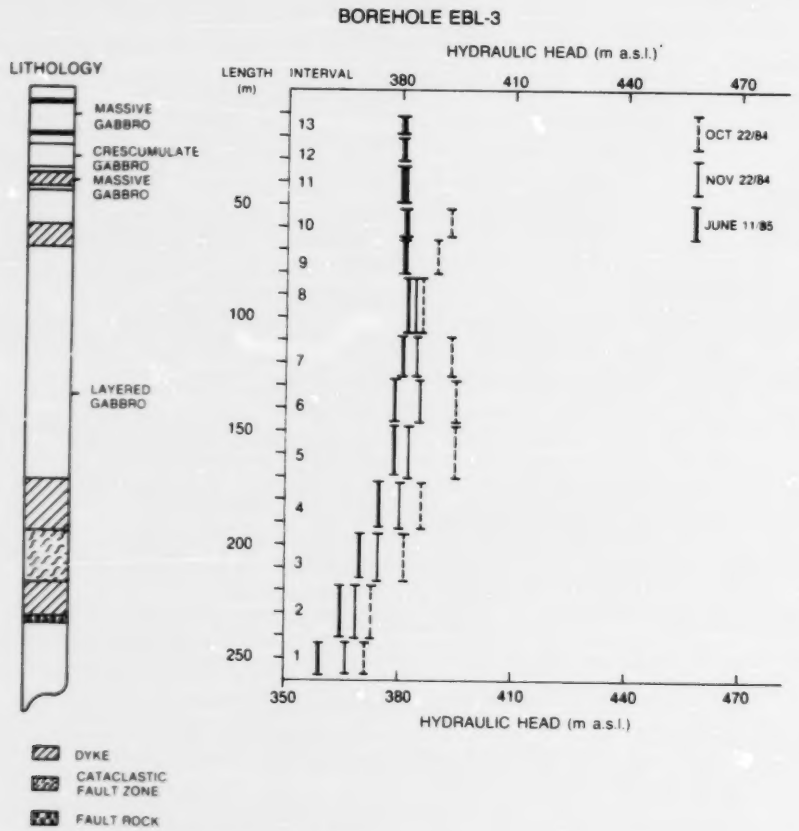

Figure 28. Composite lithological and hydrogeological log for borehole EBL-3; lithological data from core logging and hydraulic head data from pressure profiling in multiple-packer casings.

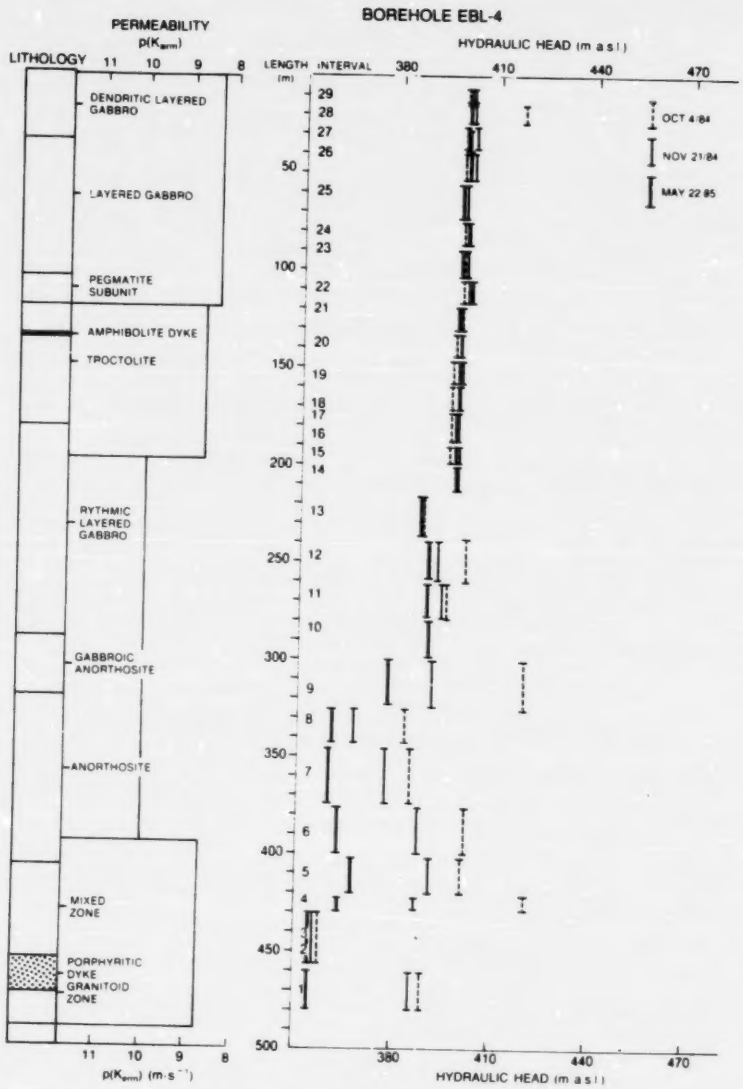

Figure 29. Composite lithological and hydrogeological log for borehole EBL-4; lithological data from core logging, permeability data from PIP testing, and hydraulic head data from pressure profiling in multiple-packer casings.

Hydraulic Head Monitoring

METHODOLOGY

Measurements of hydraulic head were obtained from both P-series and EBL-series boreholes under both open-borehole and packer-isolated test conditions. Hydraulic heads were determined from either fluid level or fluid pressure measurements and elevation data obtained from surface levelling and borehole directional surveys. Fluid level measurements were obtained using an electric-contact, water-level tape accurate to ±5 mm. Fluid pressure measurements were made using a submersible pressure transducer probe with accuracy of ±0.10 m.

Hydraulic heads in the P-series boreholes were determined from fluid level measurements. Hydraulic heads in the EBL-series boreholes were determined from (1) fluid level measurements during open-borehole and PIP- and packer-isolated test conditions and (2) fluid pressure measurements using the multiple-packer casings.

Interpretation of ground-water flow in systems with fluids of variable density requires determinations of equivalent freshwater and environmental-water heads (Lusczynski, 1961; Jorgensen *et al.*, 1982). Hydraulic heads calculated from fluid level measurements obtained in the P-series boreholes and the upper 300 m of the EBL-series boreholes are thought to represent equivalent freshwater and environmental-water heads because of the low total dissolved solids concentrations (see Chapter 7) and therefore relatively uniform density of the sampled ground waters. Ground waters below depths of 300-400 m show increasing salinity and density with depth. Hydraulic heads for these test intervals must be expressed as equivalent freshwater heads for determination of horizontal flow potentials and as environmental-water heads for determination of vertical flow potentials. Because fluid pressures and not fluid levels are measured using the multiple-packer casing system, the calculated hydraulic heads from the casing monitoring include the effects of variable density fluid and therefore represent equivalent freshwater heads. Fluid density measurements are necessary to express freshwater heads as environmental-water heads (Lusczynski, 1961).

The most comprehensive program of hydraulic head monitoring was completed in the EBL-series boreholes using the multiple-packer casings in the period October 1984 to October 1985. Fifteen or sixteen complete pressure profiles were obtained for each borehole during this one-year period. During the pressure profiling of boreholes EBL-1, 2 and 3 the fluid level within the plastic casing was filled to surface and hydraulic head values were determined from the elevation of the pressure port and the difference in pressure reading between the inside of the fluid-filled casing and in the test interval. A significant leak in the plastic casing at depth in borehole EBL-4 prohibited maintenance of fluid level at the top of the casing during pressure profiling. Hydraulic heads in borehole EBL-4 were therefore calculated from elevation data and from absolute pressure measurements recorded for the test interval that were corrected for downhole temperature effects.

A check of the integrity of the casing installation and the reliability of calculated hydraulic heads was performed in boreholes EBL-1 and EBL-2 during October 1985. Pressure profile measurements were obtained for each test interval with the casing fluid level at surface and at a depth of 8-23 m below surface. Comparison of the two pressure profiles identified test intervals with hydraulic connection to the inside of the casing and therefore unrepresentative and excessively high hydraulic heads.

RESULTS AND INTERPRETATION

P-Series Boreholes

Hydraulic head data were calculated for the P-series boreholes under open-borehole and packer-isolated conditions. The open-borehole fluid levels were generally 1.0-3.0 m below ground surface. Borehole P-2 was flowing at 1.5 m above ground surface, and borehole P-6 had a static water level of about 7.0 m below ground surface.

The most reliable estimates of hydraulic head in the P-series boreholes were obtained from the results of single-packer and straddle-packer testing. The results for 4-m length test intervals are tabulated in Appendix A. These hydraulic heads should be considered approximate as the straddle packers isolated the test intervals for relatively short periods (i.e. several hours to several days) compared with the duration of open borehole conditions (i.e. several

months). The approximate hydraulic head profile generated by the straddle-packer testing, however, provides important information on the pattern of ground-water flow in the vicinity of each borehole.

The hydraulic head distribution in the area of boreholes P-1 to P-6 is controlled by the presence of the 050 and 130 lineaments. These structural discontinuities have higher hydraulic conductivity than the surrounding rock mass and act as drains or sources for ground-water flow in the vicinity of each borehole. Boreholes P-1, 3 and 4 intersect the 130 lineament and show upward gradients of 3×10^{-2} to 9×10^{-2} from the lineament to surface. The 130 lineament is also thought to intersect borehole EBL-2 at about 123-m depth and at this depth shows hydraulic head 3-4 m greater than overlying test intervals, suggesting channelling of surface ground water to depth along the lineament. Similarly, ground water flows upward from the 050 lineament intersecting boreholes P-2 and P-5 with gradients of about 1×10^{-2}. However, 050 lineament intersections with boreholes P-6 and P-8 show that the lineament also behaves as a drain for ground water from both overlying and underlying rock with gradients of 4×10^{-2} to 6×10^{-1}. This combination of source and sink relations with the surrounding rock mass suggests that complex vertical flow regimes are likely to exist within the two structural discontinuities.

The approximate horizontal direction of flow within each structural lineament, however, can be estimated from comparison of hydraulic head data in each borehole, assuming the lineaments are hydraulically continuous. The hydraulic heads (Table 10) suggest that ground-water flow

Table 10. Hydraulic Heads of the 050 and 130 Lineament Structures and the Base of the Troctolite Horizon

Borehole	Approximate intersection depth (m)	Hydraulic head (m a.s.l.)
050 Lineament		
P-2	25.0-34.6	392
P-5	88.5-97.6	395
P-6	41.0-49.5	372
P-8	34.4-38.5	398
P-14	23.9-28.8	360
130 Lineament		
P-1	35.3-42.0	393
P-3	17.0-31.8	392
P-4	42.0-54.0	391
EBL-2	122.0-124.0	379
Base of the troctolite horizon		
EBL-1	210	399.8
EBL-2	122	379.7
EBL-4	184	398.0

m a.s.l. = Metres above sea level.

along each lineament reflects surface topography and surface drainage (see Section on Surface Drainage Pattern in Chapter 2) with flow directed to the northeast along the 050 lineament and to the southeast along the 130 lineament.

Ground-water flow in the shallow (0 to 50-m depth) rock mass of the north half of the plateau area also reflects surface topography. Flow is directed downward and to the topographic depressions created by the 050 and 130 structural lineaments (see Fig. 31 in Chapter 7).

Hydraulic heads measured in boreholes P-12 and P-13 which intersect splays of the Folson Lake Fault show vertically downward flow with gradients of 1×10^{-2} to 3×10^{-2}.

Ground water flows in areas without major structural lineaments also show a strong recharge component. Vertical gradients of 1×10^{-2} to 3×10^{-2} were observed in boreholes P-7, 9, 10 and 11.

EBL-Series Boreholes

Open-borehole fluid levels in boreholes EBL-1, 2, 3 and 4 averaged 6.0, 14.0, 10.0 and 8.0 m below ground surface, respectively, during 1983 and 1984.

Table 11. Hydraulic Heads Measured During 1984 PIP Testing

Interval	Depth (m)	Hydraulic head (m a.s.l.)
EBL 1-5	0-147	401.9
EBL 1-4	147-298	399.9
EBL 1-3	298-512	394.8
EBL 1-2	512-650	388.8
EBL 1-1	650-851	Not accessed
EBL 2-5	0-75	394.4
EBL 2-4	75-250	377.5
EBL 2-3	250-460	368.8
EBL 2-2	460-616	368.8*
EBL 2-1	616-836	368.8*
EBL-3	0-442	378.9
EBL 4-4	0-120	401.8
EBL 4-3	120-198	399.8
EBL 4-2	198-396	385.2
EBL 4-1	396-489	367.2

*Approximate data because of short observation period and low permeability of test interval.

Hydraulic heads measured during PIP testing in 1984 are listed in Table 11. The data shown in Table 11 were determined from fluid level measurements taken shortly after accessing each PIP-isolated interval. The hydraulic heads measured in most of the PIP-isolated intervals are considered representative because the test intervals were hydraulically isolated for periods of 7-8 months prior

to measurement. The data for test intervals EBL 2-1 and 2-2 are less reliable because of leaky PIPs and very low permeability of the test intervals.

The hydraulic heads measured in 1984 show vertical recharge gradients of 1×10^{-2}, 3×10^{-1} and 2×10^{-2} in the upper 200 m of boreholes EBL-1, 2 and 4, respectively. Between 200- and 400-m depth, the vertical gradients increase in both boreholes EBL-1 and EBL-4 to 5×10^{-2} and 3×10^{-1}, respectively. Horizontal hydraulic gradients in the area defined by boreholes EBL-1, 2 and 4 average 3×10^{-2} to the northeast in the upper 200 m and 5×10^{-2} to the southeast over the 200- to 400-m depth. The hydraulic gradients below 400-500 m are less clear because of limited data.

Hydraulic head monitoring was performed in boreholes EBL-1, 2, 3 and 4 throughout the period October 1984 to October 1985. The results of this pressure monitoring are tabulated in Appendix B as freshwater hydraulic heads. The results of selected surveys are also displayed against lithological and permeability or hydraulic conductivity logs (from PIP testing) in Figures 26 to 29. The freshwater hydraulic head profiles are expressed in metres above sea level (m a.s.l.). The first two surveys after packer inflation and a third survey in late spring prior to pumping for ground-water sampling are shown in Figures 26 to 29.

The hydraulic head profiles of boreholes EBL-1 and EBL-2, as illustrated in Figures 26 and 27, show downward gradients to about 500-m depth and upward gradients below 500 m. The hydraulic head profiles of boreholes EBL-3 and 4 indicate increasing downward gradient from surface to the bottom of the casing installations at 256.5- and 480.0-m depths.

The variability of the head measurements between 200 and 500 m and the upward gradients below 500 m in both boreholes EBL-1 and 2 prompted an integrity check of the casing installation in these boreholes. The results of this check are listed in Table 12. Table 12 shows the change in test interval pressure head between two successive pressure profiles: one performed with fluid level 8-23 m below the top of the casing and the other with the fluid level at the top of the casing. The change in test interval pressure between the two surveys is normalized to the change in fluid level within the casing between the two surveys. Intervals showing negligible pressure change are considered to have reliable hydraulic heads. Because some fluid is likely exchanged between the interior of the casing and the test interval during seating of the pressure probe, a maximum change of 10% in pressure reading or 1-2 m is also considered a reasonable but less reliable head measurement. Pressure changes of 10% to 50% between surveys indicate that the interval shows hydraulic head that reflects both the level of the fluid in the casing and the *in situ* hydraulic conditions. Pressure changes greater than 50% indicate that a significant leak exists between the casing and the test interval and that hydraulic head measurement in the test interval is unreliable. Because most of the pressure profiling was completed with the fluid level at the top of the casing, the calculated hydraulic heads in those intervals showing pressure changes during the integrity check would always be higher than the *in situ* or real hydraulic heads.

Table 12. Results of Integrity Check on Multiple-Packer Casings in Boreholes EBL-1 and EBL-2

Interval	Change in pressure head in percent*	
	EBL-1	EBL-2
1	55	17
2	64	–
3	71	64
4	27	–
5	27	19
6	24	1
7	0	7
8	1	29
9	20	0
10	17	24
11	0	37
12	100	86
13	8	71
14	58	80
15	16	73
16	0	73
17	0	51
18	0	0
19	13	5
20	19	2
21	11	8
22	1	0
23	0	0
24	0	0
25	0	0
26	0	0
27	0	0
28	0	12
29	0	12
30	0	30
31	0	1
32	0	0
33	0	1
34	–	4

*Change in pressure head of test interval as a percentage of the change in casing fluid level. The change in fluid levels in the casings between surveys was 15-23 m for borehole EBL-1 and 8-16 m for borehole EBL-2.

The results of the integrity check and the pressure profiling in borehole EBL-1 show that the upper 200 m of the installation provides reliable hydraulic heads with uniform down gradients of $1\text{-}2 \times 10^{-2}$, but that only a few test intervals below 250-m depth (i.e., Nos. 7, 11 and 13)

provide reliable data. No reliable hydraulic head data are available for borehole EBL-1 below 500-m depth. The few reliable hydraulic head measurements between 250- and 500-m depth indicate vertical recharge gradients of about 5×10^{-2}.

The hydraulic heads in borehole EBL-2 show a more variable distribution in the upper 200 m, likely reflecting the presence of the major structural lineaments and associated fracturing. Strong recharge conditions with gradients of 3×10^{-1} are indicated to 75-m depth, whereas strong discharge or upward flow conditions are shown from 75- to 170-m depth with gradients of 2×10^{-1}. The vertical component of hydraulic gradient is directed downward from 170- to 260-m depth. Between 260- and 500-m depth the hydraulic heads are mostly unreliable showing between 50% and 85% pressure response during integrity testing of the casing. The large number of unreliable test intervals in this section of borehole may be related to the very low permeability of the rock.

Reliable hydraulic head data were obtained in borehole EBL-2 from test intervals Nos. 6, 7 and 9 between 500- and 600-m depth. A reasonable indication of hydraulic head was also measured in test interval No. 1 at the bottom of borehole EBL-2. The available hydraulic head data for borehole EBL-2 below 250-m depth indicate down gradients of about 3×10^{-2} from 250- to 500-m depth and up gradients of about 6×10^{-2} in the borehole interval of 500- to 836-m depth. Test interval No. 1 in borehole EBL-2 is open to the bottom of the borehole at 836 m from 753-m depth.

Hydraulic heads measured in borehole EBL-3 (Fig. 28) indicate negligible vertical gradients in the upper 100 m and strong recharge gradients of 1×10^{-1} below 100-m depth. The lowest test interval, No. 1, includes the open section of borehole EBL-3 from 250- to 442-m depth. If the down gradients observed in the 100- to 250-m interval continue to depth, the lowest hydraulic head associated with the Folson Lake Fault is likely less than the measured value for test interval No. 1 at 357.7 m a.s.l. This is because the hydraulic head of 357.7 m a.s.l. is a composite value over the interval 250- to 442-m depth and likely reflects higher hydraulic head near the top of the interval and lower hydraulic head near the bottom of the interval.

The hydraulic heads measured in borehole EBL-4 after May 22, 1985, are influenced by periods of pumping for the collection of ground-water samples. Intervals No. 2 and No. 3 (429- to 456-m depth) were extensively pumped (26 000 L removed) during the period June 4 to August 4, 1985. About 4000 L was removed from interval No. 22 (105- to 117-m depth) during the period October 3-9, 1985. Drawdowns in response to these fluid withdrawals are noticeable in the hydraulic head surveys completed on August 18, September 20, and October 23, 1985.

The most reliable hydraulic head record in borehole EBL-4 was obtained on May 22, 1985, and is shown in Figure 29. The upper 200 m of borehole EBL-4 shows relatively uniform vertical recharge gradients of $1\text{-}2 \times 10^{-2}$ similar to borehole EBL-1 and in contrast to borehole EBL-2. The uniform gradients in borehole EBL-4 to 200-m depth reflect the absence of major structural discontinuities in the near surface. Below 200-m depth the distribution of hydraulic head is controlled by the presence of a high-permeability, low-hydraulic head fracture zone associated with a porphyritic dyke at the basal contact of the East Bull Lake mafic pluton. Vertical gradients of $1\text{-}3 \times 10^{-1}$ are observed from 200-m depth to the fracture zone at 454-m depth. Hydraulic head of about 352 m a.s.l. was measured in this fracture zone on May 22, 1985. This hydraulic head is the lowest equilibrium value recorded in all boreholes at East Bull Lake and is lower than the elevation of adjacent Moon Lake at about 355 m a.s.l. (Fig. 2). Figure 2 also shows that the closest potential discharge point for this low-head fracture zone is along the strike of the Folson Lake Fault in the immediate vicinity of Parisien Lake (elevation about 339 m a.s.l.). Parisien Lake is located about 2.5 km southeast of borehole EBL-4.

The results of hydraulic head monitoring in the EBL-series boreholes are useful in quantifying the likely horizontal directions of ground-water flow in the upper plateau area of the East Bull Lake pluton. In addition to the general recharge conditions discussed previously, the hydraulic head data from boreholes EBL-1, 2 and 4 suggest that ground water in the upper 200 m in the area of these boreholes flows to the northeast to the intersecting 050 and 130 lineaments with a gradient of 3×10^{-2}. This result is consistent with flow directions interpreted from hydraulic head data obtained from the P-series boreholes (Fig. 31). Ground-water flow in the upper 200 m of the southern half of the upper plateau area also reflects surface drainage and topography with horizontal gradients directed to the Folson Lake Fault.

Hydraulic head measurements from the high-permeability fractures associated with the base of the troctolite horizon (Table 10) also show a hydraulic gradient of about 5×10^{-2} directed to the northeast. Because of the uniform and high permeability of the base of the troctolite horizon, it is likely that ground water drains from the overlying bedrock, flows along the base of the troctolite with minimal resistance, and discharges at surface where the unit outcrops in the topographic depression between the north end of Moon Lake and Little Bull Lake.

Between 200- and 400- to 500-m depth, horizontal hydraulic gradients in the study area are directed to the south and southeast, likely to Folson Lake Fault, with an average value of 5×10^{-2}. The hydraulic heads and gradients measured in the upper 400-500 m of the study area during pressure profiling in 1985 are generally similar to those measured during PIP testing in 1984.

Below 400- to 500-m depth we are less certain of the horizontal direction of ground-water flow because of a shortage of reliable hydraulic head measurements. We suspect that ground water in the vicinity of borehole EBL-4 flows along the fractured porphyritic dyke intersected at 454-m depth in borehole EBL-4 and toward the Folson Lake Fault. The available hydrogeological data further suggest that the Folson Lake Fault acts as a regional high-permeability pathway directing flow along the strike of the fault to the southeast. If significant quantities of flow are directed along the fault from the East Bull Lake pluton, then the decrease in elevation observed along the strike of the fault to the southeast may result in ground-water discharge from the fault in the Parisien Lake area. Lee (1983) measured ground-water discharge into Parisien Lake and also significantly larger streamflow exiting the lake than entering it. Although Lee's data do not conclusively indicate that ground-water discharges from the Folson Lake Fault to Parisien Lake, these data in conjunction with EBL borehole hydrogeological information suggest that such ground-water flow patterns are likely occurring.

Hydrogeochemical Investigations

The East Bull Lake research area is unique in the AECL nuclear fuel waste management program in that it is the only research area where it is possible to study the hydrogeological characteristics of a large mass of mafic plutonic rock (gabbro-anorthosite) on the Canadian Precambrian Shield. In particular, the EBL area represents an opportunity to investigate the hydrogeochemical characteristics and evolutionary processes in mafic rocks and to compare such processes with those in granitic rocks which have been previously documented in this country and elsewhere. Such generic hydrogeochemical information should be of practical value during governmental review of AECL's concept assessment document for the disposal of high level nuclear waste in plutonic rock on the Precambrian Shield.

In 1984, a joint NHRI-AECL hydrogeochemistry study was initiated to characterize the chemical and isotopic composition of ground water, both areally and with depth, in the EBL pluton. This was accomplished by sampling one or more zones in each of the 14 shallow (<100 m deep), air-percussion drilled P-series boreholes, and by sampling zones in three of the four deep cored EBL-series boreholes in which production injection packers (PIPs) had been installed in the autumn of 1983. PIPs were set at depths of 147, 298, 512 and 650 m in EBL-1; 75, 250, 460, and 616 m in EBL-2; and 120, 198 and 396 m in EBL-4. No PIPs had been set in EBL-3. Sampling of these PIP-isolated zones was conducted prior to their removal for subsequent borehole geophysical logging and casing installation.

The PIP set at 250 m in EBL-2 had deflated some time since its installation and had fallen onto the PIP at 460 m. The PIP was retrieved and a new PIP installed at 248 prior to sampling. Similarly, the PIP at 460 m was not adequately inflated and had to be replaced prior to sampling. Therefore the borehole length between 75 and 616 m in EBL-2 may have been hydraulically connected for a considerable period, although the timing of PIP deflation at 250 m and 460 m is not known. Flow rate measurements in EBL-2 and EBL-4 by the USGS indicated downward flows of up to 300 and 800 $mL \cdot min^{-1}$, respectively. Therefore vertical mixing occurs in these holes when the major water producing fractures are not isolated by packers.

Selected intervals in the EBL-series boreholes were sampled in 1985 in order to obtain a more accurate chemical characterization of the saline ground water at depth and more representative samples of high hydraulic conductivity zones identified in boreholes EBL-1, 2 and 4, during testing in 1984. No deep sampling was conducted in EBL-2 in 1985 because of the very low hydraulic conductivity at depth in this borehole.

METHODOLOGY

The P-series boreholes were sampled in 1984 using single-packer and straddle-packer assemblies connected to PVC standpipe (see Section on Packer Tests in Chapter 4) into which a Bennett pneumatic pump could be lowered for sampling. There was also sufficient annular space to sample outside the pipe with the same pump. Sampling zones were selected on the basis of hydraulic conductivity data and on the degree of fracturing as determined from borehole acoustic televiewer logs. Open hole testing over the entire lengths of boreholes P-6, P-7, P-11, and P-14 was conducted because of the absence of identifiable, higher permeability zones in these holes. A Keck electrical pump was used for sampling boreholes P-6 and P-7.

Sampling of boreholes EBL-1, 2 and 4 in 1984 was conducted by wire-line swabbing inside AQ drill rod attached to each PIP except for the PIP at 650 m in EBL-1 which could not be accessed because of rock-fall material on top of it. The borehole sections above the top PIP in boreholes EBL-2 and EBL-4 were sampled with a peristaltic pump. It should be emphasized that swabbing inside the drill rod is not the preferred method for hydrogeochemical sampling because of metal contamination problems presented by the drill rod itself and organic contamination from the liberal application of pipe-thread lubricants. For example, a DOC concentration of 32 $mg \cdot L^{-1}$ has been measured in water swabbed from 512-650 m in EBL-1. Characterization of the major ion chemistry, however, should not be seriously compromised by this method. A more serious contamination problem is presented by the drill water used during the drilling of boreholes EBL-1 to 4. Fortunately, the drill water (collected from local surface waters) was tagged with the organic dye Rhodamine WT, so that at least a qualitative assessment of the level of contamination was provided by monitoring for Rhodamine

WT during swabbing using a Turner fluorometer. Conductivity was also monitored at the same time as Rhodamine WT. Once the level of contamination was reduced as low as practically feasible, a squeeze pump was lowered to a depth of 25-50 m inside the AQ rod to collect the final set of ground-water samples for chemical and isotopic analyses.

In 1985, sampling was conducted inside the multiple-packer casing following the opening of selected pumping ports. At each sampling depth, water was initially air-lifted from the casing using an air compressor. An electrical timer was used to activate the compressor for approximately 1 min every hour. This allowed sufficient time for the water level to recover to an acceptable depth inside the casing prior to the next activation. Conductivity and Rhodamine WT concentrations were monitored during the air-lifting operations. A squeeze pump set at a depth of approximately 50 m was used to collect the final set of ground-water samples for chemical and isotopic analyses.

Anion concentrations were measured routinely during the monitoring phase of sampling in each of the P-series and cored boreholes. Alkalinity was determined by potentiometric titration; chloride, by mercuric nitrate titration; and sulphate, by the Thorin titration. It was also necessary to know the bicarbonate and sulphate concentrations in the field in order to add the appropriate amount of reagents during sampling for the precipitation of carbonate and sulphate samples for isotope analyses. Anions were measured in the final sample set in the field lab, since alkalinity and sulphate may be susceptible to degradation during storage. Ground-water pH, redox potential, and dissolved oxygen were monitored in a flow cell during pumping. Ferrous iron was measured colorimetrically (2,2 bipyridyl method) with a spectrophotometer.

Samples for anions, cations, and trace elements were filtered in the field through 0.45-μm cellulose membrane filters. The cation and trace element samples were acidified with 4 $mL \cdot L^{-1}$ HCl and 8 $mL \cdot L^{-1}$ HNO_3, respectively. Samples for dissolved organic carbon were filtered through 0.45-μm silver membrane filters fitted to a glass syringe and stored in clean, pre-combusted glass bottles. Dissolved gas samples were collected in stainless steel cylinders for analysis at the Whiteshell Nuclear Research Establishment (WNRE), Atomic Energy of Canada Limited. Rare gas samples were collected in copper tubes, crimped at both ends with pinch-off tools, and sent to McMaster University (W.B. Clarke) for analyses. Isotope samples were collected for ^{18}O, ^{2}H, ^{3}H, ^{13}C, ^{14}C, ^{34}S and ^{18}O-SO_4 for analyses at the University of Waterloo (P. Fritz) and for $^{87}Sr/^{86}Sr$ measurements at McMaster University (R.H. McNutt). Radon was measured in the field and samples were collected for $^{234}U/^{238}U$ analyses at WNRE (Bottomley *et al.*, 1986). The Sr isotope results are not all available at this time and are not discussed in this report.

Cation, anion, and trace element analyses were conducted at the NHRI River Road laboratory in Ottawa. Analytical procedures for the NHRI lab are described in Appendix C. Duplicate samples of the final sample set were collected from some zones for analyses at the WNRE.

RESULTS

Sample Representativeness

Table 13 is a summary of the most representative analytical results for major and minor ions from each of the P-series boreholes and from the PIP-isolated zones in each of the cored boreholes sampled in 1984. Representative trace metal results for the same year are listed in Table 14. The results from the P-series sampling are believed to be representative of the actual spatial variability in hydrogeochemistry in the upper 50-100 m of the pluton. Samples from each of the zones in the cored boreholes, however, contained varying amounts of Rhodamine WT, indicating contamination with drill water. The amount of Rhodamine WT observed in each zone depended in a complex way on the average Rhodamine WT concentration in the drill water, which has been estimated by Raven *et al.* (1984) as varying between 5 and 34 $\mu g \cdot L^{-1}$; the history of Rhodamine WT injection in each borehole; and on the mixing proportions of drill water with ground water. Therefore the representativeness of the EBL-series borehole results is open to question.

The amount of swabbing that could be conducted at each zone was constrained by the hydraulic conductivity of the interval and by the field schedule. This limited the amount of time spent attempting to flush out the drill water contamination. For example, approximately 1.5×10^5 L was swabbed (over 12 days) from the top zone (147-298 m) of EBL-1 during which the Rhodamine WT concentration dropped from about 76 to 40 $\mu g \cdot L^{-1}$. This corresponds to a Rhodamine WT mass of almost 9 g. Although a total of approximately 37 g of Rhodamine WT was injected during drilling, most of this was discharged onto the surface with the drill water return flow. Therefore it is likely that most of the Rhodamine WT injected into the borehole fractures occurred within this top zone. This does not mean that the top zone was the most contaminated volumetrically because the Rhodamine WT in the drill water used for drilling the bottom half of the hole was as much as an order of magnitude lower in concentration than during the initial period of Rhodamine WT injection. Therefore, although the drill water contamination in the top zone

of EBL-1 was clearly the most visible, some of the other zones in boreholes EBL-2 and -4 were probably contaminated with a larger percentage of drill water,

Chemical analyses of ground waters sampled during 1985 are presented in Tables 15 (major and minor elements) and 16 (trace metals). The amount of water air-lifted from these zones ranged from 3700 L for EBL-2 (111-126 m) to 26 000 L for EBL-4 (429-456 m). Higher salinity water was recovered from EBL-4 (429-456 m) in 1985 than in 1984. Figure 30 shows the trend in electrical conductivity with increasing volume of ground-water withdrawal. Two plateaus in conductivity were reached during this test, and it is likely that still higher plateaus would have been reached had testing continued. The Rhodamine WT concentration at the end of this test was 0.3 $\mu g \cdot L^{-1}$ compared with a value of 1.6 $\mu g \cdot L^{-1}$ measured during the 1984 sampling of this zone.

The chemistry of the ground water sampled in 1985 from the high hydraulic conductivity fracture zone at the base of the troctolite in EBL-1 (204-213 m) was similar to that measured in 1984. Approximately 6300 L was removed in 1985, but the Rhodamine WT concentration during sampling was still high at 24 $\mu g \cdot L^{-1}$ but lower than the final concentration of 41 $\mu g \cdot L^{-1}$ measured during swabbing in 1984.

Table 13. Summary of Most Representative Analyses for 1984 of Ground-Water Chemistry (major and minor elements) for P-series and EBL-series Boreholes

Borehole	Depth (m)	Ca^{2+}	Mg^{2+}	Na^{+}	K^{+}	Sr^{2+}	Alk	SO_4^{2-}	Cl^{-}	F^{-}	Br^{-}	Si	B	pH	S.I.$_c$	C.B. (%)
P-1	32-53.3	1.9	0.1	53	0.4	<0.06	139*	6.7†	0.6	<0.1	0.06	7.3	0.42†	9.1*	-0.17	0.2
P-2	24.5-38.1	1.7	0.2	55	0.4	<0.06	131*	9.0*	0.8	<0.1	0.05	8.6		9.6*	0.10	3.0
P-3	0-16	17.3	3.8	24	0.8	0.14	127*	8.6†	1.0	0.2	0.04	7.0	0.20†	7.3*	-0.98	1.0
P-3	16-38.1	1.1	0.2	58	0.5	<0.06	156*	7.5*	0.8	0.5	0.05	10.5	0.66†	9.3*	-0.20	2.9
P-4	0-35	25.0	4.7	8	1.6	<0.06	103*	3.6	0.9	<0.1	0.05	6.6		7.7*	-0.51	6.2
P-5	0-22	5.1	0.7	44	1.0	<0.06	123*	3.0†	1.0	0.3	0.03	6.8	0.61†	8.9*	0.02	3.2
P-5	88.5-97.6	1.6	0.3	59	0.3	<0.06	149*	6.0*	1.2	<0.1	0.03	9.1		9.4*	0.01	0.3
P-6	0-68	15.4	3.8	26	0.6	<0.06	120*	10.0*	0.6	0.3	0.04	4.0	0.30†	8.4*	0.05	0.4
P-7	0-39.6	22.8	1.1	3.9	0.9	0.12	68*	12.0	0.6	<0.1	0.04	5.2	<0.1†	9.0*	0.53	1.5
P-8	0-20	12.2	1.4	3.1	2.0	0.12	69*	6.2	0.9	<0.1	<0.02	4.8		6.5*	-2.17	17.0
P-9	0-12	15.8	2.2	4.4	0.6	<0.06	63*	5.7	0.5	<0.1	0.11	8.0		6.2*	-2.39	1.3
P-9	12-43.2	19.3	3.2	19	10.7	0.09	109*	29.6	1.2	<0.1	0.14	8.4		7.3*	-1.01	2.3
P-10	0-34.5	19.2	4.5	5.5	0.7	<0.06	82*	11.2*	2.8	<0.1	0.09	9.4		6.1*	-2.31	6.2
P-10	34.5-38.5	24.9	5.8	8.4	0.4	0.09	115*	12.5*	2.1	<0.1	0.12	9.0		6.6*	-1.57	2.5
P-10	66.3-70.3	20.7	5.5	10.6	0.7	<0.06	123*	12.0*	1.6	<0.1	0.11	8.0		7.8*	-0.42	8.1
P-10	82-98.7	19.2	4.2	17.8	1.0	0.09	112*	12.5*	1.1	<0.1	0.11	7.7		7.6*	-0.67	0.5
P-11	0-49.2	32.4	7.3	9.5	6.8	0.20	157	12.5	1.3	0.2	0.08	7.0	0.1†	6.8*	-1.15	1.3
P-12	0-37	5.9	1.6	45	13.2	0.11	110*	34.5*	0.7	0.2	0.05	4.0	0.9†	9.4*	0.44	3.3
P-12	38-48.6	4.1	0.9	40	6.8	0.12	116*	18.0*	0.9	0.4	0.13	6.8	1.5†	8.9*	-0.08	2.8
P-13	0-22	6.9	1.9	35	7.9	0.13	105*	17.0*	1.2	0.1	0.11	9.3		9.0*	0.18	2.6
P-14	0-43.3	23.1	5.5	2.6	1.6	0.15	93*	5.9	0.2	<0.1	0.10	6.7		7.5*	-0.78	3.2
EBL-1	147-298	2.4	0.4	84	0.5	<0.06	197	4.3	17.9	<0.1	0.10	12.5	1.0†	9.4	0.29	0.3
EBL-1	298-512	5.5	0.1	233	0.8	0.10	66*	17.8†	321*	<0.1	1.6	14.7	2.81†	10.2*	0.45	0.5
EBL-1	512-650	20.5	4.2	100	1.0	0.16	119	16.0†	81	<0.1	<0.02	5.2		7.7	-0.42	11.4
EBL-2	0-75	20.0	6.3	16	0.7	0.12	144*	29†	4.0	<0.1	0.17	5.4	0.12†	6.5*	-1.70	2.9
EBL-2	75-248	0.4	0.6	65	0.2	<0.06	157*	9.9*	10.9*	0.35	0.04	12.1	1.04†	10.4*	-0.13	3.4
EBL-2	248-460	0.5	0.3	74	0.5	<0.06	130*	21.5	31*	<0.1	0.3	14.4		9.7	-0.34	2.6
EBL-2	460-616	228	1.6	570	1.1	1.53	38*	11.4	1237	1.6	3.30	4.4		8.0	0.12	0.8
EBL-2	616-836	293	1.7	584	2.1	2.37	29*	20.0*	1350	2.0	2.05	1.5	0.20†	7.4	-0.47	1.5
EBL-3	0-443	25.7	6.0	16	0.4	0.19	125*	3.7	1.2	<0.1	0.05	4.6		7.5*	-0.62	7.1
EBL-4	0-120	13.3	4.8	15	0.9	<0.06	96*	9.0*	0.8	<0.1	0.05	7.7		6.7*	-1.79	1.4
EBL-4	120-198	1.6	0.6	78	0.4	<0.06	213*	1.6	1.7	0.4	0.03	15.8	2.16†	10.9*	0.44	1.2
EBL-4	198-396	3.6	0.9	72	0.4	<0.06	186	2.0	30.7	0.3	0.04	12.8		10.2	0.83	7.8
EBL-4	396-489	279	2.0	845	2.8	3.49	71*	77	1780	3.5	5.74	6.1		7.7	0.12	2.1

*Field analysis - field pH values were measured in a flow cell.
†WNRE lab analysis.

S.I.$_c$ = Calcite saturation index = $\log \frac{IAP}{K_T}$ where IAP = ion activity product and K_T is the equilibrium constant for the reaction $CaCO_3 \rightleftharpoons Ca^{2+} + CO_3^{2-}$

C.B. = Charge balance.

Note: Concentrations are in milligrams per litre; alkalinity is reported as milligrams per litre bicarbonate.

Table 14. Summary of 1984 Trace Metal Concentrations ($mg \cdot L^{-1}$) in Ground Waters from the P-Series and EBL-Series Boreholes

Borehole	Depth (m)	Fe	Mn	Ni	Zn	Cr
P-1	32-53.3	0.11	<0.04	<0.06	<0.02	<0.06
P-2	24.5-38.1	<0.04	<0.04	<0.06	<0.02	0.13
P-3	0-16	0.37	0.12	<0.06	0.40	0.12
P-3	16-38.1	<0.04	<0.04	<0.06	0.07	0.07
P-4	0-35	<0.04	<0.04	<0.06	0.15	0.18
P-5	0-22	0.06	<0.04	<0.06	0.27	0.25
P-5	88.5-97.6	<0.04	<0.04	<0.06	0.18	0.09
P-6	0-68	<0.04	<0.04	<0.06	<0.02	<0.06
P-7	0-39.6	<0.04	<0.04	<0.06	0.04	<0.06
P-8	0-20	0.18	0.05	0.11	1.66	<0.06
P-9	0-12	0.53	0.05	<0.05	0.03	<0.06
P-9	12-43.2	0.30	0.05	<0.06	0.94	<0.06
P-10	0-34.5	<0.04	0.06	0.11	0.79	0.30
P-10	34.5-38.5	0.15	0.08	0.11	0.51	<0.06
P-10	66.3-70.3	0.26	0.06	<0.06	0.39	0.10
P-10	82-98.7	<0.04	0.05	0.06	0.15	<0.06
P-11	0-49.2	0.23	0.25	<0.06	0.13	0.13
P-12	0-37	0.07	0.06	<0.06	0.10	0.15
P-12	38-48.6	0.08	0.05	<0.06	0.18	<0.06
P-13	0-22	<0.04	<0.04	<0.06	0.05	0.10
P-14	0-43.3	0.13	0.08	<0.06	0.12	<0.06
EBL-1	147-298	<0.04	<0.04	<0.06	<0.02	<0.06
EBL-1	298-512	0.14	<0.04	<0.06	<0.02	0.09
EBL-1	512-650	<0.04	0.13	<0.06	0.04	<0.06
EBL-2	0-75	18.7	0.82	<0.06	0.42	0.09
EBL-2	75-248	1.13	<0.04	0.13	<0.02	<0.06
EBL-2	248-460	0.30	<0.04	<0.06	0.08	0.09
EBL-2	460-616	0.12	0.13	0.15	0.39	<0.06
EBL-2	616-836	0.14	0.79	0.13	0.15	<0.06
EBL-3	0-443	<0.04	0.14	<0.06	0.10	0.16
EBL-4	0-120	3.2	0.22	<0.06	0.18	0.17
EBL-4	120-198	<0.04	<0.04	<0.06	<0.02	<0.06
EBL-4	198-396	<0.04	<0.04	0.07	0.06	<0.06
EBL-4	396-489	<0.04	<0.04	<0.06	0.04	0.19

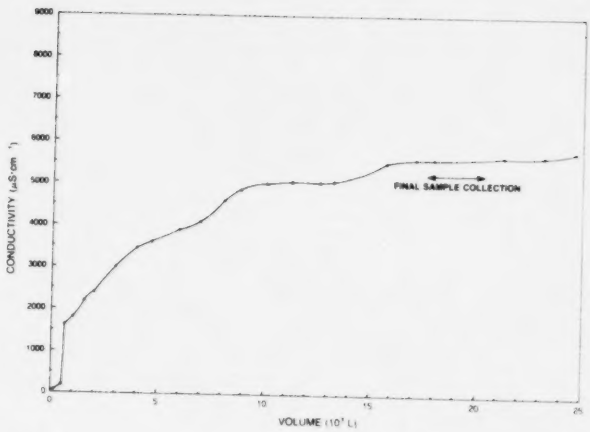

Figure 30. Plot of electrical conductivity vs. volume of water withdrawn from EBL-4 (429-456 m) in 1985.

Most of the water sampled from EBL-1 (504-650 m) in 1985 was produced from the 504-537 m casing-packer interval, since the four pumping ports below this depth were found to produce very little water. The water chemistry is similar to that recovered from the swabbed interval of 298-512 m in 1984 (Table 13). Based on fracture information it is likely that a fracture zone between 504 and 512 m (possibly at 510 m; see Section on Borehole EBL-1 in Chapter 4) produced most of the water during both the 1984 and 1985 tests. Approximately 7800 L of water was withdrawn from this zone in 1985, and the Rhodamine WT concentration was 7 $\mu g \cdot L^{-1}$ compared with a concentration of 24 $\mu g \cdot L^{-1}$ in the final samples from the 298 to 512 m interval in 1984.

The high hydraulic conductivity fracture at the base of the troctolite was also sampled in 1985 in borehole EBL-2 (111-126 m). Approximately 3700 L of ground water was withdrawn from this zone and the final Rhodamine WT concentration was 0.6 $\mu g \cdot L^{-1}$. The chemistry of this

Table 15. The Most Representative Chemical Analyses (major and minor elements) of Ground-Water Samples Collected from Selected Intervals in the EBL-Series Boreholes, 1985

Borehole	Depth (m)	Ca^{2+}	Mg^{2+}	Na^{+}	K^{+}	Sr^{2+}	Alk	SO_4^{2-}	Cl^{-}	F^{-}	Br^{-}	Si	pH	$S.I._c$	C.B. (%)
EBL-1	204-213	2.6	0.7	76	0.04	<0.06	190	3.5	17.8	<0.1	0.17	13.5	9.9*	0.57	2.4
EBL-1	504-650	8.5	0.3	205	0.10	0.09	69	14.5	310	0.6	1.66	19.3	9.8*	0.55	4.2
EBL-2	111-126	3.0	1.0	66	2.44	<0.06	172	3.4	6.8	<0.1	0.04	10.2	10.1*	0.70	1.7
EBL-4	105-117	1.3	2.9	60	0.75	<0.06	150	2.9	3.1	<0.1	<0.02	8.9	9.1	-0.31	6.0
EBL-4	429-456	455	2.2	1160	3.4	6.2	14	108	2580	0.6	10.8	9.2	8.5*	0.23	1.2

*Field analysis - field pH values were measured in a flow cell.

$S.I._c$ = Calcite saturation index = $\log \frac{IAP}{K_T}$ where IAP = ion activity product and K_T is the equilibrium constant for the reaction $CaCO_3 \rightleftharpoons Ca^{2+} + CO_3^{2-}$

C.B. = Charge balance.

Note: Concentrations are in milligrams per litre; alkalinity is reported as milligrams per litre bicarbonate.

Table 16. Representative Trace Metal Concentrations ($mg \cdot L^{-1}$) in Ground Waters from Selected Intervals in the EBL-Series Boreholes, 1985

Borehole	Depth (m)	Cu	Fe	Mn	Ni	Zn	Cr	Pb
EBL-1	204-213	<0.02	0.56	<0.02	<0.06	0.02	0.09	0.12
EBL-1	504-650	<0.02	0.06	0.02	<0.06	<0.02	0.11	0.10
EBL-2	111-126	<0.02	0.58	<0.02	0.16	<0.02	0.12	<0.10
EBL-4	105-117	<0.02	0.10	<0.02	0.06	<0.02	<0.06	<0.10
EBL-4	429-456	0.02	0.13	<0.02	0.30	0.04	0.07	0.12

Table 17. Dissolved Gas Composition of East Bull Lake Ground Waters

Borehole	Depth (m)	Total gas ($cc \cdot kg^{-1}$)	He (vol. %)	N_2 (vol. %)	O_2 (vol. %)	Ar (vol. %)	CO_2 (vol. %)	H_2 (vol. %)	CH_4 (vol. %)
P-1	32-53.3	22.8	<0.01	92.30	5.06	1.83	0.79	–	–
P-3	0-16	35.6	<0.02	72.40	1.36	1.44	24.80	<0.02	–
P-3	16-38.1	25.8	<0.02	95.60	0.18	2.04	0.27	1.87	–
P-4	0-35	30.3	<0.01	84.90	0.61	1.75	12.70	–	–
P-5	0-22	25.2	<0.02	96.50	0.56	1.86	1.11	–	–
P-5	88.5-97.6	46.3	<0.02	94.10	3.39	1.76	0.74	–	–
P-6	0-68	20.1	<0.02	85.3	6.08	1.67	7.00	<0.02	–
P-8	0-20	9.0	<0.02	79.20	0.64	1.54	18.40	0.17	0.08
P-9	0-12	46.8	<0.05	58.40	0.64	1.17	39.80	<0.05	<0.05
P-10	34.5-38.5	77.9	<0.02	81.30	11.10	0.94	6.52	0.16	0.04
P-10	82-98.7	21.5	<0.02	90.00	2.98	1.36	5.68	<0.02	<0.02
P-11	0-49.2	32.9	<0.02	64.20	0.04	1.40	34.20	0.20	<0.02
P-12	38-48.6	21.6	<0.05	96.00	1.32	1.78	0.95	<0.05	<0.05
P-13	0-22	33.2	<0.02	94.70	1.87	1.75	1.59	0.07	<0.02
P-14	0-43.3	24.2	<0.05	83.90	0.71	1.88	13.50	<0.05	<0.05
EBL-1	147-298	24.5	<0.01	96.50	0.57	1.99	0.97	–	–
EBL-1*	204-213	31.8	0.46	91.10	0.32	6.51	0.65	0.41	0.61
EBL-1	298-512	27.8	1.39	94.70	1.94	1.57	0.34	–	–
EBL-1*	504-650	27.5	1.16	94.50	0.04	1.79	0.08	1.86	0.52
EBL-2	75-248	35.2	<0.05	96.00	1.09	2.39	0.51	<0.05	<0.05
EBL-2*	111-126	26.1	<0.02	96.10	1.50	1.88	0.18	0.07	0.28
EBL-3	0-443	24.0	<0.05	79.60	3.99	1.63	14.80	<0.05	<0.05
EBL-4	8-120	52.5	<0.01	61.80	3.23	1.42	33.50	–	–
EBL-4	120-198	27.6	<0.02	90.00	2.01	1.84	6.12	–	–
EBL-4*	429-456	41.3	6.72	89.50	0.12	1.59	0.67	0.04	1.37

*Denotes 1985 analysis.

Table 18. Helium and Neon Concentrations and $^3He/^4He$ Ratios in 1984 EBL Ground Waters

Borehole	Depth (m)	He (meas.)	He (corr.)	Ne (meas.)	$^3He/^4He$ (corr.)
P-3	0-16	9.14×10^{-8}	6.26×10^{-8}	3.1×10^{-7}	2.58×10^{-6}
P-3	16-38.1	2.56×10^{-7}	2.24×10^{-7}	3.2×10^{-7}	3.72×10^{-7}
P-5	0-22	1.54×10^{-6}	1.45×10^{-6}	5.4×10^{-7}	9.44×10^{-8}
P-5	88.5-97.6	2.15×10^{-6}	2.02×10^{-6}	6.5×10^{-7}	0.81×10^{-7}
P-6	0-68	6.37×10^{-8}	4.93×10^{-8}	2.6×10^{-7}	1.94×10^{-6}
P-7	0-39.6	8.04×10^{-8}	5.74×10^{-8}	2.9×10^{-7}	1.29×10^{-6}
P-8	0-20	1.78×10^{-7}	1.66×10^{-7}	2.5×10^{-7}	6.19×10^{-7}
P-10	0-34.5	1.83×10^{-7}	1.66×10^{-7}	2.7×10^{-7}	1.15×10^{-6}
P-10	35.5-38.5	3.15×10^{-7}	2.89×10^{-7}	3.0×10^{-7}	6.58×10^{-7}
P-10	66.3-70.3	4.42×10^{-7}	4.07×10^{-7}	3.3×10^{-7}	3.43×10^{-7}
P-10	82-98.7	3.84×10^{-7}	3.49×10^{-7}	3.3×10^{-7}	2.49×10^{-7}
P-11	0-49.2	6.91×10^{-8}	5.47×10^{-8}	2.6×10^{-7}	1.59×10^{-6}
P-12	38-48.6	1.56×10^{-6}	1.52×10^{-6}	3.6×10^{-7}	9.60×10^{-8}
P-13	0-22	1.59×10^{-6}	1.56×10^{-6}	3.1×10^{-7}	8.56×10^{-8}
P-14	0-43.3	6.63×10^{-8}	4.90×10^{-8}	2.7×10^{-7}	3.04×10^{-6}
EBL-1	147-298	4.33×10^{-6}	4.26×10^{-6}	4.4×10^{-7}	3.47×10^{-8}
EBL-1	298-512	7.70×10^{-4}	7.62×10^{-4}	2.8×10^{-5}	5.34×10^{-9}
EBL-1	512-650	2.60×10^{-6}	2.60×10^{-6}	1.9×10^{-7}	4.17×10^{-8}
EBL-4	0-120	2.51×10^{-3}	2.51×10^{-3}	1.3×10^{-6}	1.73×10^{-8}
EBL-4	120-198	8.25×10^{-7}	7.62×10^{-7}	4.3×10^{-7}	2.41×10^{-6}

Note: Measured He concentrations and $^3He/^4He$ ratios have been corrected ($He_{corr.}$) assuming Ne concentrations greater than solubility (2.1×10^{-7} cc STP/g H_2O at 5°C) are the result of air contamination. All concentrations are in cc STP/g H_2O.

Table 19. Isotopic Composition of 1984 East Bull Lake Ground Waters

Borehole	Depth (m)	^{18}O ‰SMOW	^{2}H ‰SMOW	^{3}H (T.U.)	^{34}S ‰CDT	^{18}O-SO_4 ‰SMOW	^{13}C ‰PDB	^{14}C (%MOD)
P-1	32-53	-11.8	-82.2	N.D.	+4.0	+3.5	-17.6	7.8
P-2	24.5-38	-11.9	-86	20	–	–	-14.5	30.0
P-3	0-16	-11.9	-85.1	44	+4.6	+6.5	-22.0	14.2
P-3	16-38	-12.0	-87.2	N.D.	+6.8	+7.5	-14.2	12
P-4	35-55	-11.5	-88	50	+3.5	+6.4	–	–
P-5	0-22	-15.8	-124	N.D.	+16.0	+8.7	-12.8	75
P-5	88.5-97.6	-17.8	-136	26	+21.2	+6.2	–	32.7
P-6	0-68	-11.7	-80.9	49	+3.7	+8.5	-17.1	25.3
P-7	0-39	-10.2	-73	59	+10.1	+6.1	–	–
P-8	0-20	-10.5	-76.9	77	+8.2	+5.7	-20.5	N.D.
P-9	0-12	-11.6	-80.7	53	+3.7	+5.2	-22.3	100
P-9	12-43	-11.6	-83.9	62	–	–	–	–
P-10	0-34.5	-11.5	-79.1	69	+6.3	+8.9	-23.9	132
P-10	34.5-38.5	-11.3	-78.5	53	+5.8	+7.0	-21.1	117
P-10	66.3-70.3	-11.2	-79.1	37	+1.6	+9.1	-20.5	79
P-10	82-98.7	-11.2	-79.8	22	+8.4	+7.1	-19.4	63
P-11	0-49.2	-11.2	-81.3	33	+11.2	+9.8	-25.1	–
P-12	0-37	-11.6	-80.2	18	+13.5	+10.8	-17.3	–
P-12	38-49	-12.0	-83.0	19	+11.6	+9.7	-17.2	52
P-13	0-22	-11.9	-84.2	N.D.	+4.0	+10.2	-16.1	69
P-14	0-43	-11.8	-82.6	92	+3.4	+3.4	-17.5	35.0
EBL-1	147-298	-13.8	-111	72			-15.2	38
EBL-1	298-512	-12.4	-95	13			-18.9	–
EBL-1	512-650	-11.4	-84	32	+30.3	+8.9		
EBL-2	0-75	-10.4	-74.6	53				
EBL-2	75-248	-14.1	-103.4	15				
EBL-2	248-460	-13.5	-103.2	34				
EBL-2	460-616	-8.7	-65.4	48				
EBL-2	616-836	-8.6	-67.0	62	+6.9	+6.8		
EBL-3	0-443	-11.4	-79.8	66			-18.9	39
EBL-4	0-120	-10.9	-76.7	25			-19.2	44
EBL-4	120-198	-15.0	-104.9	N.D.	+4.6	+8.7	-11.9	–
EBL-4	198-396	-14.1	-103.8	23				
EBL-4	396-489	-11.4	-78.0	24				

SMOW = Standard mean ocean water.
CDT = Canyon Diablo troilite.
PDB = Pee Dee *Belemnitella americana*.
MOD = Modern.
N.D. = Not detected.

Note: The precision of the tritium analyses is ±10 T.U.

water is similar to the chemistry of the ground water sampled from the basal troctolite in borehole EBL-1 (204-213 m).

The other zone sampled in 1985 (EBL-4, 105-117 m) was the high hydraulic conductivity fracture zone associated with the pegmatite subunit in the layered gabbro. This zone probably produces a significant amount of the water which flows down the borehole when it is left open (see Section on Borehole EBL-4 in Chapter 4).

The dissolved gas composition of EBL ground waters is shown in Table 17, and the He and Ne concentrations and $^{3}He/^{4}He$ ratios as determined by W.B. Clarke are shown in Table 18. The isotopic composition of the ground waters is listed in Table 19.

1984 Sampling

Major and Minor Elements and Trace Metals

Ground waters in the P-series boreholes are generally of the Na/HCO_3 or Ca/HCO_3 type with low TDS (<200 $mg \cdot L^{-1}$) and low chloride (0.2-2.8 $mg \cdot L^{-1}$) concentrations. There is a clear trend for the Ca/HCO_3 type to evolve to Na/HCO_3 waters with depth and also laterally along the inferred direction of ground-water flow (see Section on

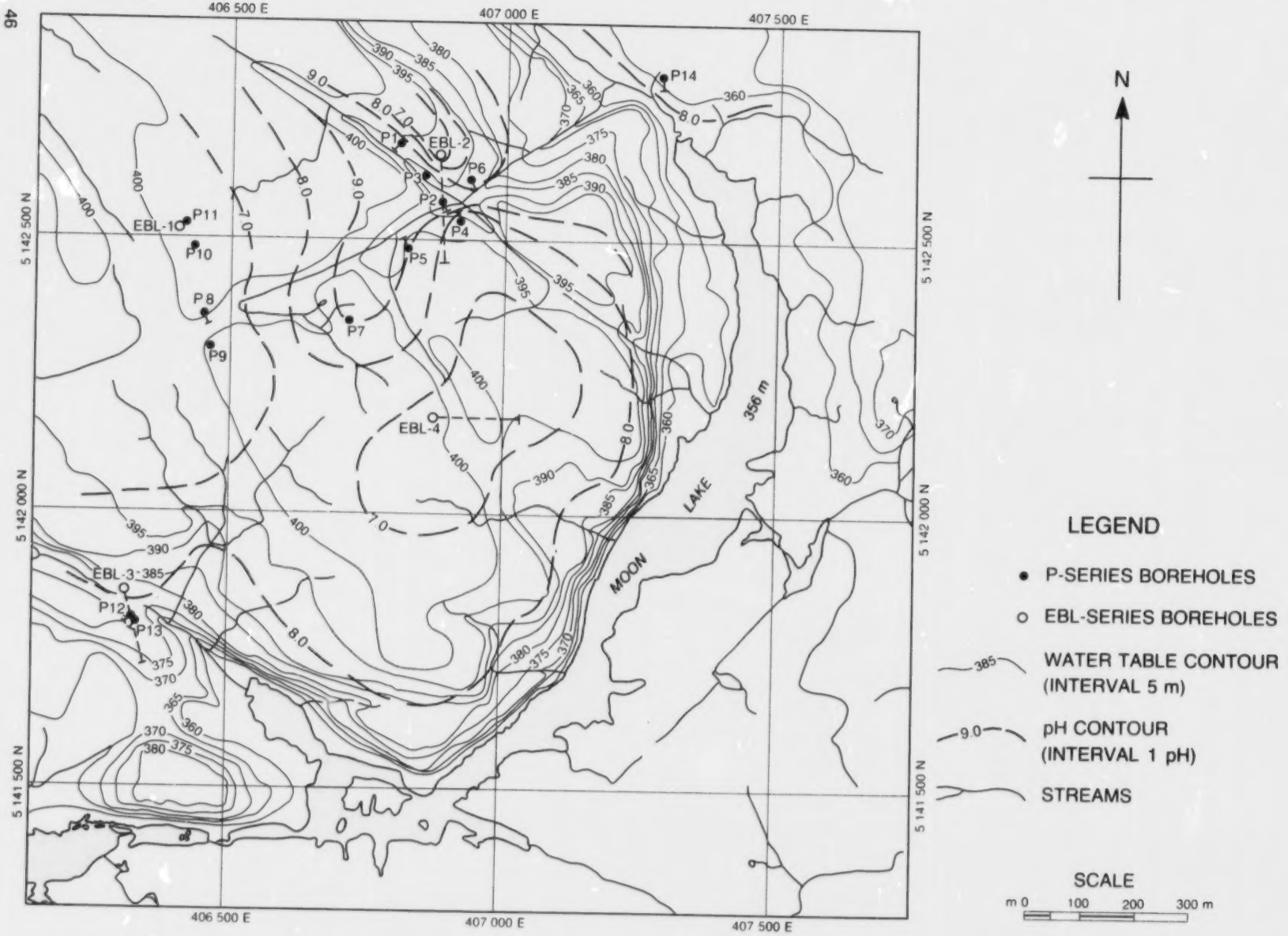

Figure 31. Water table map for EBL based on water-level measurements in all boreholes on May 2, 1984 and the topography of the area. Also shown are pH contours for the shallow ground water (< 100 m) based on maximum measured values in each borehole during 1984.

P-Series Boreholes in Chapter 6, and Fig. 31). Associated with the Ca/HCO_3 to Na/HCO_3 evolution is a large increase in pH, which ranges from 6.1 in areas of suspected groundwater recharge (P-8, P-10, P-11) to 9.6 in areas of groundwater discharge (i.e. flowing boreholes P-2 and P-3). The Ca/HCO_3 ground waters are also undersaturated with respect to calcite, whereas the Na/HCO_3 waters are saturated or supersaturated. Other notable characteristics are the higher Mg^{2+} concentrations in the Ca/HCO_3 waters; the high K^+ concentrations in boreholes P-9, P-11, P-12, P-13; and the high SO_4^{2-} concentrations in P-9, P-12 and P-13. Compared with granitic terrain areas, the Sr^{2+} concentrations in the P-series ground waters are very low.

The ground water above the top PIP in boreholes EBL-2 and EBL-4 was of the Ca/HCO_3 type as was the ground water sampled during open hole pumping of EBL-3. The zone above the top PIP in EBL-1 was not sampled. Since the drill rod had been left connected to the top PIP in EBL-2 and EBL-4 over the winter, these zones were contaminated with iron (up to 22 $mg \cdot L^{-1}$ in EBL-2). With increasing depth the water chemistry changes from Ca/HCO_3 to Na/HCO_3 and then to Na/Cl. The highest TDS water (3100 $mg \cdot L^{-1}$) was observed at a depth of 396-489 m in EBL-4 and is provided by a large fracture zone at a depth of about 454 m. High pH ground waters (as high as 10.4) occur in each of EBL-1, 2 and 4, and this has resulted in relatively large Si concentrations via the dissociation of silicic acid ($pK_1 \simeq 9.8$). These waters are also saturated with respect to calcite. The saline Na/Cl waters have lower pH values and alkalinity but significantly higher concentrations of Br^-, F^-, and Sr^{2+} than the Na/HCO_3 waters.

Representative trace metal concentrations (Fe, Mn, Ni, Zn and Cr) in the EBL ground waters are listed in Table 14. Concentrations of Cu, Pb and Al in all samples were below their detection limits of 0.03, 0.10 and 0.40 $mg \cdot L^{-1}$, respectively. The high iron concentrations measured in the EBL boreholes are probably the result of contamination from the drill rods. This is particularly noticeable in samples from zones in EBL-2 at 0-75 m and 75-248 m, and in EBL-4 at 0-120 m. The most important observation is the high Cr concentration in some zones which does not appear to be related to contamination based on the apparent lack of correlation between Cr concentrations and other metals. Chromium is known to be relatively abundant in pyroxenes and olivine, and may occur as chromite. These minerals are the most likely source of Cr in the EBL ground waters. The Ontario drinking water standard for Cr (as Cr^{6+}) is 50 $\mu g \cdot L^{-1}$, a level which may be exceeded in at least 16 of the analyses listed in Table 14. However, only total Cr was measured in these samples, not the Cr speciation (Cr^{6+} or Cr^{3+}).

Dissolved Gases

Nitrogen is the major gas present in the EBL ground waters, which is not unexpected considering that it comprises 78% of the atmosphere. Figure 32, however, shows that these ground waters contain much larger N_2 concentrations than can be explained by the temperature-dependent solubility of atmospheric N_2 in water. Line "A" in Figure 32 shows the Ar-N_2 solubility relationship at various temperatures in water that is in equilibrium with the atmosphere (WEA) at 1 atm. pressure. Argon is generally a conservative atmospheric gas and is therefore a convenient parameter with which other gas concentrations in ground waters may be compared. Lines "B" and "C" show the Ar-N_2 concentrations as a function of temperature that would result by the addition of 10 $mL \cdot kg^{-1}$ and 20 $mL \cdot kg^{-1}$ H_2O, respectively, of excess air to air-equilibrated water.

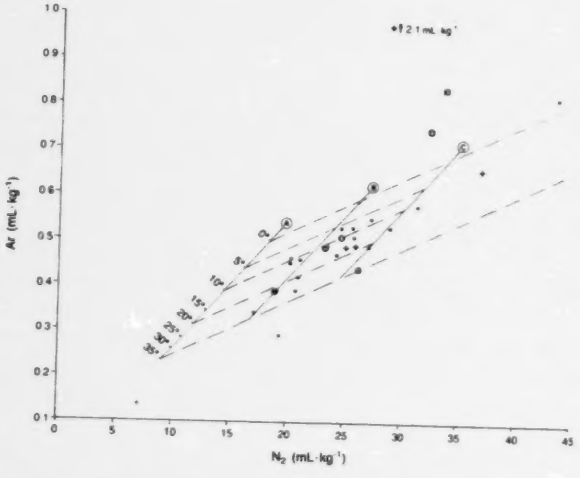

Figure 32. Concentrations of N_2 and Ar in the EBL-series (open circles and crosses) and P-series (solid circles) ground waters. Line *A* is the Ar-N_2 solubility relationship at various temperatures for water equilibrated with the atmosphere (WEA) at 1 atm. pressure. Lines *B* and *C* depict the Ar-N_2 concentrations that would result from the addition of 10 and 20 $mL \cdot kg^{-1}$ H_2O, respectively, of air to WEA.

The ground waters should plot close to line "A" if there is no other source of N_2 or Ar for these waters. Almost all these waters, however, exhibit large excesses of N_2. Contamination by N_2 leaking from packers or pumps used for sampling might be responsible for excess N_2 in some samples, but we observed no physical indications during sampling that such leaks were occurring. Moreover, the magnitude of the N_2 excess produced by leaks would be highly non-reproducible compared with the consistently large N_2 excesses actually observed. Denitrification is not

likely to be responsible for the N_2 excess, since NO_3^- concentrations in these ground waters are generally <0.2 $mg \cdot L^{-1}$.

The most likely mechanism responsible for excess N_2 in these waters is the trapping of air bubbles and eventual solution of these bubbles by infiltrating water in the unsaturated zone (Heaton and Vogel, 1981; Vogel *et al.*, 1981). Indeed, many of the EBL samples fall near a line joining the 10°C WEA position with varying amounts of excess air (up to ≃20 $mL \cdot kg^{-1}$ H_2O). A mean annual ground-water recharge temperature at EBL of 5°C to 10°C is probably reasonable, since the average annual temperature is about 3.8°C (Leech and Cooper, 1982). Excess Ar, possibly related to weathering of K-rich minerals such as biotite, is present in three EBL-series borehole ground waters. Samples plotting well below the 10°C line (i.e. Ar deficiency), however, are more difficult to explain, since the high temperatures suggested for the initial air equilibration are unrealistic. A nitrogen-isotope study of the gaseous nitrogen would help resolve the origins of the excess N_2 (Vogel *et al.*, 1981).

The solubility of atmospheric He at 5°C is 4.8×10^{-8} cc STP/g H_2O with a $^3He/^4He$ ratio of 1.36×10^{-6}. Air injection into the sample during sampling or analyses will increase the He concentration above solubility, as will the incorporation of excess air during ground-water recharge as discussed earlier. To determine the amount of radiogenic He present in the sample (derived from the alpha decay of actinide elements in the rocks), it is necessary to subtract the air-injected component from the measured concentration. The solubility of atmospheric neon is 2.1×10^{-7} cc STP/g H_2O at 5°C and does not vary significantly with temperature. Therefore measured He concentrations can be corrected for air contamination by assuming that measured neon concentrations in excess of 2.1×10^{-7} cc STP/g H_2O are due to an air component and this, in fact, is what has been done in Table 18.

Corrected He concentrations range from 4.90×10^{-8} to 2.02×10^{-6} in the P-series ground waters and from 7.62×10^{-7} to 2.51×10^{-3} in the EBL-series ground waters. Thus significant amounts of radiogenic He are present in most of the EBL ground waters, but these values are generally much lower than in the Lac du Bonnet granitic batholith where uranium enrichment is present on fracture minerals (Bottomley *et al.*, 1984). In contrast, both the ground water and rock of the EBL pluton are low in uranium (Bottomley *et al.*, 1986). Several P-series ground waters have low He concentrations and $^3He/^4He$ ratios greater than atmospheric as the result of ^3He production from tritium decay.

Environmental Isotopes

The isotopic composition of East Bull Lake ground waters is listed in Table 19. The ^{18}O and ^2H compositions are shown in Figure 33, which also shows the Global Meteoric Water Line ($\delta^2H = 8\,\delta^{18}O + 10$) of Craig (1961). The $\delta^{18}O$ content of the P-series ground waters is generally between -11.0 ‰ and -12.0 ‰, and these waters plot close to the global meteoric water line. These values can be taken as representative of modern ground water recharged under present climatic conditions. Borehole P-5, which is the deepest of the P-series boreholes, has an unusual isotopic composition because the top zone (0-22 m) is about 4 ‰ lighter in $\delta^{18}O$ and the bottom zone (88.5-97.6 m) 6 ‰ lighter relative to the other P-series ground waters. The chemistry of P-5 is not dissimilar to the other Na/HCO_3 P-series ground waters, suggesting that recharge conditions for P-5 ground water were climatically quite different from the other ground waters but the hydrogeochemical evolutionary processes have remained unchanged. The present day mean annual isotopic composition of precipitation is reflected in the isotopic composition of other P-series ground waters. Borehole P-5 also has an unusually heavy $\delta^{34}S$ composition, again reflecting sources or processes (possibly sulphate reduction) not experienced by the other P-series ground waters which have $\delta^{34}S$ and $\delta^{18}O$-SO_4 contents similar to precipitation-sulphate in the Great Lakes Basin (Nriagu and Coker, 1978). The positive $\delta^{18}O$-SO_4 values suggest sulphide oxidation by meteoric water has not been a major source of dissolved sulphate in the P-series ground waters.

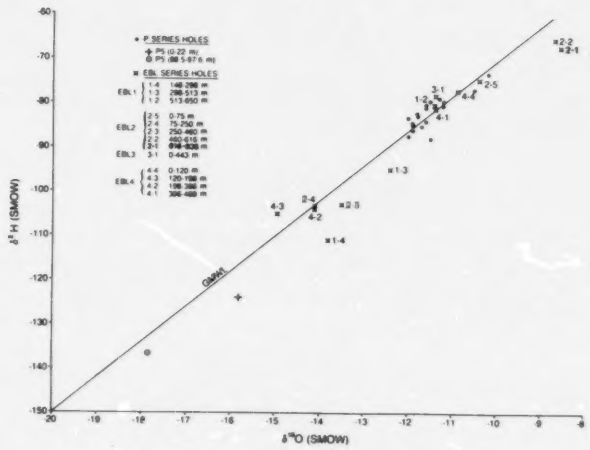

Figure 33. Plot of the stable isotope (^{18}O-^2H) compositions of EBL ground waters based upon the most representative sample collected from each test interval. Also shown is the Global Meteoric Water Line (GMWL) of Craig (1961). SMOW – Standard mean ocean water.

The ^{18}O-^{2}H compositions of ground waters in boreholes EBL-1 to EBL-4 are all heavier than P-5, but several zones contain ground water lighter than the other P-series ground waters. These zones contain Na/HCO_3 waters, whereas the Na/Cl waters tend to plot near the P-series ground waters or are even heavier. This could reflect the fact that these Na/Cl waters were severely contaminated with isotopically heavier drill water which had $\delta^{18}O$ values of -7 ‰ to -9.5 ‰ (Raven *et al.*, 1984).

The ^{18}O-^{2}H data have thus identified Na/HCO_3 waters that are isotopically depleted with respect to modern, shallow ground water in the EBL pluton. These waters appear to have been recharged under considerably cooler climatic conditions or else reflect the presence of a glacial meltwater component at the time of recharge, as suggested by the very light ground waters in P-5. The presence of tritium in the EBL boreholes confirms the Rhodamine WT results which indicate that the *in situ* ground water has been contaminated with drill water (18-74 T.U.). Therefore the actual ^{18}O-^{2}H compositions of these waters may be isotopically lighter than shown in Figure 33.

The low ^{14}C activities in waters from P-1, P-3 and P-8 are unusual, considering their light $\delta^{13}C$ values and the fact that most of the fracture calcites in the pluton have $\delta^{13}C$ values near -3 ‰ (Bottomley, unpublished data). Therefore, although ^{14}C dilution by dead carbon may explain the low ^{14}C activities, the dead carbon-14 source appears to be light in $\delta^{13}C$. This suggests that methane oxidation may have to be considered as a source of shallow water carbonate as well as mixing of older and deeper ground water with shallow younger water. Carbon-14 age modelling will be conducted when all analyses have been received and the results discussed in a later paper.

1985 Sampling

Sampling of selected intervals in 1985 confirmed the presence of high pH, Na/HCO_3 ground water supersaturated with respect to calcite in the high hydraulic conductivity fracture zone at the base of the troctolite in boreholes EBL-1 and EBL-2 (Table 15). This water also contains relatively high Fe concentrations (Table 16). Nitrogen is the major dissolved gas in the troctolite fracture zone, but significant amounts of CH_4 and H_2 are present, as is He in borehole EBL-1. Very large concentrations of dissolved Ar are also present in the troctolite zone in EBL-1 (Fig. 32), suggesting a mineral source for the excess Ar.

Sampling in 1985 also confirmed the presence of saline Na/Cl ground water, with a TDS of at least 4.3 $g \cdot L^{-1}$ in the fracture zone at a depth of about 454 m in EBL-4. If continuation of pumping had been possible even higher salinities would have been expected at this depth. Large concentrations of He and CH_4 were measured in this ground water, but the Ar concentration is of apparent atmospheric origin (Fig. 32).

The water chemistry sampled from the bottom of EBL-1 (504-650 m) in 1985 was not of higher chlorinity than that measured in 1984 at 298-512 m. In fact, the waters are chemically very similar. However, the high Rhodamine WT concentrations still present in this water indicate that contamination with drill water is still severe. It is also likely that a component of shallow ground water is present in this zone, since downward flow would have occurred in this hole when it was left open. Therefore we must conclude that the *in situ* salinity at depth in the vicinity of EBL-1 is unknown. The dissolved gas composition at this depth, however, indicates strongly reducing conditions are present, since concentrations of H_2 and CH_4 are high compared with O_2. This suggests that contamination by relatively shallow ground water (which is itself contaminated with drill water) is more significant than by direct injection of drill water which, presumably, was well oxygenated. If this is the case and if the Rhodamine WT concentration measured in EBL-1 (204-213 m) of 24 $\mu g \cdot L^{-1}$ is representative of the shallow water component, then one can estimate that the *in situ* ground water has been diluted by only about 30% by shallow ground water. This indicates that the *in situ* chlorinity in the fracture zone at 504-512 m is less than 500 $mg \cdot L^{-1}$.

The chemistry of the ground water in EBL-4 (105-117 m) is of the Na/HCO_3 type and is of relatively high alkalinity compared with the saline Na/Cl water at depth. Unfortunately, alkalinity is a non-conservative parameter and cannot be used to estimate the degree of mixing of shallow ground water with the saline water, since mixing of the two waters should cause carbonate precipitation. Moreover, Rhodamine WT concentrations measured during sampling of the upper 200 m of EBL-4 in 1984 were low and similar to the low concentrations observed in the saline ground water during 1985. Therefore for EBL-4, Rhodamine WT is an unsuitable parameter to estimate the dilution of the deep ground water by shallow ground water prior to borehole isolation. The reduced nature of the saline ground water as indicated by the high CH_4 concentration relative to O_2 and the high concentration of He suggests that shallow ground water is likely a more important source of contamination than the direct injection of drill water.

Isotope analyses of samples collected during 1985 have not been completed and will be discussed in detail in a later paper. However, the very light $\delta^{18}O$ water previously

observed only at P-5 has also been measured (-16.4 ‰) in water from the troctolite zone of EBL-2 at 111-126 m. This suggests that this isotopically light water may be present throughout the troctolite zone in the northeastern portion of the pluton. The $\delta^{18}O$ of the saline water collected from the fracture zone at 450 m in EBL-4 in 1985 was -11.9 ‰. This confirms the observation made on the basis of the 1984 measurements that the saline water has an isotopic composition similar to that of the P-series ground waters and to modern precipitation.

DISCUSSION

The East Bull Lake ground water is characterized by distinct hydrogeochemical zonation both areally and vertically, as shown on a trilinear plot of major ion compositions (Fig. 34). The area near the intersection of the 050 and 130 lineaments is an area of ground-water discharge with boreholes P-2 and P-3 having above ground hydraulic heads. The Folson Lake Fault at the southern end of the study area also appears to be a ground-water flow boundary for the shallow flow system defined by the water table map (Fig. 31). Hydraulic head measurements in EBL-3 indicate flow is downward along the fault to a depth of at least 250 m. The Na/HCO_3 ground waters in the P-series boreholes are restricted to these discharge areas. The recharge area is characterized by Ca/HCO_3 waters. The evolution from Ca/HCO_3 to Na/HCO_3 ground water in the P-series boreholes is clearly suggested in the trilinear plot of Figure 34. The transformation of Ca/HCO_3 to Na/HCO_3 ground waters also occurs with increasing depth, as indicated by the analyses of ground waters from the EBL-series boreholes which are characterized by large downward hydraulic gradients. The same phenomenon has been observed at other areas in granitic rocks and at EBL it is likely the result of ion exchange reactions on secondary fracture minerals, since the decrease in Ca^{2+} and Mg^{2+} milliequivalents is nearly balanced by the increase in Na^+. Silicate weathering does not seem to be a likely explanation, since Si concentrations do not show any clear trend during this evolution. Moreover, weathering in the absence of ion exchange would be expected to buffer the Ca concentration. Large increases in Si, however, do occur in the high pH ground waters of the EBL-series boreholes, and this is likely the result of silicic acid dissociation which would promote silicate dissolution.

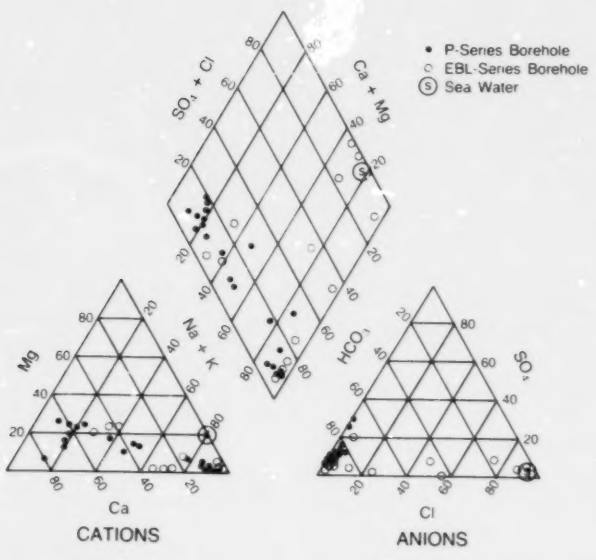

Figure 34. Trilinear plot of the major ion composition (% of total milliequivalents) of EBL ground waters.

Despite the fact that Mg is abundant in the EBL gabbros, Mg concentrations in the ground waters are low with the exception of some of the Ca/HCO_3 ground waters. This is surprising, since Mg in the olivine of the troctolite, for example, should be released much faster than Ca from calcic plagioclase (Siegel and Pfannkuch, 1984). Pyroxenes should also release Mg rapidly. The troctolite unit was sampled in 1984 in EBL-1, 2 and 4 within depth intervals of 148-298 m, 75-250 m, and 120-198 m, respectively, and in EBL-1 and EBL-2 in 1985. In all cases Mg^{2+} concentrations did not exceed 1 $mg \cdot L^{-1}$. Since the troctolite is known to be serpentinized (Ejeckam *et al.*, 1984), it is possible that serpentine, talc, and/or chlorite formation are buffering Mg^{2+} concentrations.

Serpentinization of ultramafic rocks can occur at low temperatures (<100°C), in which case lizardite or chrysotile are the usual serpentine minerals formed (Moody, 1976). Barnes and O'Neil (1969) and Barnes *et al.* (1972) have shown that serpentinization can occur at near surface temperatures in the western United States and that high pH, Ca/OH waters containing very low Mg^{2+} concentrations (<1 $mg \cdot L^{-1}$) are associated with the serpentinization process there. In contrast, weathering of serpentine was found to produce Mg/HCO_3 waters.

Thermodynamic calculations of the ground-water chemistry in the troctolite in boreholes EBL-1, 2 and 4 indicate supersaturation with respect to chrysotile, $Mg_3Si_2O_5(OH)_4$, and undersaturation with respect to forsterite olivine, Mg_2SiO_4, and clinoenstatite pyroxene, $MgSiO_3$. Thus there is the potential for present day serpentinization in which Mg^{2+} released from olivine and pyroxene is conserved. The fact that the EBL troctolite ground waters are Na/HCO_3 in composition rather than Ca/OH could be the result of the previously mentioned Ca^{2+}-Na^+ exchange reactions in water still containing relatively high

concentrations of carbonate alkalinity. Although the troctolite ground waters are saturated with respect to calcite, isotopic measurements of fracture calcites in the troctolite have not identified calcites that may have precipitated from present day ground waters (Bottomley, unpublished data).

The iron released from olivine appears to be largely conserved as iron oxides, although iron concentrations were relatively high in the troctolite ground waters sampled in 1985 (Table 16). At high pH and low E_H the iron could form $Fe(OH)_2$ or Fe_3O_4 (magnetite), the latter having been observed in the serpentinized troctolite by Ejeckam *et al.* (1984). The oxidation of $Fe(OH)_2$ to Fe_3O_4 results in the release of H_2 gas, which has been previously observed in Ca/OH ground waters in serpentinized ultramafic rocks by Barnes *et al.* (1972) and Neal and Stanger (1983). Hydrogen gas has also been observed in some of the EBL ground waters, although a methane origin for the H_2 is also possible. The possibility that serpentinization is presently occurring in the EBL pluton is intriguing and requires further investigation. Oxygen-18 analyses of the serpentine and magnetite would indicate whether the present day ground waters are involved in this process.

The Na/Cl waters are found in the anorthosite unit underlying the gabbro. The anorthosite is highly altered to laumontite ($CaAl_2Si_2O_{12} \cdot 4H_2O$) along fracture surfaces. Since anorthosite is essentially a rock consisting of calcic plagioclase, it is unlikely that rock-water interactions could be responsible for the Na/Cl composition of these waters unless much of the released Ca is fixed into secondary minerals such as laumontite. It is also possible, however, that the Na/Cl composition of these waters is a primary characteristic which reflects the major ion chemistry of water that intruded into the Precambrian basement either as infiltrated sea water or formation water of unknown age. Bromine and chlorine are two relatively conservative elements, and the molar ratio of these elements has frequently been used to identify the origin of saline waters. The EBL Na/Cl waters have Br/Cl ratios of 1-2 $\times 10^{-3}$, which is similar to the sea water ratio of 3.4×10^{-3}. The EBL Br/Cl ratio is considerably smaller than the ratio for saline ground waters and brines (6×10^{-3} to 1.25×10^{-2}) in the Canadian Shield which may be the products of prolonged rock-water interactions (Frape *et al.*, 1984), but is similar to some formation waters reported by Nordstrom (1983). Mixing between an evolved Na/HCO_3 ground water and a modified Na/Cl sea water component could explain the chemistry of the deep EBL-series borehole ground waters (Fig. 34).

The Na/Cl waters have high concentrations of calcium but have Mg^{2+} and K^+ concentrations that are even lower than in many of the P-series ground waters. However, Sr^{2+} concentrations in the Na/Cl waters are many times higher than in the Ca/HCO_3 and Na/HCO_3 waters. The high Ca/Mg ratio of the Na/Cl water demands very effective removal of the Mg^{2+} if a sea water component is responsible for the salinity. Alternatively, if the salinity is the result of intensive rock-water interactions the low Mg^{2+} concentrations do not present a problem because the rock at depth is primarily anorthosite, which consists essentially of calcic plagioclase and which has a high Ca/Mg ratio. The results from the Sr isotope analyses may indicate the origin of the Sr in the Na/Cl waters (McNutt *et al.*, in preparation) and perhaps the origin of the salinity as well.

The ^{18}O-^{2}H composition of the Na/Cl water does not appear to be isotopically light relative to the P-series ground waters, although contamination with isotopically heavy drill water (Raven *et al.*, 1984) may be partly obscuring the area actually occupied by the Na/Cl waters on the ^{18}O-^{2}H plot (Fig. 33). The Na/Cl waters have isotopic compositions that plot close to the P-series ground waters on the meteoric water line, but more detailed sampling is required to determine whether this is the true isotopic end member for the Na/Cl waters or whether these are mixed samples containing a concentrated Na,Ca/Cl component enriched in ^{2}H such as in mine brines from the Canadian Shield (Frape *et al.*, 1984).

Synthesis and Summary

Hydrogeological investigations completed at the East Bull Lake research area have essentially focussed on the reliable measurement of hydraulic conductivity, hydraulic head and ground-water chemistry of a gabbro-anorthosite pluton to depths of 800 m. These measurements are fundamental to the development of a ground-water flow model of the research area and, ultimately, to the assessment of the concept of deep storage and disposal of radioactive wastes in plutonic rocks. In this chapter, the results of the hydrogeological investigations completed at the East Bull Lake research area are summarized, evaluated with respect to their reliability, and interpreted in the context of a regional ground-water flow system.

The hydraulic conductivity of the gabbro-anorthosite has been directly measured using a variety of single-borehole hydraulic test methods and indirectly inferred from the results of other borehole tests and surveys, such as fracture logging, borehole flow-meter surveys, hydraulic head monitoring, and ground-water sampling. Repeated hydraulic testing in both shallow and deep boreholes reliably indicates that the hydraulic conductivity of the rock mass decreases with depth from an average near surface value of 10^{-8} $m \cdot s^{-1}$ to less than 10^{-12} $m \cdot s^{-1}$ below 400 to 500-m depth.

Superimposed on this general hydraulic conductivity-depth trend are several permeable fracture zones that are important to the development of both shallow and deeper regional ground-water flow systems in the research area. Of particular hydrogeological significance are the 050 and 130 structural discontinuities, extensive fracturing associated with the base of the troctolite horizon, fracturing associated with a porphyritic dyke near the basal contact of the mafic pluton and the Folson Lake Fault. Hydraulic testing using various types of packer assemblies shows that these structures have significantly higher hydraulic conductivity than the surrounding rock mass.

The 050 and 130 fracture zones are subvertical and have been associated with two major structural lineaments identified on aerial photographs of the northern half of the research area. The fracture zones are expressed at surface as two linear topographic depressions which channel surface drainage to the northeast and to the southeast to Moon Lake. The fracture zones have average hydraulic conductivities of 0.6–1.0 $\times$ 10^{-7} $m \cdot s^{-1}$ which are about 10 to 50 times higher than the average hydraulic conductivity of the surrounding rock mass. The higher hydraulic conductivity of the fracture zones in conjunction with hydraulic head measurements indicates that the fracture zones are channelways for rapid movement of ground water. The observed hydraulic heads further show that these structures act as both sources and sinks of ground water for the surrounding rock mass and that complex vertical flow regimes are likely to exist within the fracture zones. Components of horizontal flow within each structural lineament are, assuming hydraulic continuity, similar to surface drainage directions.

Fracturing associated with the base of the inclined troctolite unit shows uniform and high hydraulic transmissivity of 1-3 $\times$ 10^{-7} $m^2 \cdot s^{-1}$ in three boreholes at depths of 123–210 m. The transmissivity and hydraulic head measurements indicate that ground water likely drains from the overlying bedrock, flows along the base of the troctolite to the northeast, and discharges at surface where the unit outcrops in the topographic depression between the north end of Moon Lake and Little Bull Lake.

Fracturing observed along the contact of a porphyritic dyke in borehole EBL-4 near the basal contact of the East Bull Lake mafic pluton has a reproducibly high transmissivity (2-3 $\times$ 10^{-7} $m^2 \cdot s^{-1}$) and low hydraulic head (352 m a.s.l.). This hydraulic head is the lowest equilibrium value recorded in all boreholes at East Bull Lake and is lower than the elevation of adjacent Moon Lake at 355 m a.s.l. The most likely discharge point for this low-head fracture zone is along the Folson Lake Fault in the vicinity of Parisien Lake (elevation 339 m a.s.l.) located 2.5 km southeast of borehole EBL-4. These hydraulic head relations indicate that the fracture zone is part of a more regional-scale flow system which includes the large-scale fracturing of the Folson Lake Fault.

The Folson Lake Fault is a regional-scale fault transecting the southern end of the East Bull Lake research area. The limited hydrogeological data available suggest that the fault is characterized by variable but generally higher hydraulic conductivity and low hydraulic head. It seems likely that ground water flows locally from the

research area to the fault, and along the fault to the southeast toward Parisien Lake.

Directions of ground-water flow in the major fracture zones and in the bulk rock mass are based on reliable measurements of hydraulic head and hydraulic conductivity and assumed structural and hydraulic continuity between observation points. The assumption of hydraulic continuity between observation points is difficult, if not impossible, to evaluate directly from hydraulic interference tests at East Bull Lake because of the large spatial scales and generally low hydraulic conductivity of the bedrock. Lacking hydraulic interference test results, the directions of ground-water flow can be indirectly evaluated from the isotopic and chemical characteristics of the ground water.

Hydraulic head measurements obtained from open boreholes, straddle-packers, PIPs, and multiple-packer casings are generally reproducible to depths of 400-500 m and suggest the following simple ground-water flow system for the East Bull Lake research area. Ground-water flow in the upper 200 m reflects local topography with strong recharge gradients and horizontal flow directed to the northeast to the topographic depressions created by the 050 and 130 fracture zones and to the south of the Folson Lake Fault. Superimposed on these general trends are the flow perturbations created by the 050 and 130 fracture zones and fracturing at the base of the troctolite unit. Between 200-m and 400- to 500-m depth, the hydraulic head measurements are less numerous and less reliable but indicate similar vertical gradients in boreholes EBL-1 and EBL-2, and increased vertical gradients in boreholes EBL-3 and EBL-4. Horizontal components of flow over the depth range are directed to the south and southeast. We suspect that the increased vertical gradients observed in the south and southeast part of the research area and the horizontal flow inferred to the southeast reflect drainage of the rock mass to the Folson Lake Fault possibly along fracturing near the basal contact of the pluton. Below 500-m depth there are only limited hydraulic head measurements in two boreholes (EBL-1 and EBL-2) and these measurements are of questionable reliability. The available data suggest that ground water flows up from depths of 700-800 m and then horizontally to the Folson Lake Fault. These suggested flow directions should be evaluated with more reliable and more numerous hydraulic head and fluid density measurements.

The ground-water chemistry in the upper 250 m of the EBL pluton is controlled by rock-water interactions in the fractures and not by the bulk rock composition. Along the direction of flow, northeasterly toward the intersection of the 050 and 130 lineaments and south toward the Folson Lake Fault, the ground-water chemistry changes from the Ca/HCO_3 to the Na/HCO_3 type primarily because of ion exchange reactions. The Ca/HCO_3 waters and the shallow Na/HCO_3 waters in the P-series boreholes (with the exception of P-5) have ^{18}O and ^{2}H compositions that are meteoric in origin and similar to that of the present day average annual precipitation. The deeper Na/HCO_3 waters found in P-5 and the EBL-series boreholes have isotopically lighter values. The very light values observed in P-5 and EBL-2 (111-126 m) suggest a glacial meltwater component may be present in these waters. Their presence and restriction to these zones suggest that the establishment of the post-glacial ground-water flow systems in this area has not yet flushed (to the northeast) the last remnants of glacial meltwater recharge from the large fracture zone at the base of the troctolite.

The Na/Cl water found at depth in the pluton appears to reflect the presence of either a modified sea water or ancient formation water component that infiltrated into the crystalline basement rocks. The age of this saline component is unknown, but its presence in the high hydraulic conductivity, low hydraulic head fracture zone at 454 m in EBL-4 together with the large volume of water withdrawn from this zone in 1985 suggests it is part of an active regional flow system. The high He concentration in the saline water of EBL-4 (Table 17) may be used to estimate the residence time of this water subject to certain assumptions and constraints as discussed by Bottomley *et al.* (1984). Assuming a total rock porosity of 1% and U and Th concentrations in the rock of 1 and 3 $\mu g/g$, respectively, a residence time of about 50 million years is calculated. Whether this age is reasonable depends on how closely the requisite assumptions of the helium dating technique are matched. Certainly, the U and Th concentrations assumed for the gabbro-anorthosite rocks are not too low, and there is no evidence for enrichment on the fractures (Kamineni, AECL, pers. comm.). Nevertheless, upward leakage of He from the underlying granitic rocks or from surrounding uranium-rich Precambrian metasedimentary rocks cannot be discounted at this time.

References

Aitchison, J., and J.A.C. Brown. 1957. The lognormal distribution. Cambridge University Press, Monograph 5, Cambridge, pp. 30-33.

Barnes I., and J.R. O'Neil. 1969. The relationship between fluids in some fresh alpine-type ultramafics and possible modern serpentinization, western United States. Geol. Surv. Am. Bull. 80: 1947-1960.

Barnes I., J.B. Rapp, J.R. O'Neil, R.A. Sheppard, and A.J. Gude. 1972. Metamorphic assemblages and the direction of flow of metamorphic fluids in four instances of serpentinization. Contrib. Mineral. Petrol. 35: 263-276.

Born, P. 1978. Geology of the East Bull Lake layered complex, District of Algoma, Ontario. Unpub. M.Sc. Thesis, Laurentian University, Sudbury, Ontario.

Born, P., and R.S. James. 1978. Geology of the East Bull Lake layered gabbro-anorthosite intrusion, District of Algoma, Ontario. In Current Research, Part A, Geol. Surv. Can. Pap. 78-1A, pp. 91-95.

Bottomley, D.J., J.D. Ross, and W.B. Clarke. 1984. Helium and neon isotope geochemistry of some ground waters from the Canadian Precambrian Shield. Geochim. Cosmochim. Acta, 48: 1973-1985.

Bottomley, D.J., M. Gascoyne, J.D. Ross, and J.T. Ruttan. 1986. Hydrogeochemistry of the East Bull Lake pluton, Massey, Ontario. AECL, Technical Record* TR-382.

Brown, A., and D.C. Kamineni. 1981. Preliminary report on the fracture sets of East Bull Lake pluton, western Ontario. Geological Activities Internal Report. Unpub. report available from Geological Survey of Canada, 601 Booth Street, Ottawa, Ontario, K1A 0E8.

Cooper, H.H., Jr., and C.E. Jacob. 1946. A generalized graphical method for evaluating formation constants and summarizing well field history. Trans. Am. Geophys. Union, 27: 526-534.

Cooper, H.H., Jr., J.D. Bredehoeft, and I.S. Papadopulos. 1967. Response of a finite-diameter well to an instantaneous charge of water. Water Resour. Res., 3(1): 263-269.

Craig, H. 1961. Isotope variations in meteoric waters. Science, 133: 1702-1703.

Ejeckam, R.B., R.I. Sikorsky, and D.C. Kamineni. 1984. Preliminary report of subsurface geology of the East Bull Lake Research Area (RA-7) in northeastern Ontario. Unpub. report RW-GLG-062-84, available from Earth Physics Branch, 1 Observatory Cres., K1A 0Y3.

Ermanovics, I., R.A. Gibb, S.H. Whitaker, and K.G. Raven. 1983. Advances in the geoscience surveys at the East Bull Lake Research Area (RA-7) near Massey, Ontario. In Proc. 16th Information Meeting of the Nuclear Fuel Waste Management Program, AECL, Technical Record* TR-218, pp. 51-73.

Ermanovics, I., N.M. Soonawala, R.A. Gibb, and R. Pearson. 1982. Preliminary results of geoscience surveys at the East Bull Lake Research area (RA-7) near Massey, Ontario. In Proc. 14th Information Meeting of the Nuclear Fuel Waste Management Program (1982 General Meeting), AECL, Technical Record* TR 207, pp. 143-161.

Frape, S.K., P. Fritz, and R.H. McNutt. 1984. Water-rock interactions and chemistry of ground waters from the Canadian Shield. Geochim. Cosmochim. Acta, 48: 1617-1627.

Gringarten, A.C., and H.J. Ramey, Jr. 1974. Unsteady-state pressure distributions created by a well with a single horizontal fracture, partial penetration, or restricted entry. Soc. Petrol. Eng. J., 14(4): 413-422.

Heaton, T.H.E., and J.C. Vogel. 1981. Excess air in groundwater. J. Hydrol., 50: 201-216.

Hvorslev, M.J. 1951. Time lag and soil permeability in groundwater observations. Bull. 36, Waterways Experiment Station, U.S. Army Corps Eng., Vicksburg, Mississippi, 49 pp.

James, R.S., and P. Born. 1985. Geology and geochemistry of the East Bull Lake intrusion, District of Algoma, Ontario. Can. J. Earth Sci., 22(7): 968-979.

Johnson, C.R., R.A. Greenkorn, and E.G. Woods. 1966. Pulse-testing: A new method for describing reservoir flow properties between wells. J. Pet. Technol., 18: 1599-1604.

Jorgensen, D.G., T. Gogel, and D.C. Signor. 1982. Determination of flow in aquifers containing variable-density water. Groundwater Monitoring Rev. 2(2): 40-45.

*Atomic Energy of Canada Ltd. Technical Records are unrestricted unpublished reports available from the Scientific Documents Distribution Office, Atomic Energy of Canada Limited Research Company, Chalk River, Ontario, K0J 1J0.

Kamineni, D.C., G.F. McCrank, D. Stone, R.B. Ejeckam, R. Flindall, and R. Sikorsky. 1984. Geology of the central plateau of the East Bull Lake pluton, northwestern Ontario. In Current Research, Part B, Geol. Surv. Can. Pap. 84-1B, pp. 75-83.

Lee, D.R. 1983. Groundwater discharge zones. In Proc. 15th Information Meeting of the Nuclear Fuel Waste Management Program, AECL, Technical Record* TR-216, pp. 74-79.

Leech, R.E.J., and A.J. Cooper. 1982. Preliminary terrain assessment of three potential research areas in northern Ontario, AECL, Technical Record* TR-196.

Louis, C., and Y.N. Maini. 1970. Determination of the in situ hydraulic parameters in jointed rock. Proc. 2nd Congress of Int. Soc. of Rock Mechanics, Belgrade, Pap. 1-32, pp. 235-245.

Lusczynski, N.J. 1961. Head and flow of groundwater of variable density. J. Geophys. Res., 66(12): 4147-4256.

McCrank, G.F.D., D. Stone, D.C. Kamineni, B. Zayachkivsky, and G. Vincent. 1983. Regional geology of the East Bull Lake area, Ontario. In Current Research, Part A, Geol. Surv. Can. Pap. 83-1A, pp. 457-464.

McCrank, G.F.D., D. Stone, R. Ejeckam, D.C. Kamineni, R.I. Sikorsky, and J. McEwen. 1984. Surface and subsurface geological investigations of the East Bull Lake pluton. In Proc. 17th Information Meeting of the Nuclear Fuel Waste Management, AECL. In press.

McNutt, R.H., S.K. Frape, and P. Fritz. 1984. Strontium isotopic composition of some Precambrian Shield brines. Isotope Geosci. 46: 205-215.

Moody, J.B. 1976. Serpentinization: A review. Lithos, 9: 125-138.

Moore, E.S., and W.S. Armstrong. 1943. Geology of the East Bull Lake area, Algoma District, Ontario. Ontario Department of Mines Rep. 52, Part 6, pp. 1-19.

Neal, C., and G. Stanger. 1983. Hydrogen generation from mantle source rocks in Oman. Earth Planet. Sci. Lett., 66: 315-320.

Nordstrom, K. 1983. Conceptual framework for the chemical processes in the Stripa ground waters. KBS progress report, 83-01, Stockholm, Sweden, pp. 106-115.

Novakowski, K.S., and P.A. Flavelle. 1985. Performance evaluation of multiple-packer casing installations at the Chalk River Nuclear Laboratories and the East Bull Lake study areas. Unpub. National Hydrology Research Institute Report available from Environment Canada, 11 Innovation Blvd., Saskatoon, Sask. S7K 3H8.

Nriagu, J.O., and R.D. Coker. 1978. Isotopic composition of sulphur in precipitation within the Great Lakes Basin. Tellus, 30: 365-375.

Paillet, F.L., and A.E. Hess. 1986. Geophysical well-log analysis of fractured crystalline rocks at East Bull Lake, Ontario, Canada. United States Geological Survey, Water-Resources Investigations Report 86-4052.

Raven, K.G. 1986. Hydraulic characterization of a small groundwater flow system in fractured monzonitic gneiss. National Hydrology Research Institute, Environment Canada, NHRI Paper No. 30, IWD Sci. Ser. No. 149.

Raven, K.G., J.A. Smedley, R.A. Sweezey, and K.S. Novakowski. 1984. Borehole hydrogeologic investigations at the East Bull Lake research area: Summary of 1983 activities. Unpub. NHRI rep., 91 pp.

Redford, S.W. 1983a. A detailed gravity survey of the East Bull Lake intrusion, Research Area RA-7, Algoma District, Ontario. Unpub. Contract Rep., Paterson, Grant and Watson Ltd., Toronto, 9 pp.

Redford, S.W. 1983b. A detailed ground VLF survey of the East Bull Lake intrusion, Research Area RA-7, Algoma District, Ontario. Unpub. Contract Rep., Paterson, Grant and Watson Ltd., Toronto, 7 pp.

Siegel, D.I., and H.O. Pfannkuch. 1984. Silicate dissolution influence on Filson Creek chemistry, northeastern Minnesota. Geol. Soc. Am. Bull. 95: 1446-1453.

Vogel, J.C., A.S. Talma, and T.H.E. Heaton. 1981. Gaseous nitrogen as evidence for denitrification in groundwater. J. Hydrol. 50: 191-200.

Watson, R.K. 1982. A gravity survey of the East Bull Lake intrusion, Research Area RA-7, Algoma District, Ontario. Unpub. Contract Rep., Paterson, Grant and Watson Ltd., Toronto.

Appendix A

Summary of Straddle-Packer Test Results, Boreholes P-1 to P-14

Table A-1. Summary of Packer Test Results, Borehole P-1

Test	Depth (m)*	Static water level (m)*	Hydraulic head (m a.s.l.)	T ($m^2 \cdot s^{-1}$)	K_{erm} ($m \cdot s^{-1}$)
P0101	8.00–12.10	3.51	391.8	4×10^{-7}	1×10^{-7}
P0102	12.00–16.00	2.67	392.6	2×10^{-7}	5×10^{-8}
P0103	13.00–17.00	3.35	392.0	9×10^{-8}	2×10^{-8}
P0104	16.00–20.00	2.48	392.8	5×10^{-7}	1×10^{-7}
P0105	20.00–24.00	3.30	392.0	2×10^{-7}	5×10^{-8}
P0106	24.00–28.00	2.92	392.4	2×10^{-7}	5×10^{-8}
P0107	28.00–32.10	3.14	392.2	6×10^{-8}	1×10^{-8}
P0108	32.00–36.10	2.90	392.4	3×10^{-7}	8×10^{-8}
P0109	36.00–40.10†				
P0111	40.00–44.10†				
P0112	44.00–48.10†				
P0113	48.00–52.10†				
P0114	49.20–53.30†	3.19	392.1	1×10^{-8}	2×10^{-9}
P0115	45.00–53.30†				
P0116	46.00–53.30	3.33	392.0	2×10^{-8}	3×10^{-9}
P0117	22.00–53.30	3.51	391.8	1×10^{-6}	3×10^{-8}

*Depths are measured in metres below top of casing and along borehole.
†Poor packer seal, test results unreliable.

m a.s.l. = Metres above sea level.

Table A-2. Summary of Packer Test Results, Borehole P-2

Test	Depth (m)*	Static water level (m)*	Hydraulic head (m a.s.l.)	T ($m^2 \cdot s^{-1}$)	K_{erm} ($m \cdot s^{-1}$)
P0201	9.00–12.05	−0.72	392.0	1×10^{-6}	2×10^{-7}
P0202	13.00–17.05	−0.02	391.3	1×10^{-7}	3×10^{-8}
P0203	17.00–21.05	−0.20	391.5	2×10^{-7}	6×10^{-8}
P0204	21.00–25.05	−0.36	391.6	1×10^{-8}	2×10^{-9}
P0205	25.00–29.05	−0.03	391.3	9×10^{-9}	2×10^{-9}
P0206	29.00–33.05†				
P0207	33.00–37.05	−0.01	391.3	8×10^{-7}	2×10^{-7}
P0208	37.00–38.10	1.32	396.0	1×10^{-8}	2×10^{-9}

*Depths are measured in metres below top of casing and along borehole.
†Poor packer seal, test results unreliable.

m a.s.l. = Metres above sea level.

Table A-3. Summary of Packer Test Results, Borehole P-3

Test	Depth (m)*	Static water level (m)*	Hydraulic head (m a.s.l.)	T ($m^2 \cdot s^{-1}$)	K_{erm} ($m \cdot s^{-1}$)
P0301	4.00–8.05†				
P0302	8.00–12.05†				
P0303	12.00–16.05	0.16	390.6	3×10^{-7}	7×10^{-8}
P0304	16.00–20.05	−0.03	390.8	3×10^{-7}	8×10^{-8}
P0305	20.00–24.05†				
P0306	24.00–28.05†				
P0307	28.00–32.05†				
P0308	32.00–36.05	0.08	390.7	4×10^{-7}	1×10^{-7}
P0309	32.00–38.10	−0.17	390.9	3×10^{-8}	6×10^{-9}
P0310	16.00–38.10	−0.38	391.2	3×10^{-7}	1×10^{-8}
P0311	0.00–6.00	1.08	389.7		

*Depths are measured in metres below top of casing and along borehole.
†Poor packer seal, test results unreliable.

m a.s.l. = Metres above sea level.

Table A-4. Summary of Packer Test Results, Borehole P-4

Test	Depth (m)*	Static water level (m)*	Hydraulic head (m a.s.l.)	T ($m^2 \cdot s^{-1}$)	K_{erm} ($m \cdot s^{-1}$)
P0401	8.00–12.05	3.90	389.6	2×10^{-6}	4×10^{-7}
P0402	12.00–16.05	2.43	390.9	2×10^{-8}	5×10^{-9}
P0403	16.00–20.05	2.78	390.6	2×10^{-8}	5×10^{-9}
P0404	20.00–24.05	2.62	390.8	3×10^{-8}	1×10^{-9}
P0405	24.00–28.05	2.86	390.5	2×10^{-8}	5×10^{-9}
P0406	28.00–32.05†				
P0407	32.00–36.05†				
P0408	36.00–40.05†				
P0409	40.00–44.05	2.96	390.4	2×10^{-7}	4×10^{-8}
P0410	44.00–48.05†				
P0411	48.00–52.05†				
P0412	41.00–55.00†				
P0413	35.50–55.00†				
P0414	20.50–55.00†				
P0415	14.70–55.00	2.69	390.7	5×10^{-7}	1×10^{-8}
P0416	0.00–7.70†				

*Depths are measured in metres below top of casing and along borehole.
†Poor packer seal, test results unreliable.

m a.s.l. = Metres above sea level.

Table A-5. Summary of Packer Test Results, Borehole P-5

Test	Depth (m)*	Static water level (m)*	Hydraulic head (m a.s.l.)	T ($m^2 \cdot s^{-1}$)	K_{erm} ($m \cdot s^{-1}$)
P0501	9.00–13.05†				
P0502	13.00–17.05†				
P0503	17.00–21.05†				
P0504	15.00–19.05†				
P0505	17.00–21.05†				
P0506	21.00–25.05	1.35	395.1	9×10^{-8}	2×10^{-8}
P0507	25.00–29.05†				
P0508	29.00–33.05†				
P0509	33.00–37.05	1.17	395.3	2×10^{-7}	6×10^{-8}
P0510	37.00–41.05	1.15	395.3	2×10^{-7}	5×10^{-8}
P0511	41.00–45.05†				
P0512	45.00–49.05	1.23	395.2	1×10^{-6}	3×10^{-7}
P0513	49.00–53.05	1.25	395.2	1×10^{-6}	3×10^{-7}
P0514	53.00–57.05†				
P0515	57.00–61.05	1.09	395.4	1×10^{-6}	3×10^{-7}
P0516	61.00–65.05†				
P0517	65.00–69.05	1.19	395.3	4×10^{-7}	1×10^{-7}
P0518	69.00–73.05	1.24	395.2	2×10^{-7}	4×10^{-8}
P0519	73.00–77.05	1.23	395.2		
P0520	77.00–81.05	0.74	395.7	6×10^{-7}	1×10^{-7}
P0521	81.00–85.05	0.77	395.7	2×10^{-7}	5×10^{-8}
P0522	84.30–88.35	1.05	395.4	2×10^{-7}	5×10^{-8}
P0523	88.30–92.35	1.15	395.3	3×10^{-7}	7×10^{-8}
P0524	92.30–96.35	1.24	395.2	2×10^{-7}	4×10^{-8}
P0525	33.00–97.60	1.24	395.2	4×10^{-6}	6×10^{-7}
P0526	49.00–97.60	1.24	395.2	1×10^{-6}	3×10^{-8}
P0527	77.00–97.60	0.72	395.7	6×10^{-7}	3×10^{-8}
P0528	85.00–97.60	1.04	395.4	5×10^{-8}	4×10^{-9}
P0529	88.50–97.60	0.90	395.5	2×10^{-7}	2×10^{-8}

*Depths are measured in metres below top of casing and along borehole.
†Poor packer seal, test results unreliable.

m a.s.l. = Metres above sea level.

Table A-6. Summary of Packer Test Results, Borehole P-6

Test	Depth (m)*	Static water level (m)*	Hydraulic head (m a.s.l.)	T ($m^2 \cdot s^{-1}$)	K_{erm} ($m \cdot s^{-1}$)
P0601	17.00–21.05	9.70	390.1	4×10^{-8}	1×10^{-8}
P0602	21.00–25.05	10.17	389.6	9×10^{-8}	2×10^{-8}
P0603	25.00–29.05	11.16	388.7	7×10^{-8}	2×10^{-8}
P0604	29.00–33.05	11.28	388.6	2×10^{-8}	7×10^{-9}
P0605	33.00–37.05	12.37	387.5	1×10^{-9}	3×10^{-10}
P0606	37.00–41.05	28.04	372.1	8×10^{-9}	2×10^{-9}
P0607	41.00–45.05	21.24	378.7	7×10^{-8}	3×10^{-8}
P0608	45.00–49.05	20.33	379.6†		
P0609	49.00–53.05	20.40	379.6	9×10^{-8}	2×10^{-8}
P0610	53.00–57.05	28.20	371.9	2×10^{-8}	5×10^{-9}
P0611	57.00–61.05	21.25	378.6	9×10^{-8}	2×10^{-8}
P0612	61.00–65.05	18.51	381.4	8×10^{-10}	2×10^{-10}
P0613	65.00–68.00	21.06	378.9	5×10^{-9}	1×10^{-9}

*Depths are measured in metres below top of casing and along borehole.
†Poor packer seal, test results unreliable.

m a.s.l. = Metres above sea level.

Table A-7. Summary of Packer Test Results, Borehole P-7

Test	Depth (m)*	Static water level (m)*	Hydraulic head (m a.s.l.)	T ($m^2 \cdot s^{-1}$)	K_{erm} ($m \cdot s^{-1}$)
P0701	4.00–8.09†				
P0702	8.00–12.09†				
P0703	11.00–15.09	0.75	402.4	1×10^{-9}	2×10^{-10}
P0704	15.00–19.09†				
P0705	19.00–23.09†				
P0706	23.00–27.09	1.13	402.1	1×10^{-9}	2×10^{-10}
P0707	27.00–31.09	1.53	401.6	5×10^{-10}	1×10^{-10}
P0708	31.00–35.09	1.29	401.9	1×10^{-9}	2×10^{-10}
P0709	35.00–39.09	1.32	401.9	5×10^{-10}	1×10^{-10}
P0710	39.00–39.95	1.29	401.9	1×10^{-9}	1×10^{-9}

*Depths are measured in metres below top of casing and along borehole.
†Poor packer seal, test results unreliable.

m a.s.l. = Metres above sea level.

Table A-8. Summary of Packer Test Results, Borehole P-8

Test	Depth (m)*	Static water level (m)*	Hydraulic head (m a.s.l.)	T ($m^2 \cdot s^{-1}$)	K_{erm} ($m \cdot s^{-1}$)
P0801	4.00–8.05	1.87	399.3	2×10^{-6}	5×10^{-7}
P0802	8.00–12.05	1.95	399.2	1×10^{-9}	4×10^{-10}
P0803	12.00–16.05	1.95	399.2	1×10^{-9}	4×10^{-10}
P0805	16.00–20.05	2.26	398.9	4×10^{-6}	1×10^{-6}
P0806	20.00–24.05	2.53	398.7	5×10^{-10}	1×10^{-10}
P0807	24.00–28.05	2.46	398.7	1×10^{-9}	4×10^{-10}
P0808	28.00–32.05	2.58	398.6	3×10^{-9}	8×10^{-10}
P0809	32.00–36.05	2.52	398.7	2×10^{-9}	5×10^{-10}
P0810	36.00–40.05†				
P0811	32.00–45.20	2.65	398.5	1×10^{-9}	4×10^{-10}
P0812	16.00–45.20	1.65	399.5	4×10^{-6}	1×10^{-7}

*Depths are measured in metres below top of casing and along borehole.
†Poor packer seal, test results unreliable.

m a.s.l. = Metres above sea level.

Table A-9. Summary of Packer Test Results, Borehole P-9

Test	Depth (m)*	Static water level (m)*	Hydraulic head (m a.s.l.)	T ($m^2 \cdot s^{-1}$)	K_{erm} ($m \cdot s^{-1}$)
P0901	5.00–9.05	1.10	400.4	5×10^{-6}	1×10^{-6}
P0902	9.00–13.05	1.29	400.2	2×10^{-7}	5×10^{-8}
P0903	13.00–17.05	1.29	400.2	2×10^{-9}	5×10^{-10}
P0904	17.00–21.05	1.29	400.2	1×10^{-9}	4×10^{-10}
P0905	21.00–25.05	1.29	400.2	3×10^{-10}	1×10^{-10}
P0906	25.00–29.05	1.29	400.3	3×10^{-10}	1×10^{-10}
P0907	29.00–33.05	1.40	400.1	9×10^{-10}	2×10^{-10}
P0908	33.00–37.05	1.48	400.0	1×10^{-8}	4×10^{-9}
P0909	37.00–41.05	1.27	400.2	3×10^{-9}	7×10^{-10}
P0910	41.00–43.20	1.58	399.9	1×10^{-9}	4×10^{-10}

*Depths are measured in metres below top of casing and along borehole.

m a.s.l. = Metres above sea level.

Table A-10. Summary of Packer Test Results, Borehole P-10

Test	Depth (m)*	Static water level (m)*	Hydraulic head (m a.s.l.)	T ($m^2 \cdot s^{-1}$)	K_{erm} ($m \cdot s^{-1}$)
P1001	9.00–13.05	4.45	401.0	7×10^{-8}	2×10^{-8}
P1002	13.00–17.05	5.94	399.5	3×10^{-7}	7×10^{-8}
P1003	17.00–21.05	5.04	400.4	4×10^{-7}	1×10^{-7}
P1004	21.00–25.05†				
P1005	25.00–29.05	6.14	399.3	4×10^{-8}	9×10^{-9}
P1006	29.00–33.05	5.32	400.1	2×10^{-8}	5×10^{-9}
P1007	33.00–37.09	6.53	398.8	8×10^{-7}	2×10^{-7}
P1008	37.00–41.05†				
P1009	41.00–45.05	6.00	399.4	1×10^{-8}	4×10^{-9}
P1010	45.00–49.05	5.30	400.1	5×10^{-9}	1×10^{-9}
P1011	49.00–53.05	5.77	399.7	3×10^{-8}	7×10^{-9}
P1012	53.00–57.05	5.92	399.5	6×10^{-8}	2×10^{-8}
P1013	57.00–61.05	5.92	399.5	5×10^{-9}	1×10^{-9}
P1014	61.00–65.05	6.00	399.4	2×10^{-8}	5×10^{-9}
P1015	65.00–69.05	6.00	399.4	8×10^{-7}	2×10^{-7}
P1016	69.00–73.05	6.00	399.4	3×10^{-8}	7×10^{-9}
P1017	73.00–77.05	6.00	399.4	3×10^{-8}	7×10^{-9}
P1018	77.00–81.05	6.00	399.4	2×10^{-8}	5×10^{-9}
P1019	81.00–85.05	6.05	399.4	1×10^{-7}	3×10^{-8}
P1020	85.00–89.05	4.66	400.8	8×10^{-10}	2×10^{-10}
P1021	89.00–93.05	5.78	399.6	2×10^{-7}	4×10^{-8}
P1022	93.00–97.05	5.78	399.6	1×10^{-7}	4×10^{-8}

*Depths are measured in metres below top of casing and along borehole.
†Poor packer seal, test results unreliable.

m a.s.l. = Metres above sea level.

Table A-11. Summary of Packer Test Results, Borehole P-11

Test	Depth (m)*	Static water level (m)*	Hydraulic head (m a.s.l.)	T ($m^2 \cdot s^{-1}$)	K_{erm} ($m \cdot s^{-1}$)
P1101	8.00–12.10	2.81	402.8	4×10^{-9}	1×10^{-9}
P1102	12.00–16.10	2.81	402.7	5×10^{-8}	1×10^{-8}
P1103	16.00–20.10	2.80	402.8	3×10^{-8}	7×10^{-9}
P1104	20.00–24.10	2.88	402.7	3×10^{-9}	9×10^{-10}
P1105	24.00–28.10†				
P1106	28.00–32.10	3.32	402.2	1×10^{-8}	4×10^{-9}
P1107	32.00–36.10	3.29	402.2	1×10^{-8}	4×10^{-9}
P1108	36.00–40.10	3.42	402.1	1×10^{-8}	4×10^{-9}
P1109	40.00–44.10†				
P1110	44.00–49.20	3.40	402.2	1×10^{-8}	4×10^{-9}
P1111	36.00–49.20†				
P1112	5.00–49.20	3.70	401.9	2×10^{-6}	4×10^{-7}

*Depths are measured in metres below top of casing and along borehole.
†Poor packer seal, test results unreliable.

m a.s.l. = Metres above sea level.

Table A-12. Summary of Packer Test Results, Borehole P-12

Test	Depth (m)*	Static water level (m)*	Hydraulic head (m a.s.l.)	T ($m^2 \cdot s^{-1}$)	K_{erm} ($m \cdot s^{-1}$)
P1201	4.00–48.60	2.31	376.1	1×10^{-6}	2×10^{-8}
P1202	8.00–48.60	2.49	375.9	9×10^{-7}	2×10^{-8}
P1203	12.00–48.60	2.76	375.7	9×10^{-7}	2×10^{-8}
P1204	16.00–48.60†				
P1205	20.00–48.60†				
P1206	24.00–48.60†				
P1207	28.00–48.60†				
P1208	32.00–48.60†				
P1209	36.00–48.60	3.39	375.1	4×10^{-7}	4×10^{-9}
P1210	40.00–48.60†				
P1211	44.00–48.60†				
P1212	38.00–48.60	3.83	374.7	3×10^{-8}	2×10^{-9}
P1213	12.00–48.60	2.76	375.7	1×10^{-6}	3×10^{-8}

*Depths are measured in metres below top of casing and along borehole.
†Poor packer seal, test results unreliable.

m a.s.l. = Metres above sea level.

Table A-13. Summary of Packer Test Results, Borehole P-13

Test	Depth (m)*	Static water level (m)*	Hydraulic head (m a.s.l.)	T ($m^2 \cdot s^{-1}$)	K_{erm} ($m \cdot s^{-1}$)
P1301	5.00–9.05	2.93	375.8	1×10^{-7}	3×10^{-8}
P1302	9.00–13.05	3.07	375.7	4×10^{-7}	1×10^{-7}
P1303	13.00–17.05†				
P1304	17.00–21.05†				
P1305	21.00–25.05†				
P1306	25.00–29.05†				
P1307	29.00–33.05†				
P1308	33.00–37.05†				
P1309	37.00–41.05†				
P1310	41.00–45.05†				
P1311	44.00–48.05†				
P1312	9.00–48.70	3.61	375.2	2×10^{-6}	5×10^{-8}
P1313	20.00–48.70†				
P1314	31.00–48.70	3.53	375.3	5×10^{-8}	3×10^{-9}
P1315	40.00–48.70	3.51	375.3	5×10^{-8}	6×10^{-9}

*Depths are measured in metres below top of casing and along borehole.
†Poor packer seal, test results unreliable.

m a.s.l. = Metres above sea level.

Table A-14. Summary of Packer Test Results, Borehole P-14

Test	Depth (m)*	Static water level (m)*	Hydraulic head (m a.s.l.)	T ($m^2 \cdot s^{-1}$)	K_{erm} ($m \cdot s^{-1}$)
P1401	8.00–12.10	2.28	360.8	2×10^{-7}	6×10^{-8}
P1402	12.00–16.10†				
P1403	16.00–20.10	2.30	360.8	5×10^{-9}	1×10^{-9}
P1404	20.00–24.10	2.84	360.2	9×10^{-8}	2×10^{-8}
P1405	24.00–28.10	2.00	361.0	3×10^{-9}	8×10^{-10}
P1406	28.00–32.10†				
P1407	32.00–36.10	2.25	360.8	1×10^{-9}	3×10^{-10}
P1408	36.00–40.10	2.27	360.8	1×10^{-9}	3×10^{-10}
P1409	32.00–43.30	3.07	360.0	1×10^{-9}	4×10^{-10}
P1410	16.00–43.30	2.79	360.3	6×10^{-9}	2×10^{-9}
P1411	8.50–43.30	2.41	360.7	4×10^{-7}	1×10^{-8}
P1412	0.00–8.50	2.31	360.8	2×10^{-8}	4×10^{-9}

*Depths are measured in metres below top of casing and along borehole.
†Poor packer seal, test results unreliable.

m a.s.l. = Metres above sea level.

Appendix B

Summary of Hydraulic Head Measurements, Boreholes EBL-1, 2, 3 and 4, October 1984 to October 1985

Table B-1. Summary of Hydraulic Head Measurements, Borehole EBL-1

Port No.	Port elevation (m a.s.l.)	Hydraulic head (m a.s.l.)								
		Oct. 21/84	Nov. 21/84	Mar. 19/85	Apr. 11/85	May 1/85	May 2/85	May 6/85	May 7/85	May 16/85
1	-224.1	439.1	409.0	–	–	–	397.8	–	398.2	398.0
2	-204.6	442.3	411.4	–	–	–	399.7	–	399.2	399.3
3	-188.1	461.7	428.6	–	–	–	406.0	–	405.1	404.2
4	-150.6	400.6	395.4	–	–	–	396.4	–	397.3	395.1
5	-138.6	401.1	395.5	–	–	–	396.5	–	397.2	395.1
6	-104.1	397.2	395.6	–	–	–	396.4	–	397.2	395.0
7	-66.6	396.9	392.3	–	–	–	389.1	–	389.0	388.8
8	-32.1	397.7	390.9	–	–	–	393.8	–	391.9	391.5
9	-12.6	399.3	396.8	–	–	–	396.1	–	394.4	393.9
10	6.8	396.0	392.1	–	–	–	390.7	–	389.6	389.3
11	38.3	395.3	392.3	–	–	–	390.7	–	389.5	389.2
12	66.8	417.4	405.6	–	–	–	405.8	–	405.7	405.8
13	104.3	393.6	392.4	392.9	395.4	391.8	390.6	390.9	389.7	389.7
14	135.8	417.1	395.5	396.4	397.1	394.2	393.9	393.8	393.3	392.4
15	164.3	416.8	399.9	400.7	400.9	400.7	400.9	401.0	400.8	400.6
16	183.8	400.3	400.0	400.0	400.1	400.1	400.2	400.0	399.9	400.1
17	198.8	400.4	399.9	400.0	400.1	400.1	400.2	400.1	400.1	400.1
18	201.8	400.3	400.0	400.1	400.1	400.1	400.1	400.1	400.1	400.1
19	206.3	465.9	428.7	410.1	409.3	408.8	407.7	406.1	405.9	406.7
20	216.8	450.8	424.2	406.5	406.3	406.8	406.0	405.2	405.0	405.8
21	239.3	401.1	399.0	402.4	401.8	402.0	401.5	401.6	401.1	402.3
22	260.3	400.4	400.4	400.3	400.4	400.4	400.4	400.3	400.4	400.3
23	276.8	400.5	400.4	400.4	400.4	400.4	400.4	400.3	400.4	400.4
24	296.3	400.6	400.5	400.4	400.6	400.5	400.6	400.4	–	400.4
25	308.3	400.4	400.4	400.3	400.6	400.4	400.5	400.3	–	400.4
26	321.8	400.6	400.4	400.3	400.5	400.5	400.4	400.4	–	400.4
27	336.8	400.6	400.4	400.6	400.7	400.5	400.6	400.4	–	400.4
28	350.3	400.8	400.8	401.1	401.3	401.0	401.1	400.7	–	400.8
29	366.8	401.5	401.3	401.8	401.3	401.3	401.3	401.3	–	401.3
30	377.3	401.6	401.4	401.3	401.3	401.3	401.4	401.3	–	401.3
31	386.3	401.6	401.5	401.4	401.4	401.4	401.4	401.3	–	401.3
32	393.8	402.0	401.8	401.6	401.6	401.6	401.6	401.7	–	401.6
33	396.8	403.0	403.3	403.2	403.6	403.3	403.4	403.4	–	403.1

m a.s.l. = Metres above sea level.

Table B-2. Summary of Hydraulic Head Measurements, Borehole EBL-1

Port No.	Port elevation (m a.s.l.)	Hydraulic head (m a.s.l.)								
		May 23/85	June 7/85	June 9/85	July 4/85	Aug. 3/85	Aug. 28/85	Sept. 19/85	Oct. 15/85	Oct. 15/85*
1	-224.1	398.7	399.4	400.8	–	405.8†	–†	394.2	399.4	390.6
2	-204.6	400.8	401.5	403.9	–	406.1	–‡	395.5	399.4	388.7
3	-188.1	404.7	404.7	405.6	–	410.7	–‡	396.3	397.8	385.5
4	-150.6	395.9	395.1	395.5	395.5	394.2	–‡	385.1	386.2	381.6
5	-138.6	396.0	395.1	395.5	395.5	394.4	–‡	385.5	386.5	381.6
6	-104.1	395.8	395.0	395.5	395.1	394.0	–	382.8	386.0	381.8
7	-66.6	388.8	388.6	388.5	388.3	387.7	385.0	377.1	381.1	381.4
8	-32.1	392.1	390.9	390.8	391.0	391.7	395.9	386.6	381.8	381.5
9	-12.6	394.5	393.0	393.7	393.7	393.2	397.3	388.5	387.0	383.1
10	6.8	390.0	389.0	389.2	390.3	389.8	393.0	385.4	385.5	382.3
11	38.3	389.6	389.1	389.1	388.8	388.1	386.4	381.1	382.8	382.9
12	66.8	405.7	405.6	405.8	405.7	405.7	404.4	405.4	405.8	385.8
13	104.3	389.9	389.5	389.7	390.4	388.4	386.4	384.9	383.8	382.1
14	135.8	394.0	393.3	393.7	394.0	401.2	398.4	395.4	396.3	384.1
15	164.3	400.8	400.7	400.9	400.9	402.3	403.2	402.7	402.3	398.9
16	183.8	400.0	400.1	–	399.7	399.2	399.2	399.0	399.5	399.5
17	198.8	400.0	399.9	–	399.7§	399.2	399.2	399.2	399.4	399.5
18	201.8	400.0	399.9	–	399.7	399.3	399.2	399.2	399.5	399.5
19	206.3	406.3	406.3	–	406.1	407.7	406.4	406.7	403.8	400.8
20	216.8	406.3	405.5	–	405.6	405.9	405.4	405.6	403.4	399.2
21	239.3	401.3	401.3	–	401.1	400.6	401.1	401.3	401.3	399.0
22	260.3	400.1	400.1	–	399.7	399.4	399.4	399.5	399.9	399.7
23	276.8	400.2	400.1	–	399.9	399.6	399.4	399.5	400.1	400.3
24	296.3	400.4	400.2	–	399.9	399.7	399.6	399.6	400.2	400.3
25	308.3	400.3	400.2	–	399.9	399.7	399.6	399.6	400.1	400.1
26	321.8	400.3	400.2	–	399.8	399.7	399.7	399.7	400.2	400.2
27	336.8	400.4	400.4	–	400.1	399.9	401.1	399.7	400.3	400.4
28	350.3	400.7	400.6	–	400.4	400.2	400.0	400.1	400.5	400.6
29	366.8	401.2	401.2	–	400.9	400.9	400.8	400.8	401.5	401.7
30	377.3	401.3	401.3	–	401.0	400.8	400.9	400.8	401.5	401.6
31	386.3	–	401.3	–	401.1	401.0	400.9	400.9	401.6	401.8
32	393.8	401.5	401.6	–	401.3	401.1	400.6	401.1	402.0	402.3
33	396.8	403.0	403.0	–	402.5	402.4	402.8	401.9	403.6	403.9

* Integrity check of casing: profile completed with lowered water level within the casing.
† Pumping port No. 1: opened July 14, 1985; pumped August 28 to September 10, 1985; closed September 18, 1985.
‡ Pumping ports No. 2 to 5: opened August 5, 1985; pumped August 28 to September 10, 1985; closed September 18, 1985.
§ Pumping port No. 17: opened July 5, 1985; pumped July 5-11, 1985; closed July 11, 1985.

m a.s.l. = Metres above sea level.

Table B-3. Summary of Hydraulic Head Measurements, Borehole EBL-2

Port No.	Port elevation (m a.s.l.)	Hydraulic head (m a.s.l.)							
		Oct. 16/84	Nov. 20/84	Mar. 20/85	Apr. 12/85	May 2/85	May 3/85	May 7/85	May 8/85
1	-361.2	389.5	388.9	–	–	–	–	–	391.1
2	-304.2	410.1	403.7	–	–	–	398.2	–	397.3
3	-272.7	409.5	395.7	–	–	–	398.3	–	397.3
4	-238.2	384.3	379.2	–	–	–	385.2	–	384.8
5	-203.7	376.9	375.5	–	–	–	374.9	–	375.5
6	-164.2	376.2	374.6	–	–	–	372.9	–	372.9
7	-161.2	382.6	375.7	–	–	–	375.0	–	374.3
8	-145.2	386.0	377.9	–	–	–	378.0	–	375.9
9	-113.7	375.8	375.8	–	–	–	375.3	–	375.7
10	-82.2	386.2	376.0	–	–	–	373.9	–	371.9
11	-50.2	413.3	386.6	–	–	–	376.2	–	375.5
12	-23.7	394.9	389.7	–	–	–	383.1	–	380.7
13	19.8	397.8	384.7	–	–	–	378.8	–	375.0
14	45.8	389.7	389.0	–	–	–	391.1	–	390.4
15	64.8	385.6	385.7	–	–	–	386.2	–	385.9
16	96.3	389.7	385.9	383.9	384.9	387.5	386.4	385.3	386.1
17	127.8	389.8	385.7	380.2	380.4	382.4	381.8	381.7	–
18	159.3	389.0	384.4	380.2	379.8	379.5	379.6	379.8	379.7
19	184.8	386.9	384.2	381.5	381.2	381.9	382.1	380.7	380.4
20	216.3	386.5	388.8	381.0	381.9	382.1	380.0	380.5	380.0
21	235.8	396.2	394.1	395.4	394.4	395.6	396.8	395.9	396.1
22	261.3	385.1	381.1	380.2	380.7	380.9	380.7	380.9	–
23	280.8	383.6	380.0	379.1	379.5	379.7	379.7	379.8	–
24	286.8	383.3	380.0	379.0	379.5	379.7	379.8	379.7	–
25	297.3	378.8	376.8	376.2	376.2	376.2	376.2	376.3	–
26	310.8	378.9	376.4	376.2	376.5	377.4	376.7	376.7	–
27	324.3	378.6	376.0	375.1	375.8	376.4	376.0	375.9	–
28	339.3	386.1	393.1	392.5	391.2	392.0	392.3	391.3	–
29	345.3	386.2	393.0	393.0	392.1	392.7	392.9	392.0	–
30	355.8	390.6	395.7	394.2	392.5	392.4	392.1	390.9	–
31	363.3	393.6	393.5	393.3	393.5	393.3	393.4	393.5	–
32	373.8	393.3	393.5	393.3	393.5	393.3	393.4	393.5	–
33	381.3	393.7	394.0	393.8	394.0	393.9	–	394.0	–
34	385.8	394.2	394.5	395.0	394.9	394.9	394.7	395.2	–

m a.s.l. = Metres above sea level.

Table B-4. Summary of Hydraulic Head Measurements, Borehole EBL-2

Port No.	Port elevation (m a.s.l.)	Hydraulic head (m a.s.l.)							
		May 16/85	May 24/85	June 6/85	Aug. 2/85	Sept. 7/85	Sept. 18/85	Oct. 17/85	Oct. 17/85*
1	-361.2	–	392.2	393.1	396.3	–	395.6	395.2	393.9
2	-304.2	396.4	396.3	–	403.7	–	408.6	401.1	–
3	-272.7	396.4	396.2	396.6	402.6	–	408.2	401.0	395.5
4	-238.2	384.5	385.7	386.2	388.3	–	390.4	–	–
5	-203.7	375.7	375.7	374.7	–	–	373.0	374.0	371.9
6	-184.2	373.1	373.2	373.9	375.6	–	372.3	372.1	371.7
7	-161.2	372.8	372.8	372.8	373.5	–	372.4	372.1	371.2
8	-145.2	376.5	376.6	377.1	379.8	–	375.8	375.9	372.7
9	-113.7	371.7	371.3	371.0	371.0	–	370.6	370.1	370.5
10	-82.2	372.1	372.1	372.4	375.3	–	372.8	372.4	369.8
11	-50.2	375.6	376.2	376.7	378.5	–	378.5	378.2	374.0
12	-23.7	380.6	383.8	–	396.5	–	393.6	391.1	381.1
13	19.8	374.7	376.3	377.9	384.1	–	384.4	382.8	373.9
14	45.8	389.9	390.5	390.3	389.0	–	390.0	389.2	378.8
15	64.8	385.7	386.7	387.3	389.0	–	388.0	387.2	377.5
16	96.3	385.6	386.9	387.6	388.9	386.8	387.9	387.1	376.9
17	127.8	381.3	381.9	382.4	382.2	384.7	384.3	382.0	375.0
18	159.3	380.0	379.9	379.7	378.5	377.7	375.8	374.0	374.0
19	184.8	380.2	380.7	381.0	381.2	380.8	379.2	376.1	375.3
20	216.3	380.0	380.5	379.9	379.0	379.3	376.6	375.9	375.6
21	235.8	395.9	396.5	396.2	395.9	380.0†	377.3	377.4	376.2
22	261.3	380.8	380.8	380.5	379.6	379.3	376.2	377.2	377.3
23	280.8	379.7	379.7	379.3	378.3	377.9‡	374.7‡	375.5	375.7
24	286.8	379.7	379.6	379.3	378.3	378.0	374.6	375.5	375.5
25	297.3	376.0	376.2	375.5	374.6	374.7	372.8	373.8	373.9
26	310.8	376.2	376.5	376.0	374.9	374.6	373.1	373.9	373.7
27	324.3	375.9	376.1	375.4	374.4	374.2	372.8	373.7	373.8
28	339.3	390.7	391.6	392.2	383.4	382.8	379.4	379.1	373.2
29	345.3	391.1	392.2	392.2	385.9	386.2	381.2	380.2	373.8
30	355.8	389.8	391.5	389.7	389.5	388.3	389.3	387.4	383.8
31	363.3	393.4	393.1	393.0	392.3	392.3	392.4	393.5	393.3
32	373.8	393.3	393.1	393.0	392.3	392.3	392.5	393.5	393.5
33	381.3	393.8	393.7	393.6	392.9	392.9	393.0	394.0	393.9
34	385.8	394.6	394.6	394.5	393.8	394.0	393.9	394.7	394.1

* Integrity check of casing; profile completed with lowered water level within the casing.
† Pumping port No. 21: opened August 7, 1985; closed August 7, 1985.
‡ Pumping port No. 23: opened August 7, 1985; closed September 5, 1985; opened September 8, 1985; pumped September 10 and 11, 1985; closed September 18, 1985; opened September 19, 1985; pumped September 19 and 20, 1985; closed October 8, 1985.

m a.s.l. = Metres above sea level.

Table B-5. Summary of Hydraulic Head Measurements, Borehole EBL-3

Port No.	Port elevation (m a.s.l.)	Hydraulic head (m a.s.l.)							
		Oct. 22/84	Nov. 22/84	Mar. 19/85	Apr. 11/85	May 1/85	May 3/85	May 6/85	May 8/85
1	136.2	371.9	366.3	360.5	359.8	359.6	359.5	359.3	359.3
2	163.2	373.3	368.7	367.0	366.3	367.1	365.3	366.5	364.8
3	185.7	382.2	374.8	372.8	372.1	372.6	370.7	371.7	370.3
4	208.2	386.2	380.3	377.0	376.9	375.9	374.9	376.2	374.8
5	233.7	395.0	382.9	380.4	380.2	379.3	378.5	379.5	378.5
6	253.2	395.0	385.7	380.9	380.1	378.8	378.5	379.6	378.4
7	272.7	394.6	384.5	383.6	382.7	381.9	381.9	382.5	381.0
8	298.2	386.6	383.6	383.3	382.7	386.2	386.2	386.6	384.4
9	314.7	390.4	381.5	381.6	381.4	384.2	384.2	384.5	383.5
10	334.2	393.9	381.9	381.6	381.6	382.7	382.8	383.2	382.6
11	347.7	381.0	380.9	381.0	381.0	380.9	380.9	380.9	381.0
12	365.7	380.9	380.8	380.9	380.9	380.8	380.7	380.9	380.9
13	376.2	380.9	380.9	380.9	380.9	380.7	380.7	380.8	380.9

m a.s.l. = Metres above sea level.

Table B-6. Summary of Hydraulic Head Measurements, Borehole EBL-3

Port No.	Port elevation (m a.s.l.)	Hydraulic head (m a.s.l.)						
		May 15/85	May 23/85	June 11/85	Aug. 1/85	Sept. 7/85	Sept. 19/85	Oct. 23/85
1	136.2	359.3	359.0	359 0	357.9	357.9	357.9	357.7
2	163.2	364.2	365.3	365.0	364.8	366.2	363.2	363.9
3	185.7	369.3	370.8	370.4	370.5	371.7	368.6	369.3
4	208.2	373.2	374.8	374.7	374.3	374.7	371.6	373.3
5	233.7	377.9	378.6	378.5	378.5	378.4	376.6	377.3
6	253.2	378.4	378.1	378.7	378.6	378.4	377.0	377.6
7	272.7	381.5	381.4	381.2	381.9	–	379.5	380.6
8	298.2	385.6	385.4	382.4	384.0	381.6	379.8	380.7
9	314.7	383.3	383.2	381.4	381.9	380.6	379.7	380.2
10	334.2	382.4	382.8	381.6	381.8	381.2	380.4	381.1
11	347.7	380.8	380.7	380.5	380.7	380.8	380.4	381.0
12	365.7	380.7	380.6	380.4	380.5	–	380.6	380.8
13	376.2	380.7	380.5	380.4	380.6	–	380.3	380.9

m a.s.l. = Metres above sea level.

Table B-7. Summary of Hydraulic Head Measurements, Borehole EBL-4

Port No.	Port elevation (m a.s.l.)	Hydraulic head (m a.s.l.)							
		Oct. 4/84	Nov. 2/84	Mar. 20/85	Apr. 10/85	May 2/85	May 4/85	May 6/85	May 7/85
1	-32.4	389.8	390.6	–	–	–	355.7	–	–
2	-10.0	348.4	–	–	–	–	352.5	–	–
3	-7.2	348.4	354.0	–	–	–	352.6	–	–
4	8.2	420.0	387.6	–	–	–	364.3	–	–
5	27.4	398.2	390.6	–	–	–	368.4	–	–
6	41.8	402.3	387.5	–	–	–	364.6	–	–
7	71.2	385.6	377.5	–	–	–	361.1	–	–
8	95.1	383.1	367.2	–	–	–	361.2	–	–
9	107.7	419.2	391.7	381.0	381.5	380.3	379.4	–	378.8
10	137.1	–	–	391.9	392.8	392.5	391.1	–	392.1
11	155.3	395.5	394.1	388.5	392.7	392.5	390.9	–	392.1
12	173.5	401.2	392.3	388.8	389.9	390.8	389.9	–	390.9
13	194.5	388.8	388.2	388.3	386.6	388.1	387.3	–	388.4
14	215.5	397.0	398.0	397.8	397.1	398.3	396.8	–	398.2
15	222.5	396.1	398.5	398.5	398.5	398.6	397.6	–	398.5
16	232.3	396.3	–	398.6	398.1	398.6	–	398.3	398.5
17	240.7	396.3	398.7	398.6	398.3	398.7	397.7	398.4	398.4
18	247.7	396.8	398.4	398.4	398.3	398.8	397.6	398.5	398.5
19	260.3	396.7	398.9	398.7	398.7	398.8	398.0	398.7	398.6
20	278.5	397.7	378.7	398.8	398.1	398.9	398.2	399.0	398.8
21	291.1	398.7	397.5	397.9	397.9	398.4	397.8	398.5	398.1
22	303.7	399.1	401.8	401.2	401.4	401.5	400.8	401.6	401.3
23	319.1	399.2	399.7	398.8	398.7	399.3	–	399.4	399.1
24	331.7	398.5	399.4	398.5	397.3	399.2	–	399.5	399.2
25	347.1	398.7	399.7	398.6	398.2	399.1	–	399.7	398.8
26	365.3	399.0	401.5	400.6	400.8	400.8	–	401.2	400.8
27	377.9	399.2	401.6	402.1	400.8	401.0	–	401.3	400.8
28	387.7	417.2	401.7	400.8	401.0	401.1	–	401.4	401.0
29	394.7	399.3	401.8	400.8	401.0	401.1	–	401.6	401.0

m a.s.l. = Metres above sea level.

Table B-8. Summary of Hydraulic Head Measurements, Borehole EBL-4

Port No.	Port elevation (m a.s.l.)	Hydraulic head (m a.s.l.)							
		May 8/85	May 8/85	May 16/85	May 22/85	Aug. 1/85	Aug. 28/85	Sept. 20/85	Oct. 23/85
1	-32.4	355.1	–	354.7	354.7	349.1	–	353.1	353.1
2	-10.0	352.6	–	352.2	–	350.1*	–	350.4	349.6
3	-7.2	352.1	–	352.3	352.4	350.2*	–	350.3	349.8
4	8.2	365.5	–	365.1	363.6	361.2	–	361.5	362.7
5	27.4	369.5	–	369.4	367.7	365.6	–	365.6	366.8
6	41.8	365.3	–	364.6	363.1	360.8	–	361.5	362.6
7	71.2	361.2	–	360.8	360.5	358.8	–	358.6	358.1
8	95.1	361.4	–	360.8	360.8	360.9	–	358.9	357.4
9	107.7	378.7	–	379.1	378.1	374.3	374.8	373.9	370.6
10	137.1	391.1	–	390.9	390.8	391.2	390.3	388.7	387.1
11	155.3	391.5	–	390.8	390.5	391.1	389.3	387.4	385.8
12	173.5	390.0	–	390.3	390.5	390.0	389.5	388.1	385.5
13	194.5	387.1	–	387.3	387.8	387.7	387.2	385.8	384.3
14	215.5	397.6	–	397.2	397.8	397.7	397.2	395.9	394.8
15	222.5	397.6	–	397.5	398.0	398.1	397.4	396.0	395.1
16	232.3	397.7	–	397.7	398.0	397.9	397.5	396.2	395.3
17	240.7	397.1	–	397.6	398.4	398.0	397.5	396.3	–
18	247.7	398.0	–	397.7	398.1	398.0	397.7	396.3	395.5
19	260.3	398.2	–	397.9	398.3	398.3	397.7	396.5	395.8
20	278.5	398.5	–	398.2	398.5	398.6	377.9	396.7	396.0
21	291.1	397.6	–	397.9	398.0	398.7	397.8	396.8	389.2†
22	303.7	400.9	401.4	400.9	401.0	400.9	400.0	399.1	398.0
23	319.1	398.8	399.2	398.8	398.9	–	398.2	397.3	396.7
24	331.7	399.0	399.0	398.9	399.0	398.7	398.2	397.5	396.8
25	347.1	399.1	398.8	399.1	398.7	395.9	398.2	399.7	396.6
26	365.3	400.6	400.8	400.5	400.7	401.2	400.0	399.3	398.8
27	377.9	400.8	400.9	400.7	400.9	401.4	400.0	399.4	399.0
28	387.7	387.6	387.4	400.8	400.9	401.5	400.1	399.5	399.1
29	394.7	401.0	401.0	400.9	401.1	401.6	400.2	399.6	399.2

*Pumping ports No. 2 and No. 3, opened June 4, 1985, pumped June 4 to August 4, 1985, closed August 7, 1985.
†Pumping port 21, opened October 2, 1985, pumped October 3 to October 9, 1985, closed October 9, 1985.

m a.s.l. = Metres above sea level.

Appendix C

Analytical Methods for Major and Minor Elements and Trace Metals

Analytical Methods for Major and Minor Elements and Trace Metals

CATION AND TRACE METAL ANALYSES

Cation and trace metal analyses were carried out by atomic absorption spectroscopy. The analytical speed, ease of operation, and relative lack of interferences made it the choice for these determinations. A brief summary of system descriptions, interferences, results and discussion are reported for the analyses of East Bull Lake geochemical samples collected in 1984 and 1985.

The instrumentation employed for this study consisted of an Instrumentation Laboratory Atomic Absorption Spectrophotometer model 251, equipped with both air-acetylene and nitrous oxide burners. An R-955 photomultiplier tube and an Ebert monochromator fitted with step-wise curved slits capable of a minimum band pass of 0.04 nm were used. Single-element hollow cathode lamps, and sodium and potassium discharge lamps without electrodes were used as light sources. An Esterline Angus recorder was used to record the outputs.

All standard reference solutions were prepared from reagent grade chemicals, or were purchased as stock 1000 $mg \cdot L^{-1}$ solutions. Water was purified with a Milli-R.O., Milli-Q system (Millipore Corp.).

Interferences in atomic absorption are of several types: chemical, matrix, and ionization. Chemical interferences occur when the element being determined combines chemically with another reactive component in the same sample. The resulting component influences the atomization process in the flame and thus alters the number of free atoms available to absorb light. Chemical interferences were controlled through the addition of a releasing agent, i.e., in the case of calcium, 2000 $mg \cdot L^{-1}$ lanthanum.

Matrix interferences occur when physical properties such as viscosity or surface tension differ between sample and standard. These interferences may occur when samples contain high concentrations of dissolved salts. Matrix interferences were controlled by diluting the sample until the dissolved salt effect was negligible.

Ionization interferences occur when the flame temperature is high enough to ionize a significant fraction of the element being determined. This interference was controlled by the addition of 2000 $mg \cdot L^{-1}$ potassium or cesium, depending on the element of interest.

Analyte linearities are based on Beer's law and also on the instrument's capabilities. All of the samples analyzed for cations were pretreated for interference effects and diluted to fall within the linear range of that specific element. Curve corrections were not applied as an alternative to dilution.

Overall precisions were calculated based on calibration curves of least squares with the overall precision, $St = mx + c$, where x = the concentration of the sample determined in milligrams per litre, and c = the zero concentration intercept. The difference in overall precisions for various elements can be associated with analyte linearities. Silicon is linear to 150 $mg \cdot L^{-1}$ and has a relatively high degree of precision (±4.4%), whereas magnesium is linear to 0.4 $mg \cdot L^{-1}$ and its associated precision is much lower (±15.8%). The analyte precisions are of the order Sr>Si>Ca >Na>K>Mg, with silicon linear to a higher concentration than Sr>Ca>Na>K>Mg.

Total trace metals were determined by direct aspiration into either an air-acetylene or a nitrous oxide flame. All standards and samples were in 8 $mL \cdot L^{-1}$ concentrated nitric acid. Overall precisions were calculated using $St = mx + c$.

Sensitivities are again based on calibration curves of least squares, and minimum detection limits are based on 1% absorption, or 0.0044 absorbance units (Table C-1).

ANION ANALYSES

The technique of ion chromatography (I.C.) has gained wide acceptance for the analyses of inorganic ions in a variety of aqueous matrices and was used for anion analyses of the East Bull Lake samples.

Table C-1. Linear Ranges, Overall Precisions, Minimum Detection Limits and Sample Treatments for Ionization Interferences for Cations or Trace Metals Analyzed

Element	Minimum detection limits ($mg \cdot L^{-1}$)	Linear range ($mg \cdot L^{-1}$)	Precision (±%)	Sample/standard treatment
Calcium	0.05	0.05–3.0	5.5	2000 $mg \cdot L^{-1}$ La^{3+} in 4 $mL \cdot L^{-1}$ HCl; air/acetylene flame
Magnesium	0.003	0.003–0.4	15.8	2000 $mg \cdot L^{-1}$ La^{3+} in 4 $mL \cdot L^{-1}$ HCl; air/acetylene flame
Potassium	0.01	0.01–0.4	15.4	2000 $mg \cdot L^{-1}$ Cs^{+} in 4 $mL \cdot L^{-1}$ HCl to control ionization of K^{+}; air/acetylene flame
Sodium	0.001	0.001–1.0	11.1	2000 $mg \cdot L^{-1}$ K^{+} in 4 $mL \cdot L^{-1}$ HCl to control ionization of Na^{+}; air/acetylene flame
Silicon	0.8	0.8–150	4.4	Samples and standards in 4 $mL \cdot L^{-1}$ HCl; nitrous oxide/acetylene flame
Strontium	0.06	0.06–5.0	3.3	2000 $mg \cdot L^{-1}$ K^{+} in 4 $mL \cdot L^{-1}$ HCl added to control strontium ionization; nitrous oxide/acetylene flame
Aluminum	0.40	0.40–60	8.5	2000 $mg \cdot L^{-1}$ K^{+} in 8 $mL \cdot L^{-1}$ HNO_3; nitrous oxide/acetylene flame
Chromium	0.06	0.06–5.0	11.5	8 $mL \cdot L^{-1}$ HNO_3; nitrous oxide/acetylene flame
Copper	0.03	0.03–4.0	10.8	8 $mL \cdot L^{-1}$ HNO_3; air/acetylene flame
Iron	0.04	0.04–5.0	10.4	8 $mL \cdot L^{-1}$ HNO_3; air/acetylene flame
Lead	0.1	0.1–15.0	12.0	8 $mL \cdot L^{-1}$ HNO_3; air/acetylene flame
Manganese	0.04	0.04–3.0	16.0	8 $mL \cdot L^{-1}$ HNO_3; air/acetylene flame
Nickel	0.06	0.06–5.0	18.5	8 $mL \cdot L^{-1}$ HNO_3; air/acetylene flame
Zinc	0.02	0.02–1.0	13.0	8 $mL \cdot L^{-1}$ HNO_3; air/acetylene flame

Field analyses of East Bull Lake ground waters indicated a wide variety of matrices including varying pH (6–10), conductance values of 100-6000 $\mu S \cdot cm^{-1}$ and chloride values of less than 1.0 to about 2500 $mg \cdot L^{-1}$. As I.C. was chosen as the analytical method for anion determinations, investigations were undertaken to determine whether varying pH and high chloride concentrations had any effect on the separation and quantification of desired anions.

All anions were analyzed by ion chromatography on a Dionex System 12 ion chromatograph, equipped with a 4 × 30 mm anion concentrator, a 4 × 250 mm anion separator column, and a hollow fibre suppressor unit.

Standard anion eluent, 0.0024 *M* Na_2CO_3/0.0030 *M* $NaHCO_3$, was used. A 100-μL sample injection loop and a flow rate of 138 $mL \cdot h^{-1}$ were used. Eluted anions were detected by a Dionex Conductance Meter followed by quantification employing a Hewlett-Packard 3390A reporting integrator.

Electrochemical detection of bromide and iodide was performed with a Dionex Ion-Chrom/Amperometric detector. The cell consists of a working silver electrode 1.3 cm long × 0.178 cm in diameter, an Ag/AgCl reference electrode separated from the flowing stream by a Nafion cation exchange membrane and a platinum counter electrode. The applied potential for bromide and iodide was +0.20 volts.

Total alkalinities were determined using a Metrohm Herisau E536 Potentiograph, a Dosimate E535 automatic titrator, and a Metrohm AG 9100 comination pH electrode. Alkalinities are reported as milligrams per litre bicarbonate.

All the standard inorganic anion solutions, as sodium or potassium salts, were prepared from reagent grade chemicals. Water was purified with a Milli-R.O., Milli-Q system (Millipore Corp.).

Chromatograms of standard anion solutions of fluoride, chloride, nitrite, nitrate and sulphate at pH values of 2.5, 5.5, 11.5 indicated that pH is not a factor in the separation and quantification of anions by I.C. In all cases the values obtained were within the limits of precision. The addition of HCl precluded assessment of pH effect on chloride determination.

Ion chromatography analyses of ground waters with chloride values of 100–1500 $mg \cdot L^{-1}$ were also examined. Chloride additions of 100, 500 and 1000 $mg \cdot L^{-1}$ were added to the "standard anion" solutions (2 $mg \cdot L^{-1}$ F^{-}, 20 $mg \cdot L^{-1}$ NO_2^{-}, 20 $mg \cdot L^{-1}$ NO_3^{-}, 30 $mg \cdot L^{-1}$ $SO_4^{=}$).

Separation and quantification of anions were then determined.

From the chromatograms integration of peaks revealed that chloride additions have no significant effect on the separation and quantification of fluoride, nitrate or sulphate. Similar studies have shown that sulphate response is linear in the range 0-80 $mg \cdot L^{-1}$ in the presence of chloride concentrations up to 4000 $mg \cdot L^{-1}$. Problems encountered upon chloride addition were the separation and quantification of nitrite. Chloride additions of 500-1000 $mg \cdot L^{-1}$ resulted in the loss of chloride/nitrite peak separation.

Analyses of East Bull Lake ground waters for nitrite required special attention. Chloride values for P-holes remained low enough to quantify nitrite. Boreholes EBL-1, 2 and 4 had varying chloride values. Some were low enough to allow for separation of Cl^- and NO_2^- and quantification; a large number, however, were not. Values for nitrite cannot be assigned to boreholes with chloride values in excess of 500 $mg \cdot L^{-1}$. Nitrate values for boreholes 1, 2 and 4 are typically <0.2 $mg \cdot L^{-1}$. Nitrate is quantifiable in high chloride solutions. With such low amounts of nitrate in boreholes 1, 2 and 4, it is believed that nitrite values were <0.2 $mg \cdot L^{-1}$. Determination of nitrite by I.C. may be accomplished by passing the sample through a silver-charged exchange resin to precipitate out the high Cl^- as AgCl.

Chloride concentration was not a concern in the electrochemical detection of bromide and iodide. A solution containing 2500 times as much chloride as bromide had little effect on the determination of bromide, since the standard electrode potential, E°, for the oxidation of Ag to AgCl is positive.

Linearities obtained using the Dionex System 12 were based on two principles: (1) the maximum amount of analyte that could be detected without sample treatment (dilution) and (2) deviation from calibration curves at a value greater than precision allowed.

Sensitivities for the individual anions were established based on standard calibration curves of least squares. Minimum detection limits were based on the resolution of peak height to baseline noise. Quantitative limits were established based on the analyte signal being five times that of the baseline signal. Assuming the analyte does not overload the concentrator column, the minimum detection limits may be improved by increasing the injection volume from 100 to 200 μL.

Precision or reproducibility was calculated based on a homogeneous sample, regardless of whether or not the observed values were widely displaced from the mean as a result of systematic or constant error present in a measurement. Precision is expressed in terms of percent relative standard deviation from the mean (R.S.D.). Results reported are based on the integration of 20 injections of "standard anions" run in conjunction with sample analyses (Table C-2).

Table C-2. Linearities, Sensitivities, and Precisions for Various Anions as Determined by I.C.

Anion	Linearity ($mg \cdot L^{-1}$)	Sensitivity ($mg \cdot L^{-1}$)	Precision (% R.S.D.)
Fluoride	0.2-10.0	0.2	5.0
Chloride	0.2-10.0	0.2	5.4
Nitrite	0.2-40.0	0.2	4.1
Nitrate	0.2-80.0	0.2	8.6
Sulphate	2.0-80.0	2.0	10.0
Bromide	0.02-2.0	0.02	5.0
Iodide	0.04-10.0	0.04	5.8